

HIGHER ORDER SLIDING MODE CONTROL BASED SR MOTOR CONTROL SYSTEM DESIGN



by

Muhammad Rafiq
PE093011

A thesis submitted to the
Department of Electronic Engineering
in partial fulfillment of the requirements for the degree of
DOCTOR OF PHILOSOPHY IN ELECTRONIC ENGINEERING

Faculty of Engineering
Mohammad Ali Jinnah University
Islamabad
June, 2012

Copyright © 2012 by Muhammad Rafiq

All rights reserved. Reproduction in whole or in part in any form requires the prior written permission of Muhammad Rafiq.

*Dedicated to my wife,
all of my teachers, parents and friends.*

ACKNOWLEDGEMENT

All praises to Allah Subhanahu Wa Ta'ala, the Most Gracious and the Most Merciful, who blessed me with knowledge and enabled me to complete this report. All respects to Holy Prophet Hazrat Muhammad (P.B.U.H) who is the last messenger, who has given us a complete code of life.

I would like to thank my supervisor Dr. Fazal-ur-Rehman for his valuable assistance and cooperation during this work. His valuable suggestions and guidance have always fueled my research work and made me enthusiastic about this interesting field. I would like to acknowledge Dr. Saeed-ur-Rehman and Dr. Aamer Iqbal Bhatti for their consistent guidance and support throughout this work. Without their guidance and help this research work would not have been possible. Their valuable opinions and their logical way of thinking are a great asset for me.

My gratitude for financial support goes to Higher Education Commission and Mohammad Ali Jinnah University Islamabad.

Special thanks to Dr. Irfan Awan, Dr. Nayyar Masood Dar, Dr. Masood Nadeem, Dr. Ghulam Shabbir, Dr. Shaukat Iqbal, Dr. Rana M. Ramzan, Dr. M. Arif, Qarab Raza Butt, Dr. M. Iqbal, Qudrat Khan, Kamran Nadeem, Ms. Umaima Kamran, and Dr. Syed Hameed Qaiser for all encouragement and motivation at all stages of my work. I am also thankful to Qarab Raza Butt for his careful proofreading, review of my research papers and this document, and providing help in simulating the model and controllers. I am also thankful to Dr. Sohail Iqbal for his help while simulating the model in Matlab. I would extend my appreciation to all of my research fellows at Control and Signal Processing Research Group (CASPR) Mohammed Ali Jinnah University Islamabad and CASE for their useful technical support.

I am also grateful to all my friends and relatives from Ahmadpur East and Hayatpur for their encouragement and well wishes during my research work.

Special thanks to Mr. and Mrs. Naveed Iqbal and Mr. and Mrs. Jehangir Bhutta for providing good research environment.

May Allah reward them in the world and thereafter (Amen).

ABSTRACT

This thesis presents a novel scheme for speed regulation/tracking of Switched Reluctance (SR) motors based on Higher-Order Sliding-Mode technique. In particular, a Second-Order Sliding-Mode Controller (SOSMC) based on Super Twisting algorithm is developed. Owing to the peculiar structural properties of SRM, torque produced by each motor phase is a function of phase current as well as rotor position. More importantly, unlike many other motors the polarity of the phase torque in SR motors is solely determined by the rotor position and is independent of the polarity of the applied voltage or phase current.

SR motor needs an electronic commutation scheme for its operation. So design of commutation scheme plays an important role in motor efficiency and performance. This commutation scheme is embedded in its power supply as switching timers. The existing commutation schemes cause high power loss and based on those commutation schemes, the existing controller techniques for SR motor show low robustness especially when motor's parameters change. Therefore a new commutation scheme is developed which optimizes power consumption in motor phases. On the bases of this commutation scheme, a new controller technique is used to design controller for SR motor which is highly efficient, simple to design and easy to implement and also provides sufficient robustness against parameter variations and unknown disturbances. The proposed controllers take advantage of this property and incorporate a commutation scheme which, at any time instant, selects to energize only those motor phases for the computation of control law, which can contribute torque of the desired polarity at that instant. This feature helps in achieving the desired speed regulation/tracking objective in a power efficient manner as control efforts are applied through selective phases and phases producing the torque of opposite polarity are kept switched off. This approach also minimizes the power loss in the motor windings reducing the heat generation within the motor.

The common techniques for designing the SR Motor controls are fuzzy logic control, Artificial Neural Network (ANN) and feedback linearization. Fuzzy logic control provides sufficient robustness against parameter variations but at a high computational cost. Artificial Neural Network (ANN) shows good dynamic response

against unknown disturbances but problem in using this technique is requirement of a large training data set. In the feedback linearization technique, nonlinear control problem is transformed into linear control problem and then any one of the well established and mature linear controller techniques are applied on the resulting system. Feedback linearization cannot be applied to all types of nonlinear systems; and in case of parameters uncertainties, the robustness cannot be guaranteed. All the deficiencies in discussed techniques can be overcome by introducing sliding mode control which is simple, easy to implement and provides robustness. The inherent problem of chattering in classical FOSMC can further be improved by using higher order sliding mode control (HOSMC).

In order to highlight the advantages of Higher-Order Sliding-Mode controller, a classical First-Order Sliding-Mode controller (FOSMC) is also developed and applied to the same system. The comparison of the two schemes shows much reduced chattering and low power consumption in case of SOSMC. This feature is especially very important for SR motor control, due to reduced chattering; wear and tear problem of actuators is reduced. The responses of synthesized controllers are also investigated against changes in moment of inertia which could be due to engagement of load; stator phase resistance which could vary due to temperature variations in winding during operation and coefficient of viscous friction as a model uncertainty. The performance of the proposed SOSMC controller for speed regulation is also compared with that of another sliding mode speed controller published in the literature and also with dynamic sliding mode controller. The same technique is also applied on position control problem and, FOSMC and SOSMC are developed for position regulation problem; making it possible candidate for servo drive application.

TABLE OF CONTENTS

Acknowledgement	v
Declaration	vi
Abstract	vii
Table of contents	ix
List of Figures	xii
List of Tables	xvi
List of Publications.....	xvii
List of acronyms.....	xviii

Chapter 1

Introduction.....	1
1.1 Switched Reluctance Motor (SR motor)	1
1.1.1 Basic Operation of SR Motor.....	2
1.1.2 Torque Production Principle	3
1.1.3 Inductance verses rotor position relationship.....	5
1.1.4 Advantages and Disadvantages of SR Motor.....	7
1.1.5 SR Motor Applications.....	9
1.2 Motivation	10
1.3 Contribution of the Thesis.....	11
1.4 Organization of the Thesis	12
1.5 Conclusion.....	13

Chapter 2

Mathematical Model and proposed commutation scheme for SR motor	14
2.1 Model Description.....	14
2.1.1 Electrical Subsystem	16
2.1.2 Mechanical Subsystem.....	17
2.2 Commutation Scheme	18
2.2.1 Proposed Commutation Scheme	18
2.3 PI Controller for speed control application.....	23

2.3.1	Controller Effort	25
2.3.2	Speed Response of PI Controller to a Sinusoidal Signal	26
2.3.3	Robustness Comparison	27
2.4	Conclusion.....	32

Chapter 3

First Oder Sliding Mode Control	33
3.1 Existing Techniques for the Control of SR Motor	33
3.2 Sliding Mode Technique for the Control of SR Motor	37
3.3 Sliding mode control examples	39
3.3.1 Example 1.....	40
3.3.2 Example 2.....	41
3.3.3 Example 3.....	44
3.4 First Oder Sliding Mode Controller (FOSMC) Design.....	48
3.4.1 Case-1: Regulation Problem.....	50
3.4.2 Case-2: Tracking Problem.....	52
3.5 Simulation Results of FOSMC using Proposed Commutation scheme	53
3.5.1 Comparison of Speed Response of FOSMC and SMC to A Step Command	53
3.5.2 Comparison between FOSMC and SMC With Respect To Power Loss, Input Phase Voltages and Torques in Speed Regulation Problem	54
3.5.3 Comparison of Speed Response of FOSMC and SMC to a Sinusoidal Signal.	57
3.5.4 Position Response of FOSMC to A Step Command.....	57
3.6 Drawbacks of Conventional SMC and FOSMC	58
3.7 Conclusion.....	60

Chapter 4

Higher-Order Sliding-Mode Control.....	61
4.1 Background	61
4.2 Higher Order Sliding Mode.....	64
4.3 Second order sliding mode algorithms.....	64
4.3.1 Twisting Algorithm	64
4.3.2 Sub-Optimal Algorithm.....	66
4.3.3 Drift Algorithm	67

4.3.4	Super-Twisting Algorithm	68
4.3.5	Example.....	70
4.4	Simulation Results of HOSM Using STA and Commutation Scheme	76
4.4.1	Comparison of Speed Response of FOSMC and SOSMC to A Step Command.....	77
4.4.2	Comparison of Position Response of FOSMC and SOSMC to A Step Command.....	81
4.4.3	Comparison between FOSMC and SOSMC With Respect to Power Loss, Input Phase Voltages and Torques in Speed Regulation Problem.....	83
4.4.4	Comparison between FOSMC and SOSMC With Respect to Power Loss, Input Phase Voltages and Torques in Position Regulation Problem	87
4.4.5	Comparison of Speed Response of FOSMC and SOSMC to A Sinusoidal Signal	90
4.5	Conclusion.....	92

Chapter 5

	ROBUSTNESS OF THE PROPOSED CONTROL	93
5.1	Robustness.....	93
5.1.1	Robustness against External Load.....	93
5.2	Robustness against Parameters Variation	97
5.2.1	Comparison of Speed/Position Responses of SR Motor with Changes in J .	98
5.2.2	Comparison of Speed/Position Responses of SR Motor with Changes in B	100
5.2.3	Comparison of Speed/Position Responses of SR Motor with Changes in R	102
5.3	Conclusion.....	104

Chapter 6

	Conclusions and Future Work.....	105
	References.....	108

LIST OF FIGURES

Figure 1.1: Operation of SR motor. (i) Phase B is aligned. (ii) Phase C is aligned.....	2
Figure 1.2: Solenoid and its characteristics. (i) A solenoid. (ii) Flux vs. mmf characteristics.....	3
Figure 1.3: Basic rotor position definition in 2-poles SR motor.....	6
Figure 1.4: Inductance profile.....	6
Figure 2.1: Division of one electrical cycle into 12 distinct region for commutation purposes.	20
Figure 2.2: Block diagram of commutation schemes.	22
Figure 2.3: Speed response of PI for a step command.....	23
Figure 2.4: Error plots of speed response of PI for a step command.....	24
Figure 2.5: A close up view of speed response of PI controller for a step command. The high magnitudes of speed ripples are clearly noticeable.	24
Figure 2.6: Controller effort during the simulated period for a simulation run of 1.0 second.	25
Figure 2.7: Controller effort in transient state when commutation scheme was used.	25
Figure 2.8: Controller effort in initial stage of steady state when commutation scheme was used.....	26
Figure 2.9: Speed response of PI controller against the sinusoidal signal.....	26
Figure 2.10: Speed error response of PI controller for sinusoidal signal.....	27
Figure 2.11: Speed response with torque load.....	28
Figure 2.12: A close up view of speed response against sudden change in torque load.	28
Figure 2.13: Speed response with variations in moment of inertia J.	29
Figure 2.14: A close up view of speed response with changes in J.....	29
Figure 2.15: Speed response with variations in coefficient of friction B.	30
Figure 2.16: A close up view of speed response with changes in B.....	30
Figure 2.17: Speed response with variations in resistance R.....	31
Figure 2.18: A close up view of speed response with changes in R.....	31
Figure 3.1: Sliding motion phase portrait.	42
Figure 3.2: Controller effort.....	43
Figure 3.3: System Trajectories.	43
Figure 3.4: Sliding Surface.	44
Figure 3.5: Speed response.	46

Figure 3.6: Tracking error response.....	46
Figure 3.7: Current response.....	47
Figure 3.8: Controller effort.....	47
Figure 3.9: Speed response of SMC and FOSMC to a step command.....	53
Figure 3.10: Power loss in SMC and FOSMC during the entire simulation period of one second.....	55
Figure 3.11: 3-phase voltages during initial stage of steady state response.	55
Figure 3.12: 3-phase current during initial stage of steady state response.	56
Figure 3.13: Torques during initial stage of steady state response.	56
Figure 3.14: Speed response of FOSMC and SMC against sinusoidal signal.	57
Figure 3.15: Position response of FOSMC to a step command.....	58
Figure 3.16: Error plot of position response of FOSMC to a step command.	58
Figure 3.17: A close-up of speed response of conventional SMC and FOSMC to a step command.	59
Figure 3.18: A close-up of steady state position response of FOSMC to a step command.....	59
Figure 4.1: Phase trajectory of twisting algorithm.....	65
Figure 4.2: Phase trajectories of sub-optimal algorithm.....	66
Figure 4.3: Phase trajectories of drift algorithm.	67
Figure 4.4: Evolution of Switching Surface during the super twisting controller action; minimizing the error between reference signal and desired output.	68
Figure 4.5: Phase portrait using FOSMC.....	72
Figure 4.6: Phase portrait using SOSMC.....	72
Figure 4.7: Controller effort using FOSMC.	73
Figure 4.8: Controller effort using SOSMC.	73
Figure 4.9: System trajectories using FOSMC.	74
Figure 4.10: System trajectories using SOSMC.	74
Figure 4.11: Sliding surfaces of FOSMC and SOSMC	75
Figure 4.12: Driver circuit used for energizing motor phases.	76
Figure 4.13: Speed response of FOSMC and SOSMC to a step command.	77
Figure 4.14: A Close-up View of Response of both FOSMC and SOSMC to a step command. The high magnitude of chattering signal of FOSMC is clearly noticeable.	78
Figure 4.15: Error plot of Speed Response of FOSMC and SOSMC to a step command.....	78

Figure 4.16: A Close-up View of Error plot of Speed Response for FOSMC and SOSMC to a step command. The reduced amount of error magnitude is clearly visible.....	79
Figure 4.17: Speed Response and Speed error plot of FOSMC and SOSMC to a step command for a relative speed of 20 rad/s.	79
Figure 4.18: A close up view of Speed Response of both FOSMC and SOSMC to a step command in the starting and steady state regions. The high magnitude of chattering signal of FOSMC is clearly visible.....	80
Figure 4.19: Control effort using FOSMC.....	80
Figure 4.20: Control effort using SOSMC.....	81
Figure 4.21: Position response of FOSMC and SOSMC to a step command.....	81
Figure 4.22: A close-up view of responses of both FOSMC and SOSMC to a step command. The high magnitude of chattering signal of FOSMC is clearly noticeable.	82
Figure 4.23: Error plot of position responses of FOSMC and SOSMC to a step command.....	82
Figure 4.24: A close-up view of error plot of position responses for FOSMC and SOSMC to a step command in initial stage of steady state.	83
Figure 4.25: Power loss in Conventional Design is about 85 kW. Using FOSMC it is about 19 KW. Using SOSMC it even lowers to about 15 kW.....	84
Figure 4.26: 3-phase voltages during initial stage of steady state response.	85
Figure 4.27: 3-phase currents during initial stage of steady state response.....	85
Figure 4.28: Torques during initial stage of steady state response.	86
Figure 4.29: Phase voltages during simulated period for a simulation run of 10 seconds when motor is directed to obtain a desired position 30 radian.....	87
Figure 4.30: Phase voltages during transient response seconds when motor is directed to obtain a desired position 30 radian.	88
Figure 4.31: Power Loss during transient state when SR motor is commanded to attain a desired position 30 radian.	88
Figure 4.32: Power Loss during transient state when SR motor is commanded to attain a desired position 30 radian..	89
Figure 4.33: 3-Phase Torque and Net Torque during transient state when SR motor is commanded to attain a desired position 30 radian.....	89
Figure 4.34: Speed response of proposed design for sinusoidal signal	90
Figure 4.35: A Close-up of Speed response of proposed design for sinusoidal signal.	90
Figure 4.36: Error response using FOSMC and SOSMC.....	91
Figure 5.1: Speed response of SR motor with sudden change in torque load.	94
Figure 5.2: A close-up view of Figure 5.1 with sudden change in Torque Load.	94

Figure 5.3: Speed response of SR motor with sudden change in torque load.	95
Figure 5.4: A close-up view of Figure 5.3 with sudden change in Torque Load.	95
Figure 5.5: Speed response during sudden change in torque load	96
Figure 5.6: Position response of SR motor with sudden change in torque load.	96
Figure 5.7: A close-up view of Figure 5.6 with sudden change in Torque Load.	97
Figure 5.8: Speed response of SR motor with sudden changes in J.	98
Figure 5.9: Position response of SR motor with sudden changes in J.	98
Figure 5.10: A close up view of Figure 5.8 with sudden changes in J.	99
Figure 5.11: Close up view of position response of controllers during initial stage of steady state against sudden change in J.	99
Figure 5.12: Speed response of SR motor with sudden changes in B.	100
Figure 5.13: Position response of SR motor with changes in B.	101
Figure 5.14: A close up view of Figure 5.12 with sudden changes in B.	101
Figure 5.15: Close up view of position response of controllers during initial stage of steady state against sudden change in B	102
Figure 5.16: Speed response of SR motor with sudden changes in R	102
Figure 5.17: Position response of SR motor with changes in R.	103
Figure 5.18: A close up view of Figure 5.16 with sudden changes in R.	103
Figure 5.19: Close up view of position response of controllers during initial stage of steady state against sudden change in R	104

LIST OF TABLES

Table 1: Parameters of SR Motor.	15
Table 2: Model Summary of Electrical Subsystem.	16
Table 3: Model Summary of Mechanical Subsystem.	17
Table 4: Parameters of DC Motor.....	45

LIST OF PUBLICATIONS

The work presented has already been submitted and published in national and international reviewed conferences and journals.

Journals

1. Rafiq M., Rehman S.U., Rehman F. R., Butt Q. A., Awan I.,” Second Order Sliding Mode Control Design of a Switched Reluctance Motor using Super Twisting Algorithm”, Simulation Modelling Practice and Theory, March 2012. (ISI Thomson IF: 0.728)
2. Rafiq M., Rehman S.U., Rehman F. U., Butt Q. R.,” Power Efficient Higher Order Sliding Mode Control of Switched Reluctance Motor for Speed Control Applications”, International Journal of Computer Science Issues. Vol. 8, No. 3, May 2011.
3. Rafiq M., Rehman S.U., Rehman F. R., Butt Q.A., ”Performance Comparison of PI and Sliding Mode for Speed Control Applications of SR Motor”, European Journal of Scientific Research, Vol. 50, No. 3. pp. 368-384, February 2011.
4. Rafiq M., Bhatti A. I., Rehman F. R., Butt Q. A., Awan I., “Position Control of Switched Reluctance Motor Using Super Twisting Algorithm“, (Submitted in Scientific Research and Essays).

Conferences

1. Rafiq M., Rehman S.U., Butt Q. R., Bhatti A. I., ”Power Efficient Sliding Mode Control of SR Motor for Speed Control Applications,”INMIC 2009, MAJU, Islamabad, Pakistan.
2. Butt Q. R., Bhatti A. I., Iqbal M., Rizvi M. A., Rafiq M., Kazmi I. H., “Estimation of Automotive Engine Parameters Part I: Discharge coefficient of throttle body”, IBCAST 2009 January, 2009 Islamabad, Pakistan.

LIST OF ACRONYMS

SRM	Switched Reluctance Motor
STA	Super Twisting Algorithm
SMC	Sliding Mode Control
PI	Proportional Integral
HOSM	Higher Order Sliding Mode
FOSMC	First Order Sliding Mode Controller
SOSMC	Second Order Sliding Mode Controller
HOSMC	Higher Order Sliding Mode Controller
DSMC	Dynamic Sliding Mode Controller
FEM	Finite Element Method
ANN	Artificial Neural Network
GA	Genetic Algorithm
ISMC	Integral Sliding Mode Control
DISMC	Dynamic Integral Sliding Mode Control
FSMC	Fuzzy Sliding Mode Control
MIMO	Multi Input Multi Output

Chapter 1

INTRODUCTION

This chapter is dedicated to a brief introduction of switched reluctance (SR) motor and its structure, highlights some of the advantages and disadvantages associated with it and the applications where its use could be beneficial in terms of power and cost optimization. The contribution of the thesis is summarized in Section 1.3. Section 1.4 gives the layout of thesis and Section 1.5 gives concluding remarks.

1.1 Switched Reluctance Motor (SR motor)

SR motors have recently received increasing interest of research community due to its simple construction, rugged mechanical structure, fault-tolerant operation capability and low cost drive electronics. Due to the absence of any windings on the rotor, SR motor is very suitable for operations at high speed and/or at high temperatures and vibrations [1]. A number of possible practical applications of SR motor increase its requirement in industrial society.

SR motor is doubly salient machine, i.e. both stator and rotor have salient poles on their laminations. Torque is generated due to the tendency of rotor poles to align themselves with the poles of the excited motor phases. The sequential excitation of the phases based on rotor position rotates the motor. Torque is nonlinear function of phase current and rotor position, and its polarity is independent of the polarity of phase current but depends only upon the relative position of the rotor poles with respect to the excited phase poles. Therefore, low cost unipolar power converters are used to drive SR motors. This fact also leads to a very important feature peculiar to this motor.

Unlike most of the other types of electrical motors, it is not necessary that all poles of motor would be generating the torque of same polarity (in the same direction; clockwise or anticlockwise). It is quite possible that at a particular instant, one or more than one phases/ poles of motor are generating torque for clockwise rotation while the remaining phases are generating the torque in counterclockwise direction. It

is quite possible for example, that in a regular 3-phase SR motor, there are certain rotor positions where only one phase is generating the torque in a clockwise direction whereas the torques generated by the other two phases are in counterclockwise direction. In such a situation/ rotor positions, the torque in the opposite of the desired direction would give a cancellation effect thus wasting power input to the motor. Therefore it would not be necessary to energize all the phases, and only phases generating the torque in the desired direction would be energized.

1.1.1 Basic Operation of SR Motor

Consider a regular 3-phase 6/4 SR motor [2]. Initially the rotor poles R_1 and R_1' are aligned with the stator poles B and B' . Here the rotor is at aligned position with respect to phase B but at unaligned position with respect to phase C . Aligned position is also called stable equilibrium point where the phase current cannot produce any phase torque at this point but slightly away from this point attracts the rotor towards it. Unaligned position is also called unstable equilibrium point where a small displacement causes the rotor away from that point. After energizing the phase C , the flux is produced through stator poles C and C' and rotor poles R_2 and R_2' which tends to bring rotor poles R_2 and R_2' into alignment with the stator poles C and C' respectively in the clock wise direction as shown in the Figure 1.1 (i).

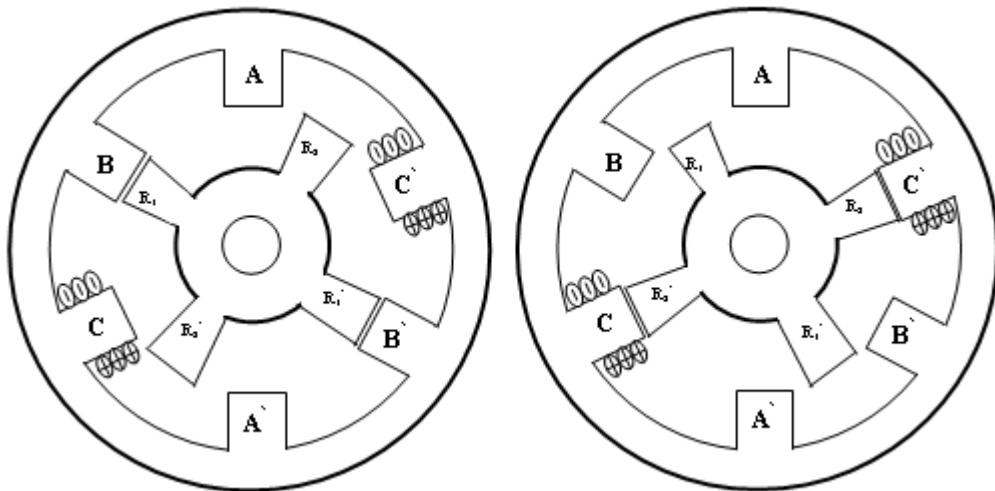


Figure 1.1: Operation of SR motor. (i) Phase B is aligned. (ii) Phase C is aligned.

After the alignment, the stator current in phase C is turned off and the subsequent situation can be seen in Figure 1.1(ii).

The rotor rotates in a step. The step angle is calculated by the following formula

$$\theta_s = \frac{2\pi}{q N_r} \quad (\text{Eq 1.1})$$

where q is the number of phases and N_r is the number of rotor poles. In this particular motor, the step angle is $\theta_s = \frac{2\pi}{3 \times 4} = 30^\circ$

Now phase A is energized, causing the poles R_1 and R_1' move towards the poles A and A' respectively. Similarly by exciting phase B , results in alignment of rotor poles R_2 and R_2' with stator poles B and B' respectively. Therefore, in three excitation in sequence CAB , moves the rotor to an angle 90 degree in the clock wise direction and for one complete revolution, current is switched in any phase as many times as the number of rotor poles in the motor. Similarly, excitation in the sequence ACB rotates the motor in the counter clock wise direction.

1.1.2 Torque Production Principle

The torque production in SR motor is described with the help of electromechanical energy conversion principle of solenoid as shown in the Figure 1.2(i) [2]. When solenoid is excited with a current i having N turns, the coil establishes a flux Φ . With the increment of excitation current, the armature will rotate towards the fixed yoke. Let x_a and x_b be two points in the air gap such that $x_b < x_a$ then their fluxes verses magneto-motive force (mmf) plot can be shown in the Figure 1.2(ii). The flux vs. mmf behaviour is linear for x_a due to dominant reluctance and makes the flux smaller in the magnetic circuit.

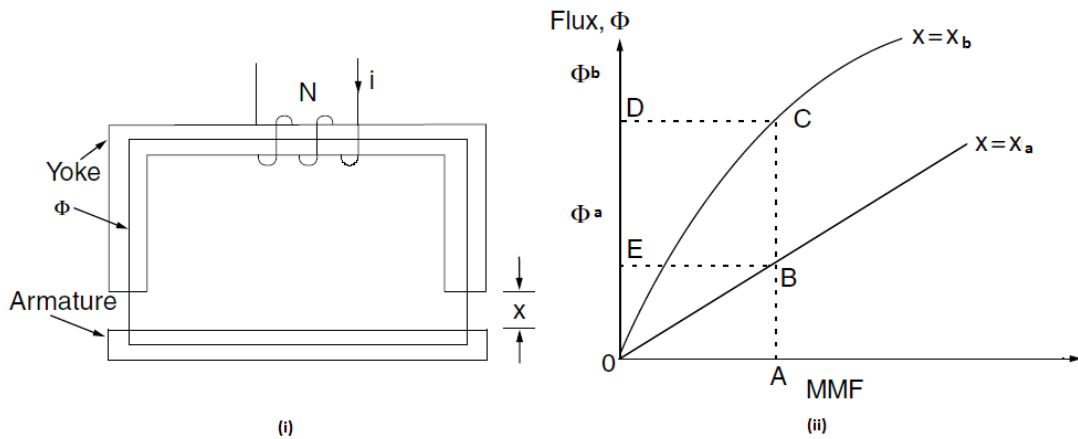


Figure 1.2: Solenoid and its characteristics. (i) A solenoid. (ii) Flux vs. mmf characteristics.

The input electrical energy W_e is expressed as

$$W_e = \int e i dt = \int i dt \frac{dN\Phi}{dt} = \int Ni d\Phi = \int F d\Phi \quad (\text{Eq 1.2})$$

where e and F are the induced electro-motive force (emf) and mmf respectively. W_e is also equal to the energy stored in the coil W_f plus the energy converted into mechanical work W_m .

$$W_e = W_f + W_m \quad (\text{Eq 1.3})$$

In case of no mechanical work, the field energy is equal to the input electrical energy given in (Eq 1.2). This field energy corresponds to the area $OBEO$ as shown in the Figure. The complement of field energy is called coenergy corresponding to the area $OBAO$. Now for x_b , field energy and coenergy correspond the area $OCDO$ and $OCAO$. In this case, the incremental input electrical energy is written as

$$\delta W_e = \delta W_f + \delta W_m \quad (\text{Eq 1.4})$$

$$\Rightarrow \delta W_m = \delta W_e - \delta W_f \quad (\text{Eq 1.5})$$

Let a constant excitation force F_1 be applied at the point A then the corresponding δW_e and δW_f are written as

$$\delta W_e = \int_{\Phi_a}^{\Phi_b} F_1 d\Phi = F_1(\Phi_2 - \Phi_1) = \text{area}(BCDEB) \quad (\text{Eq 1.6})$$

$$\delta W_f = \delta W_f|_{x=x_b} - \delta W_f|_{x=x_a} = \text{area}(OCDO) - \text{area}(OBEO) \quad (\text{Eq 1.7})$$

Now plugging (Eq 1.6) and (Eq 1.7) in (Eq 1.5) and get

$$\delta W_m = \text{area}(OBCO) \quad (\text{Eq 1.8})$$

This is the incremental mechanical energy for a given mmf F_1 . In case of rotating machine, δW_m can be expressed as

$$\delta W_m = T_e \delta\theta \quad (\text{Eq 1.9})$$

where T_e is the electromagnetic torque and $\delta\theta$ is the change in position, therefore

$$T_e = \frac{\delta W_m}{\delta\theta} \quad (\text{Eq 1.10})$$

Since F_1 is a constant excitation force so δW_m is equal to the rate of change of coenergy, therefore

$$\delta W_m = \delta W_f' \quad (\text{Eq 1.11})$$

$$\text{and } W_f' = \int \Phi dF = \int \Phi d(Ni) = \int (N\Phi) di = \int \lambda(\theta, i) di = \int L(\theta, i) i di$$

where L and λ are the inductance and flux linkage respectively. Both are the functions of rotor position and current. This change in coenergy has been occurred from rotor position θ_b to rotor position θ_a .

Now (Eq 1.10) can be written as

$$T_e = \frac{\delta W_m}{\delta \theta} = \frac{\delta W_f'}{\delta \theta} = \frac{\delta W_f'(i, \theta)}{\delta \theta} \quad |i = \text{constant} \quad (\text{Eq 1.12})$$

If inductance is a linear function of rotor position at a given phase current which is not possible in actual motor operation, (Eq 1.12) can be rewritten as

$$T_e = \frac{dL(\theta, i)}{d\theta} \cdot \frac{i^2}{2} \quad (\text{Eq 1.13})$$

$$\text{where } \frac{dL(\theta, i)}{d\theta} = \frac{L(\theta_2, i) - L(\theta_1, i)}{\theta_2 - \theta_1} \quad |i = \text{constant}$$

Now following observations can be deduced from (Eq 1.13).

- Since $T_e \propto \frac{i^2}{2}$ so unidirectional torque can be developed by applying unipolar current requiring only one power switch for current regulation in phase winding. Due to this characteristic, less hardware is used in motor convertor, making the motor more economical.
- Since torque is proportional to the square of the current so SR motor has a sufficient starting torque.

1.1.3 Inductance verses rotor position relationship derivation

Due to saturation and variation of phase current, the ideal inductance profile given in Figure 1.4 is not possible for actual motor operation; however for clarity and ease of understanding, motor is being assumed working in an unsaturated region with constant phase current. The inductance profile changes are expressed in terms of stator pole arc (β_s), rotor pole arc (β_r) and number of rotor poles (N_r). The stator pole arc is supposed to be smaller than rotor pole arc, and then, the following expressions are derived [2].

$$\theta_a = \frac{1}{2} \left[\frac{2\pi}{N_r} - (\beta_s + \beta_r) \right] \quad (\text{Eq 1.14})$$

$$\theta_b = \theta_a + \beta_s \tag{Eq 1.15}$$

$$\theta_c = \theta_b + (\beta_r - \beta_s) \tag{Eq 1.16}$$

$$\theta_d = \theta_c + \beta_s \tag{Eq 1.17}$$

$$\theta_e = \theta_d + \theta_a = \frac{2\pi}{N_r} \tag{Eq 1.18}$$

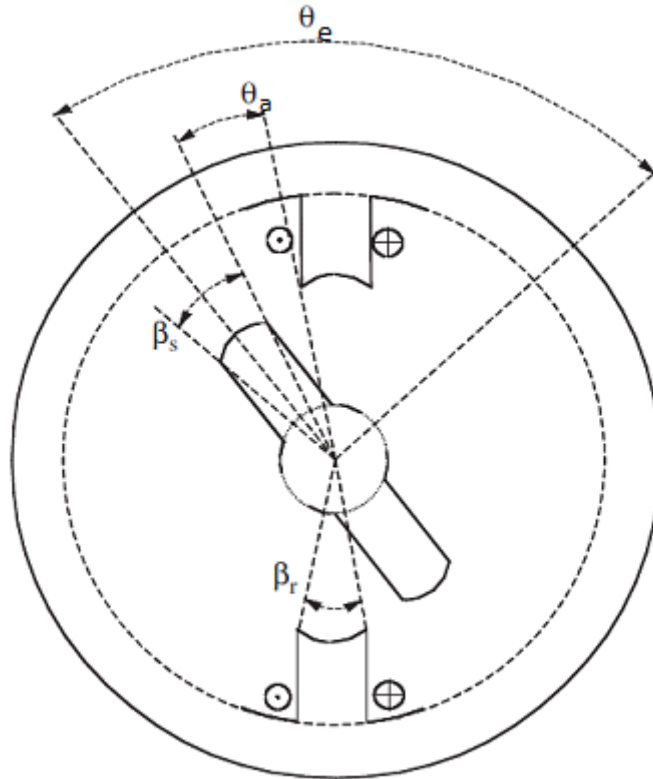


Figure 1.3: Basic rotor position definition in 2-poles SR motor.

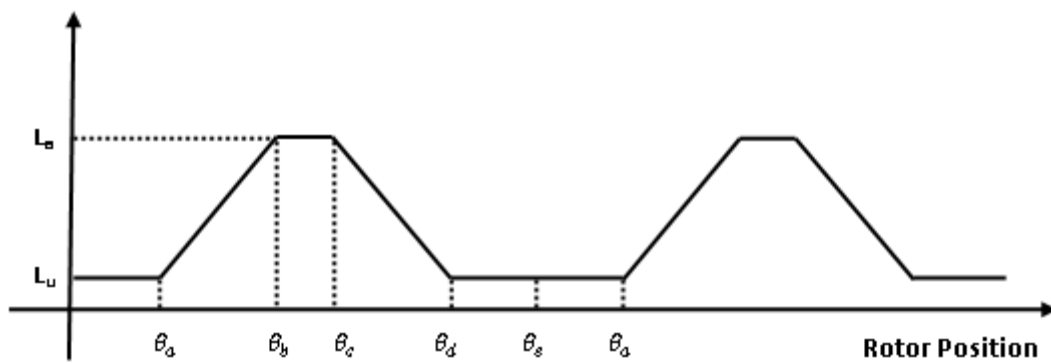


Figure 1.4: Inductance profile.

From Figure 1.4, following regions are considered.

- $0 - \theta_a, \theta_d - \theta_e$ (No over lapping)

In these regions, flux path is mainly determined by the air gap making the inductance minimum; it is almost constant. This inductance is termed as unaligned inductance (L_u). These regions do not play a part in torque production.

- $\theta_a - \theta_b$ (Partial overlapping)

Flux path in this region is generally through stator and rotor pole core. The inductance increases linearly with rotor position providing positive slope, so positive torque (conversion of electrical energy into mechanical energy) is produced. This region comes to end before the full overlapping region starts.

- $\theta_b - \theta_c$ (Full overlapping)

In this region, the inductance has maximum value, it is almost constant. This inductance is termed as aligned inductance (L_a). Since the inductance is constant so no torque is generated in this region instead of presence of phase current. This region plays an important role in providing sufficient time to make current zero or some minimum value during commutation thus avoiding negative torque.

- $\theta_c - \theta_d$ (Partial overlapping)

The inductance in this region decreases linearly with rotor position providing negative slope, so negative torque (conversion of mechanical energy into electrical energy) is produced.

1.1.4 Advantages and Disadvantages of SR Motor

The SR motor acquires some distinguished features that make it strong contestant to existing AC and DC motors in various engineering applications. The advantages of SR motor can be summed up as following [1-2]:

- SR motor preserves high efficiency over wide speed and load ranges.
- Since in SR motor, there are no brushes on rotor, and there is no winding or permanent magnets on rotor, therefore SR motor has low rotor inertia and a

high torque/inertia ratio. Due to this property, rotor has the ability to move faster.

- SR motor has simple mechanical construction. The stator and rotor has salient poles made up of laminations and there is no winding cost on rotor. Therefore the overall manufacturing cost of SR motor is low.
- Since SR motor is a brushless machine similar to AC machine, therefore its maintenance is easier than DC machine.
- Since there is no such mechanical arrangement (a brush commutator) in SR motor, and rotor is free from winding or permanent magnets, therefore rotor can move up to high speeds and low speeds/zero speed with full rated torque.
- SR motor can be used for four quadrant operation either for motoring or generating purpose.
- SR motor is shape adaptable; it can be designed as a pancake or long to adjust the available space.

SR motor has a unique inverter topology in which each leg is facilitated with a separate phase winding preventing it from a shoot through failure. Shoot through failure or shoot through fault in SR motor may be classified into two categories: machine fault and convertor fault.

- Machine fault may be phase winding open or phase winding short.
- Convertor fault may be phase switch open, phase switch short, DC voltage drop etc.

This feature makes SR motor a good fault tolerant machine.

- Due to independent stator phases, the motor operation will not be stopped in case of one or more phases loss.
- SR motor control is also possible without position sensors. The information about rotor position is achieved by means of change in inductance and change in flux during the entire electrical cycle of rotor rotation.

However, SR motor has some disadvantages which are listed below:

- SR motor needs a small air gap in order to optimize its output power density. This thing leads to increase the complexity in manufacturing SR motor and also becomes the source of inductance irregularity.
- Usually, in SR motor control, position encoder is used to estimate the rotor position but there are some situations where the encoder is not allowed (e.g. compressor), sensorless control is the best solution for such problems.
- Potential cost of SR motor drive was high but with the growth of electronic circuits, its cost is now gradually decreasing.
- The phase torque is the nonlinear function of rotor position and phase current and net torque which is equal to the sum of torques produced by all phases of the motor is usually not smooth. In order to make smoothness, complex control technique can be employed. Further, ripples are appeared in the generation of phase torque due to switching of phase current. A number of techniques have been developed in the literature in order to minimize the torque ripples [3-5].
- SR motor produces acoustic noise due to time varying phase current. Acoustic noise may be dangerous for the motor because it distorts the stator yoke with time. However, this problem can be reduced with good mechanical construction.

1.1.5 SR Motor Applications

SR motor can be used for the following purposes [2].

- General purpose industrial drive
- Application specific drive such as compressors, fans, centrifuge, and pumps etc.
- Domestic drives such as food processors, washing machine and vacuum cleaners etc.
- Electric vehicle application
- Aircraft actuators and generators. Actuators are used in defence application

- Servo drives and coolant pumps in nuclear power plant

1.2 Motivation

The thesis is aimed at design of model based controllers for power optimization of an SR motor. The mathematical model of an SR motor is highly nonlinear due to magnetic saturation effects therefore the speed/position control of this motor is important issue in industrial drive application. A number of techniques had been found in literature for speed/position control of SR motor. Each one has its own merits and demerits. Feedback linearization method was introduced in [6-9] etc. to address speed/position control problems for SR motor. However, the controller synthesis process was complex and also dependent on exact external load model. It also required complete knowledge about magnetization characteristics. The use of fuzzy logic technique was reported in [10-12] etc. for speed control problem of SR motor. However in this technique, the selection of appropriate set of rules was compulsory and the designer was required to have the knowledge about system behavior and fuzzy system so that required membership functions could be selected. Moreover, optimization of parameters in membership function was very complex. Sliding mode technique emerged from Soviet Union in 60s and attracted the attention of researchers due to its simple structure, robustness and easy implementation. Since motor control is intrinsically discrete in nature, use of sliding mode technique is ideal in electric machines because its switching control structure property is best suited for electronic power circuit. In [3, 5, 13-22], sliding mode technique had been reported on SR motor for various control issues. Along with these benefits, it had the drawback of chattering which is dangerous for electromechanical systems because it excites unmodelled dynamics that may cause unexpected problems and may cause instability. A number of techniques had been developed to avoid chattering. One of the techniques was the use of boundary layer in which the saturation function was introduced to approximate the sign function term in the sliding manifold (see, e.g., [23]). The significance of this technique was that the system trajectories were bounded to remain within the small vicinity of the sliding manifold but this caused steady state error. Another solution of chattering reduction was the use of dynamic sliding mode control [24] where the dynamic sliding surface was used to produce dynamic feedback. This method was restricted to a specific nonlinear system. One of

the possible solutions of chattering reduction was the use of higher order sliding mode (HOSM) control. Many authors applied this technique on various industrial drive applications. For example, HOSM control on DC Motor [25], induction motor [26-27], permanent magnet synchronous motor [28-29], stepper motor [30] had been found in literature for various engineering problems. The motivation of this thesis is to develop such control strategy to address speed/position problems of SR motor which should be almost chattering free and robust against parameter variation and unknown disturbances. In addition, the desired performance may be achieved in finite time.

1.3 Contribution of the Thesis

In this thesis a number of model-based sliding mode controllers are designed for power optimization and speed control of SR motors. The designed controllers are compared with PI controller for performance evaluation. A novel commutation scheme is designed for controller design because it is an essential and integral part of SR motor controls. The major individual contributions of this thesis are summarized as below.

- A novel commutation scheme for SR motor has been proposed. The proposed commutation scheme minimizes input power by exciting at the most two out of three phases of same polarity at any instant. Conversely, at least one, and at the most two phases of opposite polarity are kept off to avoid the negative contribution which causes power loss at the own expenses. Thus the motor is driven in a power efficient manner by this commutation scheme.
- A high performance second order sliding mode controller (SOSMC) for speed regulation/tracking problem of SR motor has been derived and simulated. A conventional first order sliding mode controller (FOSMC) has been developed for comparison. This technique has been applied first time for this motor application according to author's best knowledge based on extensive literature survey.
- A FOSMC for position regulation has been designed for SR motor and its robustness has been tested against parameter variations and unknown

disturbances; making it possible candidate for servo drive application. This technique has also been applied first time for position control of SR motor.

- A high performance SOSMC for position regulation problem for the same system has also been developed first time and its performance has been compared with FOSMC.

1.4 Organization of the Thesis

This thesis is organized as follows:

A mathematical model is described on the bases of physical laws in Chapter 2. It is taken from [31]. Next, a novel commutation scheme is presented for SR motor which, at any time instant, selects only those motor phases for the computation of control law, which can contribute torque of the desired polarity at that instant. This feature helps in achieving the desired speed/position regulation/tracking objective in a power efficient manner as control efforts are applied through selective phases and counterproductive phases are left un-energized. This approach also minimizes the power loss in the motor windings and thus reducing the heat generation within the motor. Using this proposed commutation scheme, a conventional PI controller is also designed and its performance is tested against parameter variation and unknown disturbances.

A first order sliding mode controller (FOSMC) is derived for SR motor and its convergence issues are also discussed Chapter 3. SR motor is highly nonlinear machine due to its nonlinear characteristics. Many nonlinear techniques were developed so far for the control of SR motor. Most of the techniques required a lot of knowledge about the dynamic system, such as phase resistance, inductance, flux linkage, inertia, coefficient of friction and external load. Moreover, the controller design and its implementation were very complex. A brief survey of these techniques on SR motor is presented in this chapter. Sliding mode technique has gained much popularity and has received considerable attention from control community due to its simple structure, inherent robustness and easy implementation. To understand this technique and how to design sliding mode controller, few examples are quoted. The designed FOSMC with proposed commutation scheme is simulated and compared with conventional SMC for speed regulation/tracking problem. FOSMC saves power

consumption and its performance is far better than conventional SMC. But sliding mode technique causes undesirable chattering. Higher order sliding mode is one of the solutions of chattering reduction.

Higher order sliding mode (HOSM) technique is introduced and its applications on different types of systems especially motors are elaborated in Chapter 4. HOSM is one of the solutions of chattering removal in addition of robustness and order reduction. Theory of HOSM control is given in detail along with design of super twisting algorithm which is one of the popular algorithms that does not require the time derivatives of sliding variable. An example from [32] is taken in order to demonstrate the performance of second order sliding mode controller (SOSMC) over FOSMC. In addition, important simulation results are given for comparison of conventional SMC, FOSMC and SOSMC over power loss, amount of voltage, and torques for speed/position regulation problem.

Chapter 5 deals with robustness, the important characteristic of the proposed controllers. The significant results are elaborated through simulation study. The performance of the proposed controllers SOSMC is tested and compared with FOSMC against parameter variation such as moment of inertia, coefficient of friction, resistance and external disturbances.

In Chapter 6, a brief review of the results of the previous chapters along with some general comments is given and proposed future work is also presented.

1.5 Conclusion

This chapter has briefly described the overall structure of thesis. SR motor and its various applications in real life have been discussed. Since due to its magnetic structure, SR motor is highly nonlinear, many nonlinear techniques have been developed for its control. The sliding mode technique was selected for controller design and analysis for speed control application in this thesis. Among these, sliding mode has received much attention from control community due to its simple structure, robustness and easy implementation but it was affected by chattering phenomenon which can be evaded by introducing HOSM control. This technique is also applied on speed control problem of SR motor. The same technique is also applied on position regulation problem; making it possible candidate for servo drive application.

Chapter 2

MATHEMATICAL MODEL AND PROPOSED COMMUTATION SCHEME FOR SR MOTOR

In order to study the dynamics of SR motor and to synthesize its controllers, a mathematical model of the system is required. In Section 2.1, model is described on the bases of physical laws. Next, the commutation scheme for SR motor is proposed in Section 2.2 and Section 2.3 discusses the design and performance of conventional PI controller against parameter variations and unknown disturbances for speed control problem. Section 2.4 concludes the chapter.

2.1 Model Description

For any controller design, the important step is to develop the reliable mathematical model that represents the system dynamics under various operating conditions. A lot of work has been done on modeling and design of SR motor. Several numbers of techniques have been found in literature for estimating the motor parameters. Finite element method (FEM) is one of the popular techniques used for mathematical modeling. It has the capability to grasp complicated geometries with relative ease. Ref. [33] has applied FEM on SR motor by incorporating its nonlinear model. Flux linkage was estimated for a particular current and rotor position. The estimated parameters were verified through simulation results at different operating conditions. Artificial neural network (ANN) has the quality of self learning and can approach the problem with any accuracy. Ref. [34] applied ANN on SR motor and proposed a model. The model consisted of further two submodels namely forward model and inverse model. Forward model was used to estimate flux linkage and torque as a function of current and rotor position whereas inverse model was used for current and flux linkage estimation depending upon torque and rotor position. The proposed model was independent of phase voltage and torque sensors and was shown to be more effective and accurate. However ANN has a drawback, the searching capability of global optimization solution and convergence rate is poor. Genetic algorithm (GA)

compensates these two deficiencies. Ref. [35] has combined both ANN and GA for SR motor modeling by exploiting the fast convergence of GA and computational accuracies of ANN. Their simulation results showed the improved convergence rate and accuracy of the proposed technique. Ref. [36] introduced new approach for developing dynamic model of SR motor. The approach was based on assumption that phase inductance profiles always have triangular shapes and its peak values depend upon phase current. It was concluded that the proposed model was very suitable for controller design.

Although the proposed controllers can be developed for any SR motor with arbitrary number of phases, for clarity of presentation and subsequent simulations, a specific 6/8, regular 3-phase commercial SR motor [31] is considered whose parameters are listed in Table-1.

Table 1: Parameters of SR Motor.

Parameter	Value
No. of Phases	3
No. of Stator Poles	6
No. of Rotor Poles	8
Inertia (J)	0.1 N.ms ²
Coefficient of Friction (B)	0.1 N.ms
Phase Resistance	4.7 Ω
DC Voltage Supply	250 V
Rated Speed	492 rad/sec
Rated Power	5 KW

The mathematical model of SR motor consists of electrical and mechanical dynamic subsystems which are described below.

2.1.1 Electrical Subsystem

Because of the concentrated nature of phase windings, the mutual inductance between various phases of SR motor is negligibly small. Thus the voltage applied to any one phase of the SR motor can be accurately described as

$$u_j(t) = R_j i_j(t) + \frac{d\lambda_j(\theta, i_j)}{dt} \quad j = 1, 2, 3 \quad (\text{Eq 2.1})$$

Where u_j , R_j , and i_j represent the input, resistance, and current in the j th phase. $\lambda_j(\theta, i_j)$ is the flux linkage in the j th phase which is a the nonlinear function of rotor position and phase current. For simplicity of notation, the explicit dependence of u_j and i_j on time 't' will be omitted in the remaining part of the thesis. The decoupling between motor phases leads to the following expression for the time derivative of phase flux linkage:

$$\frac{d\lambda_j(\theta, i_j)}{dt} = \frac{\partial \lambda_j(\theta, i_j)}{\partial \theta} \frac{d\theta}{dt} + \frac{\partial \lambda_j(\theta, i_j)}{\partial i_j} \frac{di_j}{dt} \quad (\text{Eq 2.2})$$

Substituting (Eq 2.2) in (Eq 2.1) gives:

$$u_j = R_j i_j + \frac{\partial \lambda_j(\theta, i_j)}{\partial \theta} \omega + \frac{\partial \lambda_j(\theta, i_j)}{\partial i_j} \frac{di_j}{dt} \quad (\text{Eq 2.3})$$

which can be re-written in the following form

$$\frac{di_j}{dt} = \left(\frac{\partial \lambda_j(\theta, i_j)}{\partial i_j} \right)^{-1} \left(u_j - R_j i_j - \omega \frac{\partial \lambda_j(\theta, i_j)}{\partial \theta} \right) \quad (\text{Eq 2.4})$$

Where $\frac{\partial \lambda_j(\theta, i_j)}{\partial i_j}$ represents the self-inductance of the phase and $\omega \frac{\partial \lambda_j(\theta, i_j)}{\partial \theta}$ is the back EMF produced in the j th phase.

Variables and parameters of electrical subsystem are summarized in Table 2.

Table 2: Model Summary of Electrical Subsystem.

Sr. No.	Variable/parameter	Description
1	u_j	Input voltage in j^{th} phase
2	R_j	Resistance in j^{th} phase
3	i_j	Current in j^{th} phase
4	λ_j	Flux linkage of j^{th} phase

5	θ	Rotor position
6	ω	Rotor speed
7	$\frac{\partial \lambda_j(\theta, i_j)}{\partial i_j}$	Self-inductance of the j^{th} phase
8	$\omega \frac{\partial \lambda_j(\theta, i_j)}{\partial \theta}$	Back EMF produced in the j^{th} phase.

2.1.2 Mechanical Subsystem

Mechanical subsystem can be expressed by the following relation.

$$\frac{d^2\theta}{dt^2} = \frac{1}{J} (T_e(\theta, i_j) - B\omega - T_L) \quad (\text{Eq 2.5})$$

where θ is the rotor angle and ω is the rotor speed. J and B are the moment of inertia and coefficient of friction, respectively. $T_e(\theta, i_j)$ is the total electromagnetic torque which is equal to the sum of individual torques produced by all motor phases. For simplicity, the explicit dependence of T_e on θ and i is being omitted in the remaining part of the report.

$$T_e = \sum_{j=1}^3 T_j(\theta, i_j) \quad (\text{Eq 2.6})$$

where $T_j(\theta, i_j)$ is the torque of the j^{th} phase.

$$T_j(\theta, i_j) = \frac{\partial W_c(\theta, i_j)}{\partial \theta} \quad (\text{Eq 2.7})$$

where W_c is co-energy.

$$W_c(\theta, i_j) = \int_0^{i_j} \lambda_j(\theta, i_j) di_j \quad (\text{Eq 2.8})$$

Now (Eq 2.7) takes the form as

$$T_j(\theta, i_j) = \frac{\partial}{\partial \theta} \int_0^{i_j} \lambda_j(\theta, i_j) di_j \quad (\text{Eq 2.9})$$

Variables and parameters of mechanical subsystem are summarized in Table 2.

Table 3: Model Summary of Mechanical Subsystem.

Sr. No.	Variable/parameter	Description
1	J	Moment of inertia
2	T_e	Total electromagnetic torque produced in the motor

3	B	Force of friction
4	T_L	Torque load
5	T_j	Torque of the j th phase
6	W_c	Co-energy

Now, the complete dynamic model of the SR motor can be expressed in the following state-space form:

$$\frac{d\theta}{dt} = \omega \quad (\text{Eq 2.10})$$

$$\frac{d\omega}{dt} = \frac{1}{J} (T_e(\theta, i_j) - B\omega - T_L) \quad (\text{Eq 2.11})$$

$$\frac{di_j}{dt} = \frac{\partial \lambda_j(\theta, i_j)^{-1}}{\partial i_j} (u_j(t) - R_j i_j(t) - \omega \frac{\partial \lambda_j(\theta, i_j)}{\partial \theta}) \quad (\text{Eq 2.12})$$

2.2 Commutation Scheme

As stated earlier, torque is produced in SR motor when rotor moves towards the excited phase. This sequential excitation of the phases rotates the motor which is performed through commutation scheme. Contrary to other motors, commutation in SR motor is achieved electronically instead of being operated from *AC* source or *DC* bus. To accomplish this power electronics are used to regulate the commutation of the motor's phases. The commutation scheme plays a vital role in SR motor control. The commutation scheme use position feedback either from position sensors [37-38] or from sensorless approach ([15], [39-40] etc.). The basic idea behind the commutation scheme is the selection of phase for excitation which depends upon the rotor position in order to optimize the motor performance. The detail of the commutation scheme is given in the next section.

2.2.1 Proposed Commutation Scheme

For finding proper control laws for SR motor control using FOSMC and SOSMC at each instant, in terms of phase voltages, the elements of control vector u will be

selected so as to engage only those phases which can contribute torque of the desired polarity. The selection of the appropriate motor phases at each instant depends upon the rotor position and the sign of the speed error at that instant. The commutation scheme which does this phase selection is now being explained.

Although the phase torque of SR motor is a complex non-linear function of rotor position and phase current as explained earlier, for ease in explaining the commutation scheme the researcher would refer to Figure 2.1 which shows the phase torques of a regular 3-phase SR motor at a specific value of phase currents, ignoring the effects of magnetic saturation and spatial harmonics. The figure shows the variation of phase torques as a function of rotor position within one electrical cycle. The complete electrical cycle is divided into 12 distinct regions *R1-R12* such that in each region, specific phase(s) can only produce positive torque whereas the remaining phase(s) can contribute only negative torque. For example, in region *R1*, positive torque is only produced via phase *B*, while phase *C* and phase *A* when energized provide only negative torques. Similarly in region *R3*, phases *B* and *C* provide positive torque while negative torque can only be produced by energizing phase *A*.

Thus if the rotor position lies in *R3* at a specific time instant and positive torque is required to reduce the speed error, only phases *B* and *C* should be used to compute the control laws. This would lead to achieving the desired net torque using lower voltage levels and with reduced copper losses in the motor windings. Had all the motor phases energized, not only that phase *A* would have generated counterproductive torque, other phases would had to produce higher than the required values of torques to cancel the opposing torque produced by phase *A*. This would have lead to applying higher phase voltages and an increase in copper losses too. On the other hand, if negative torque is required in this region to reduce the speed error, then only phase *A* should be energized. There is no need to energize phases *B* and *C* because they can only produce positive torques in this region, which would be counterproductive.

A similar approach is adapted in all these regions, which suggests that for a regular 3-phase SR motor, only one or at the most two phases can produce the desired polarity torque at any instant depending upon the current rotor position. Thus a judicious choice of the phases to be used in computing the control laws would result in saving net power leading to increased system efficiency.

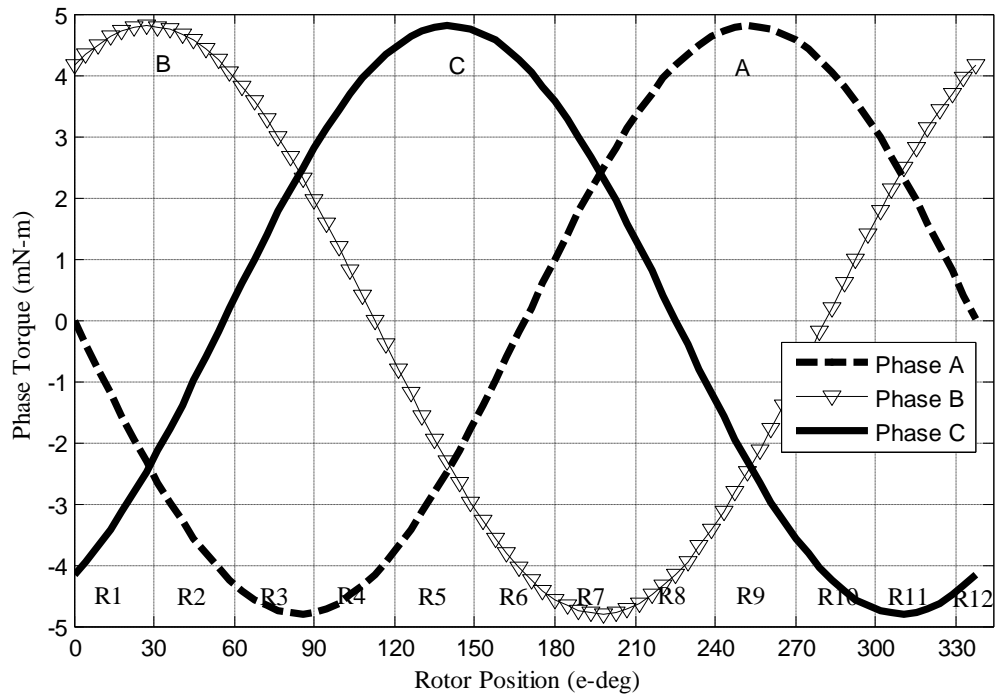
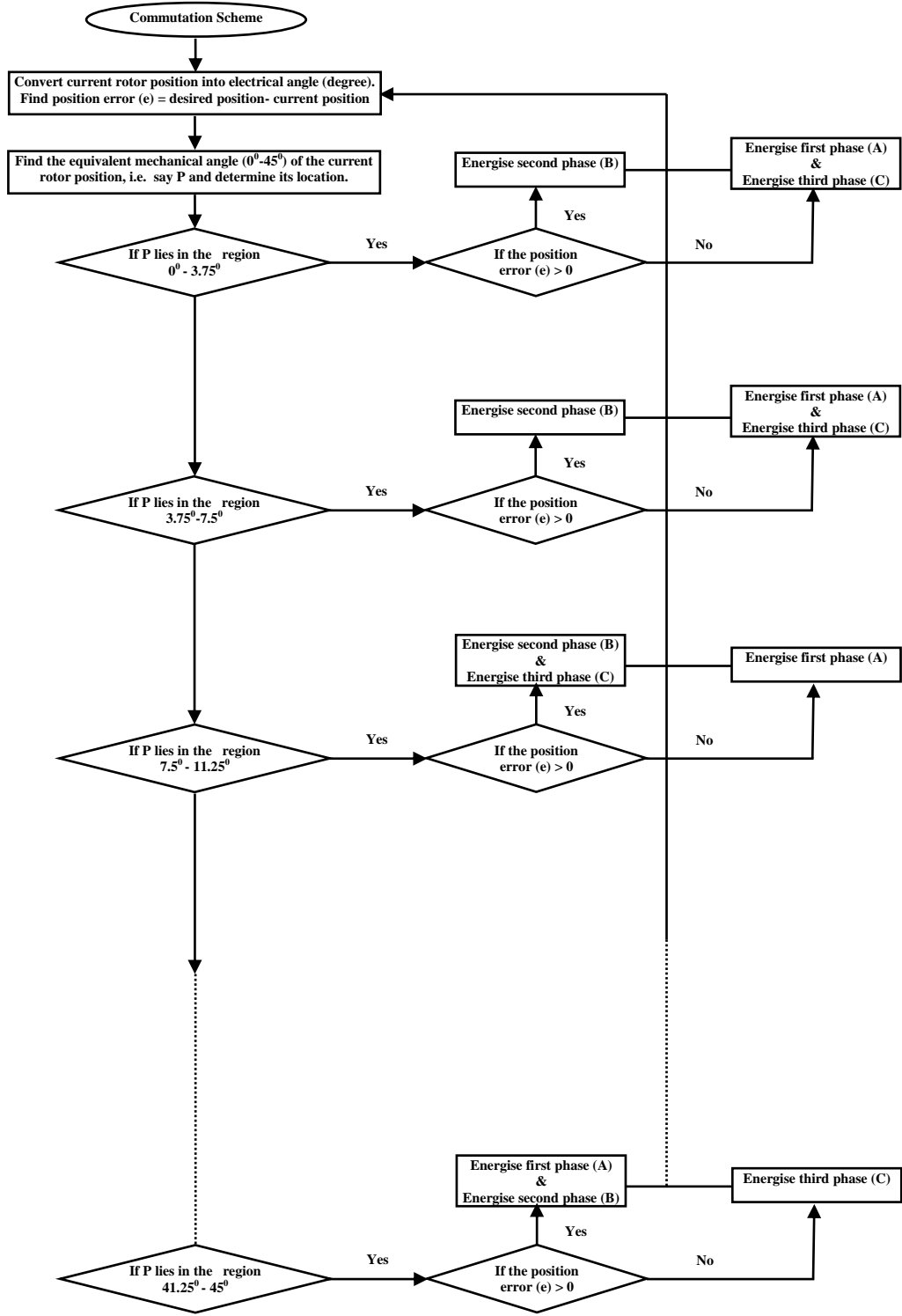


Figure 2.1: Division of one electrical cycle into 12 distinct region for commutation purposes.

To understand the above commutation scheme clearly, a flow chart is given on the next page.



To have some idea about the commutation scheme, see the Figure 2.2; for instance, position control application. Using conventional scheme (a), error is to be estimated from the estimated position and the desired position, and this error is then propagated to controller for further process. Once the error is estimated, the controller determines how much torque is required to compensate the error and then, on the bases of the desired compensating torque, required input voltages are estimated. For this particular 6/8 3-phase regular SR motor, the input values u_a , u_b , u_c are estimated by the controller and then, are applied to motor phases.

In the proposed design (b), the scheme takes present position to determine in which region the rotor of the motor lies. The scheme also takes position error to determine which polarity of the torque whether positive or negative torque is required. On the bases of this information, the scheme gives the correct phases that should be energized. Therefore, the contributing phases out of the phases given by the controller are to be selected. The selected phases may be at most two as it is the design of proposed commutation scheme. The output of commutation is applied to motor phases.

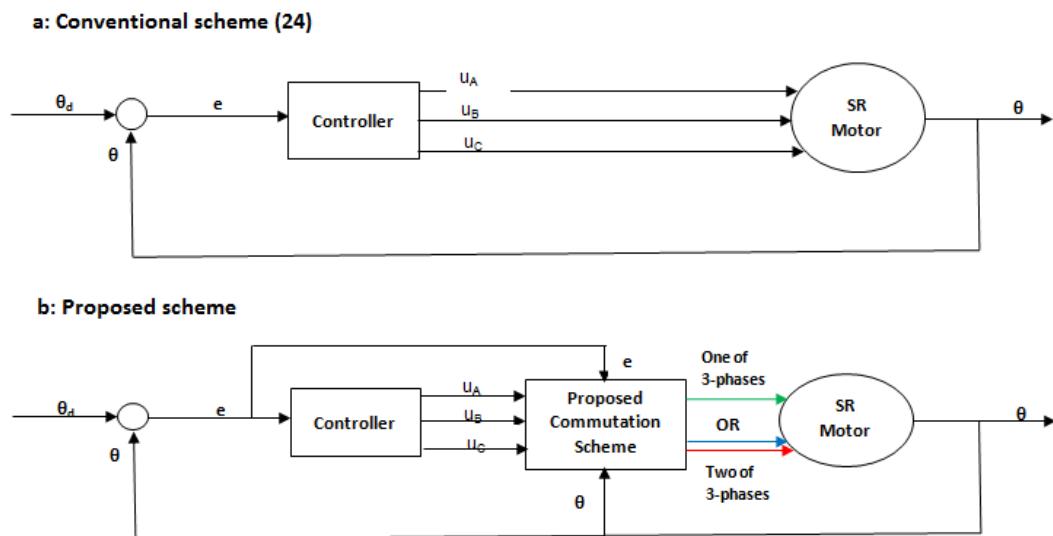


Figure 2.2: Block diagram of commutation schemes.

To apply conventional control on SR motor model represented by (Eq 2.10) - (Eq 2.12) using proposed commutation scheme described in Section 2.2, PI controller for speed regulation/tracking problem is designed and its performance is discussed in the following section.

2.3 PI Controller for speed control application

PI controllers are widely used in industries due to their design simplicity and low cost. Moreover, their implementation in analogue or digital hardware is simple and easy. Under limited operating conditions, they perform well and also their steady state performance is good. The PI controller for SR motor can be expressed as

$$u = K_p e(t) + K_i \int e(t) dt \quad (\text{Eq 2.13})$$

Where K_p and K_i are the proportional and integral gain constants. Since the motor is highly nonlinear and state variables are coupled, so it is not easy to predict the system dynamics with the help of mathematical solution. Therefore classical pole placement method is not applicable for designing PI controller. For a certain operating point, the gains K_p and K_i are tuned using trial and error method. Online tuning would require a lot of computational resources and real time response could still be in question

Speed Response of PI Controller to a Step Command

Figure 2.3 shows the speed response when motor is commanded to accelerate from zero to 10 rad/sec and its error plot is shown in Figure 2.4.

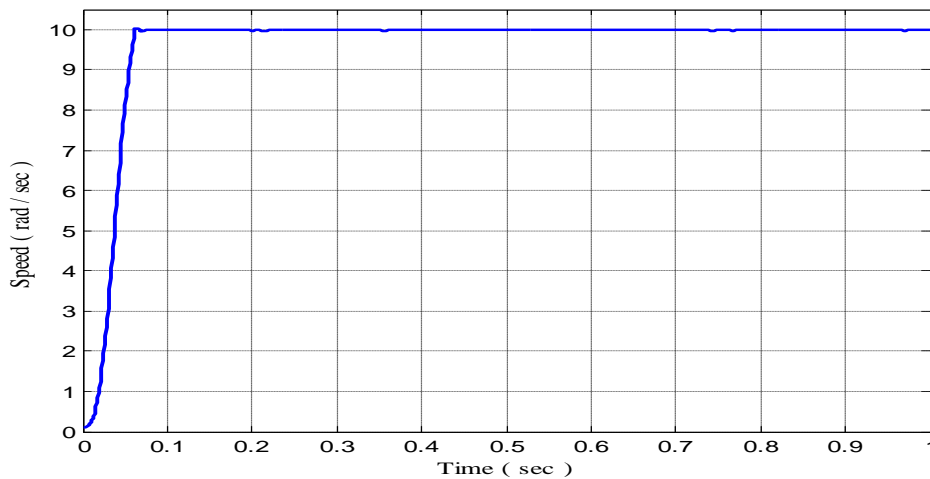


Figure 2.3: Speed response of PI for a step command.

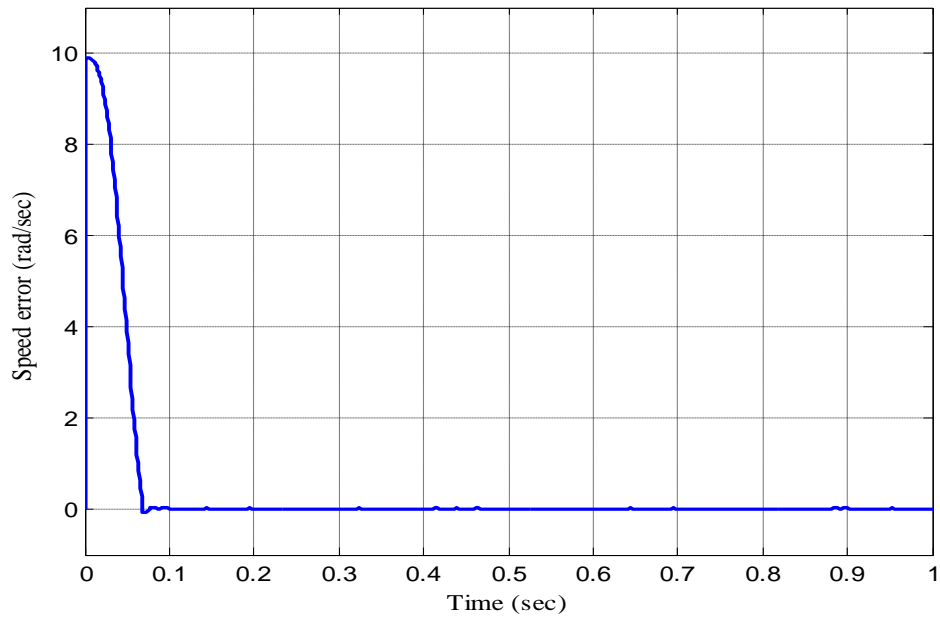


Figure 2.4: Error plots of speed response of PI for a step command.

It can be noted that the designed controller shows an initial overshoot which is reasonable and then tracks the motor speed closely to the desired speed. It is also important to see that conventional PI controller exhibits speed ripples in the range - 0.2% to 0.05% as it is reflected from Figure 2.5.

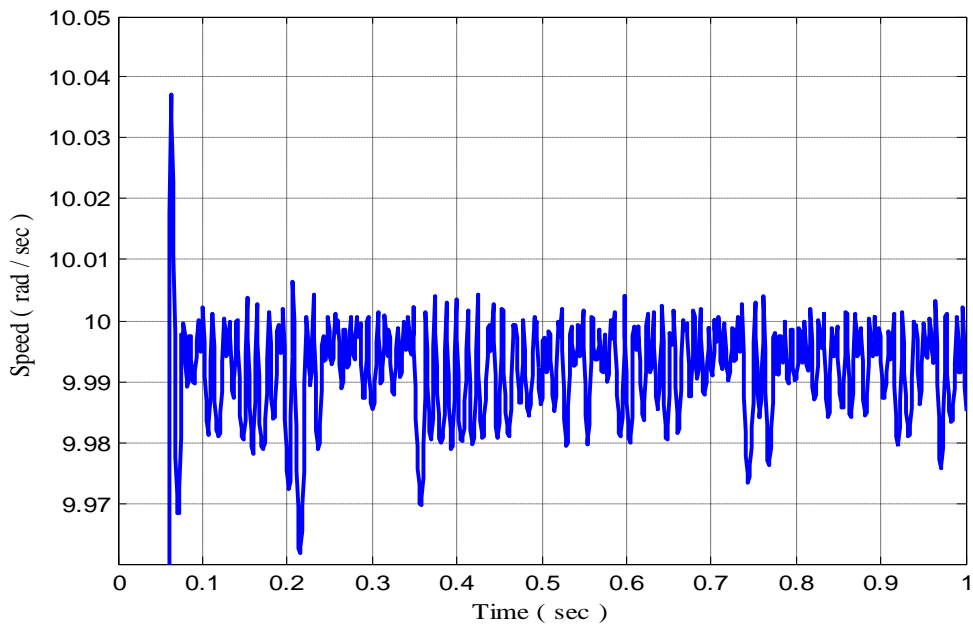


Figure 2.5: A close up view of speed response of PI controller for a step command. The high magnitudes of speed ripples are clearly noticeable.

2.3.1 Controller Effort

Controller effort is given in Figure 2.6. Due to the proposed commutation scheme, at the most two phases are energized at any instant to produce the desired net torque instead of energizing all the motor phases thus reducing heat generation within the motor. This is very much clear in Figure 2.7 and Figure 2.8.

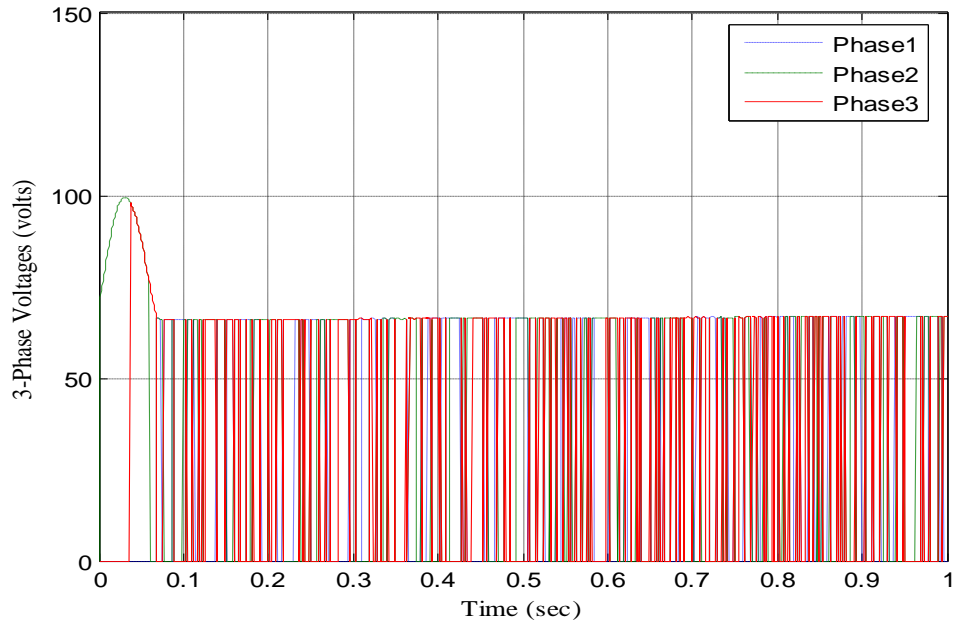


Figure 2.6: Controller effort during the simulated period for a simulation run of 1.0 second.

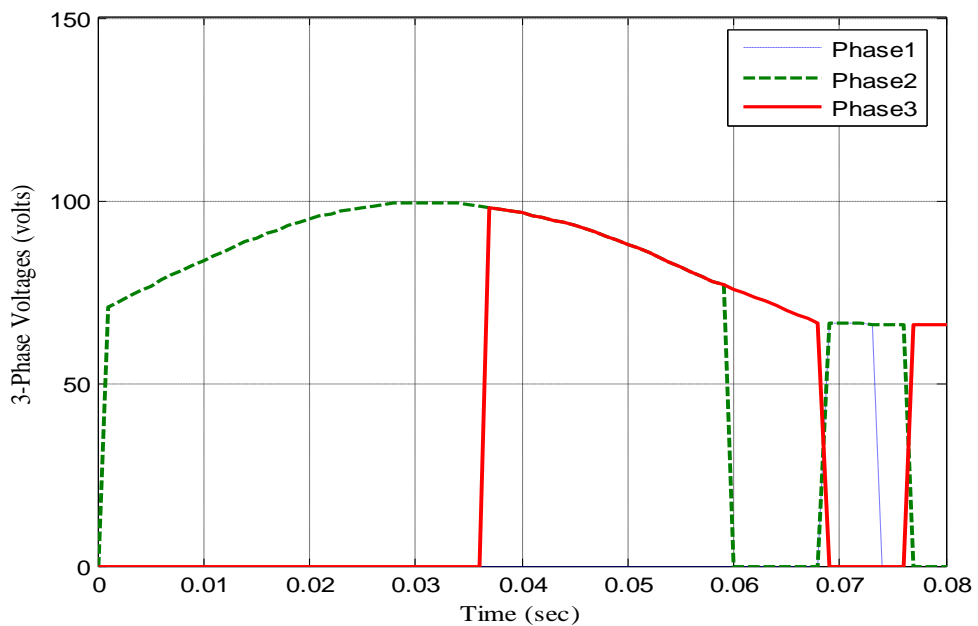


Figure 2.7: Controller effort in transient state when commutation scheme was used.

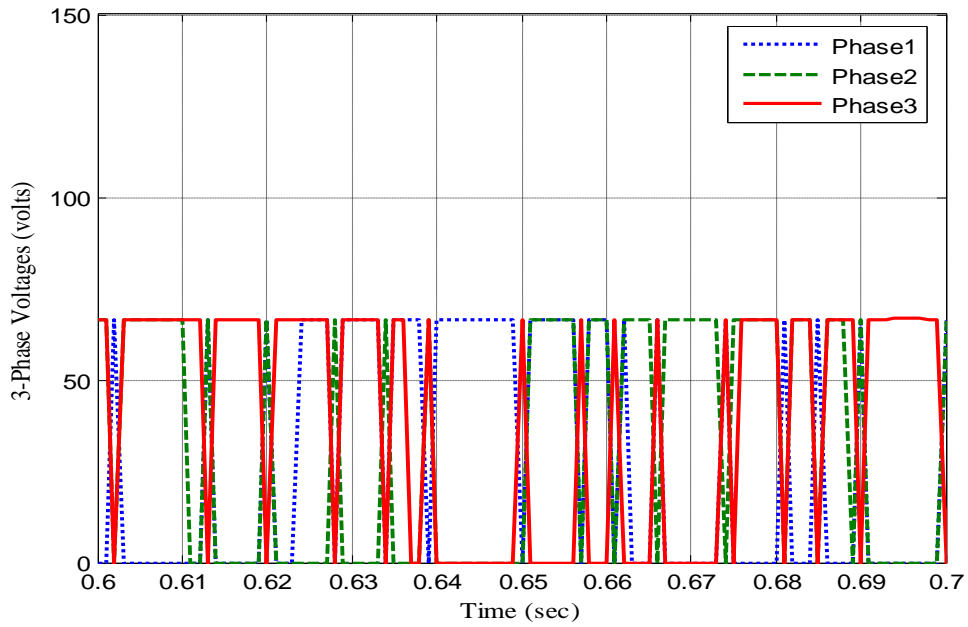


Figure 2.8: Controller effort in initial stage of steady state when commutation scheme was used.

2.3.2 Speed Response of PI Controller to a Sinusoidal Signal

Figure 2.9 illustrates the tracking response when the designed controller is following the sinusoidal trajectory. Figure 2.10 represents its respective error plot. It can be visualized that the tracking performance of PI controller is acceptable as the tracking error is low i.e. -1.5% to 2%.

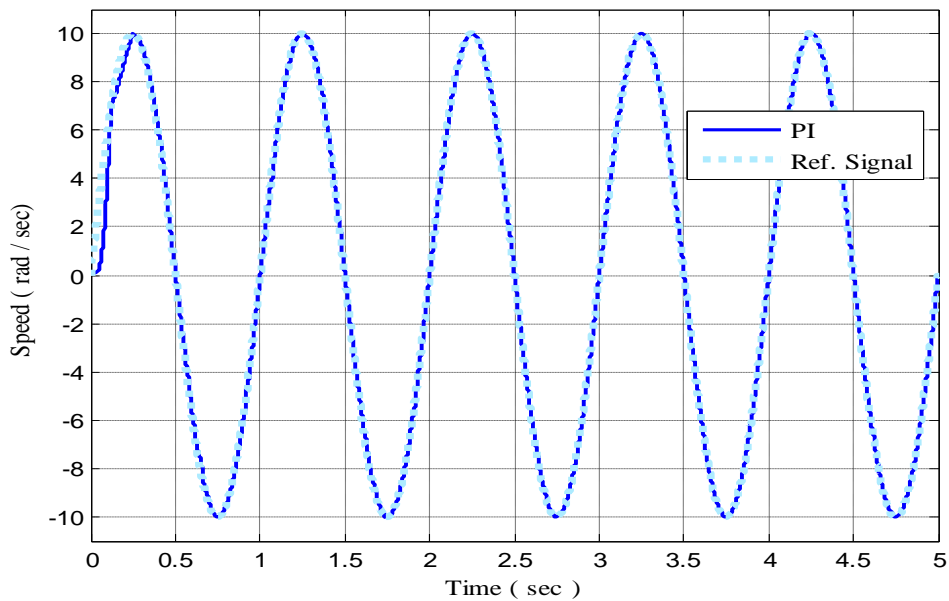


Figure 2.9: Speed response of PI controller against the sinusoidal signal..

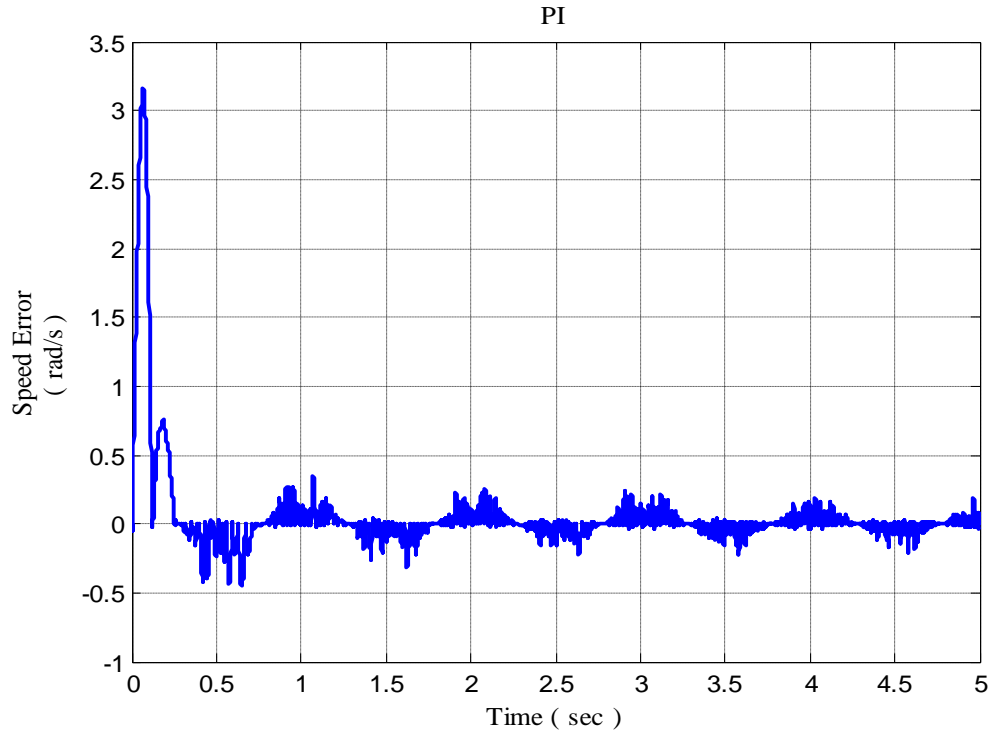


Figure 2.10: Speed error response of PI controller for sinusoidal signal.

2.3.3 Robustness Comparison

Robustness of the conventional PI controller against parameter variations and external load disturbances are depicted in Figures 2.11-2.18.

2.3.4.1 Variation in load torque

Figure 2.11 shows the speed response when SR motor is directed to follow the reference with sudden change in torque load. Initially the external torque load was zero and then suddenly a torque load of 4 N-m is applied at $t = 0.4$ second which results in a slightly larger ripples in motor speed. Finally the external torque load is withdrawn at $t = 0.5$ second and speed ripples decrease slightly. It is clear from Figure 2.12 that the maximum speed ripple using PI controller is 7% with a slight drop in speed response in transient state.

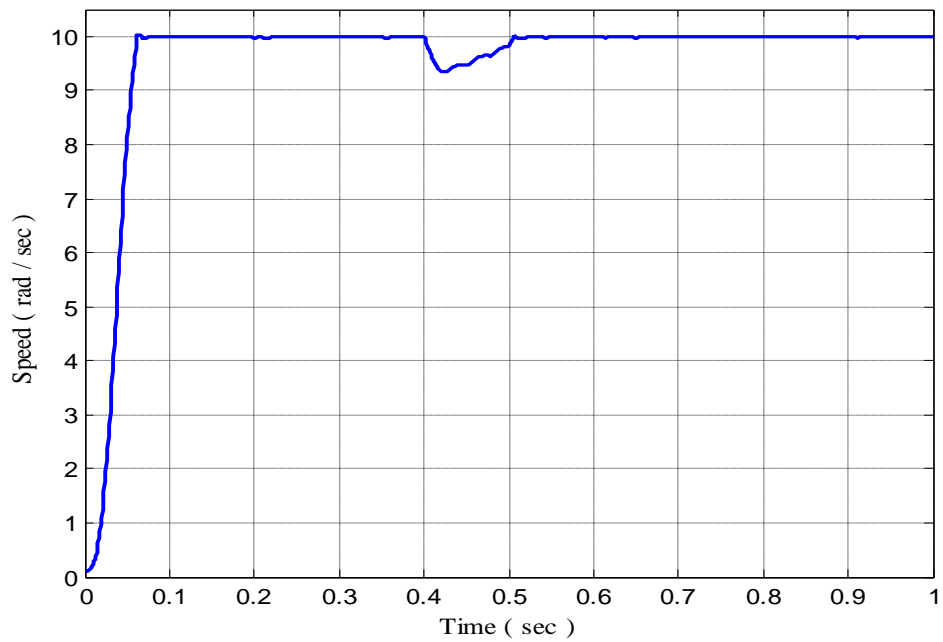


Figure 2.11: Speed response with torque load.

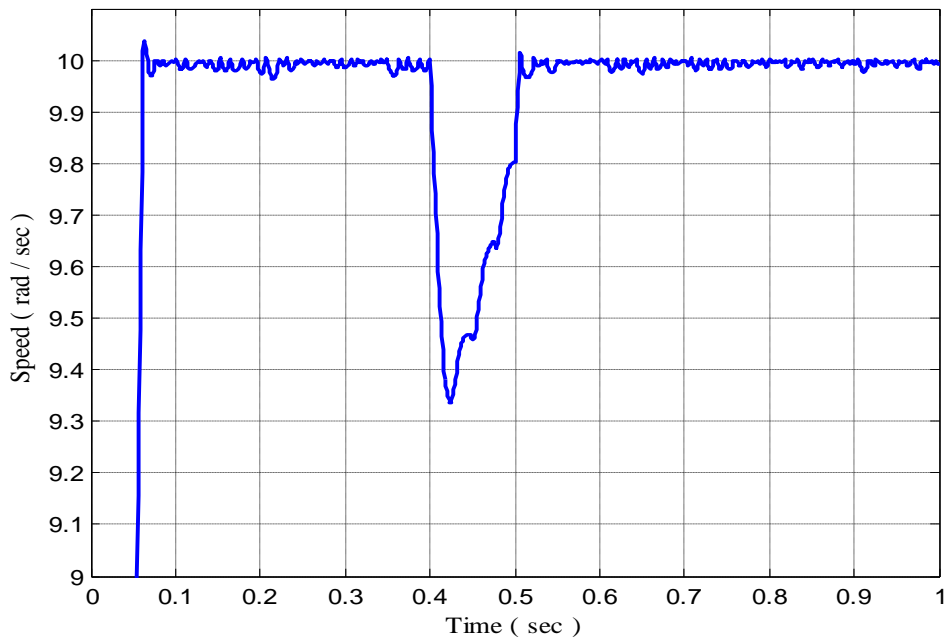


Figure 2.12: A close up view of speed response against sudden change in torque load.

2.3.4.2 Variation in moment of inertia, coefficient of friction and phase resistance

Figures 2.13-2.18 show the motor responses when system parameters moment of inertia/coefficient of friction/resistance is decreased by 50% and then increased by 100% of its original value.

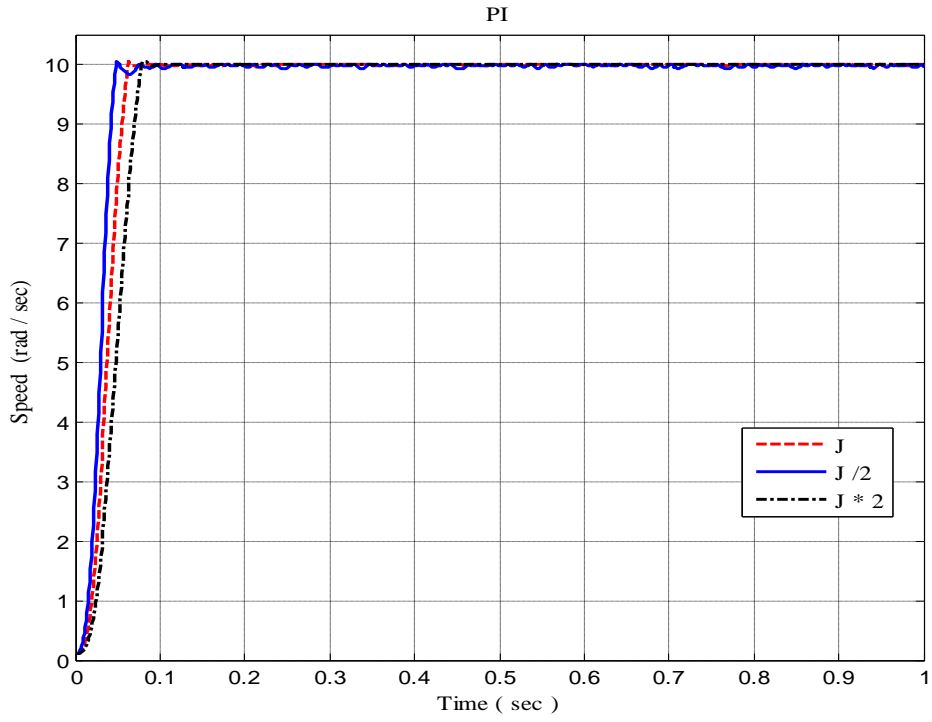


Figure 2.13: Speed response with variations in moment of inertia J .

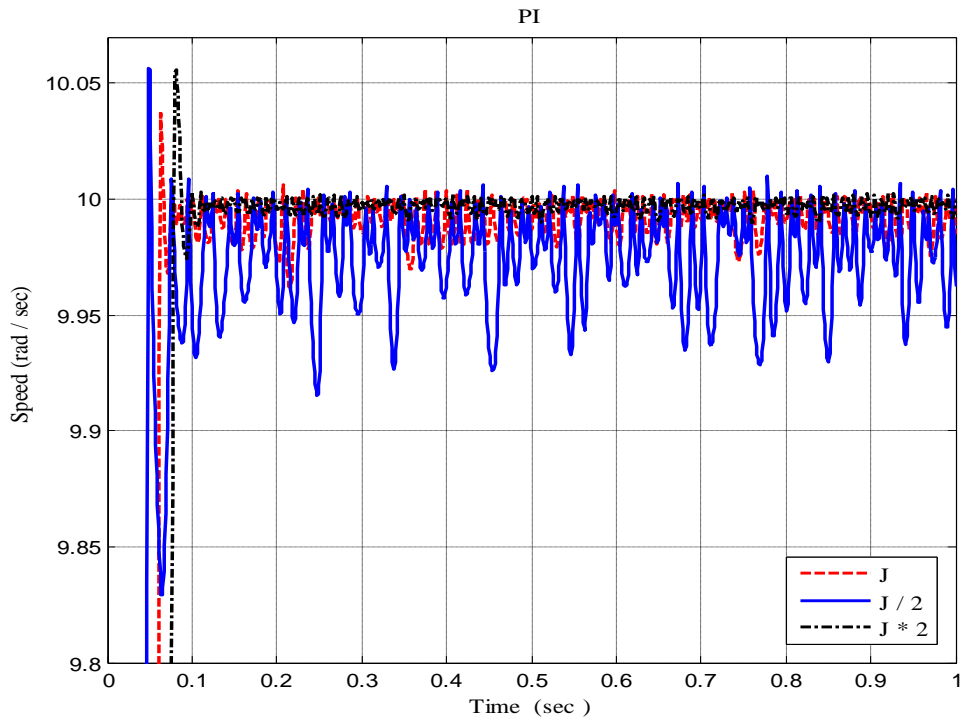


Figure 2.14: A close up view of speed response with changes in J .

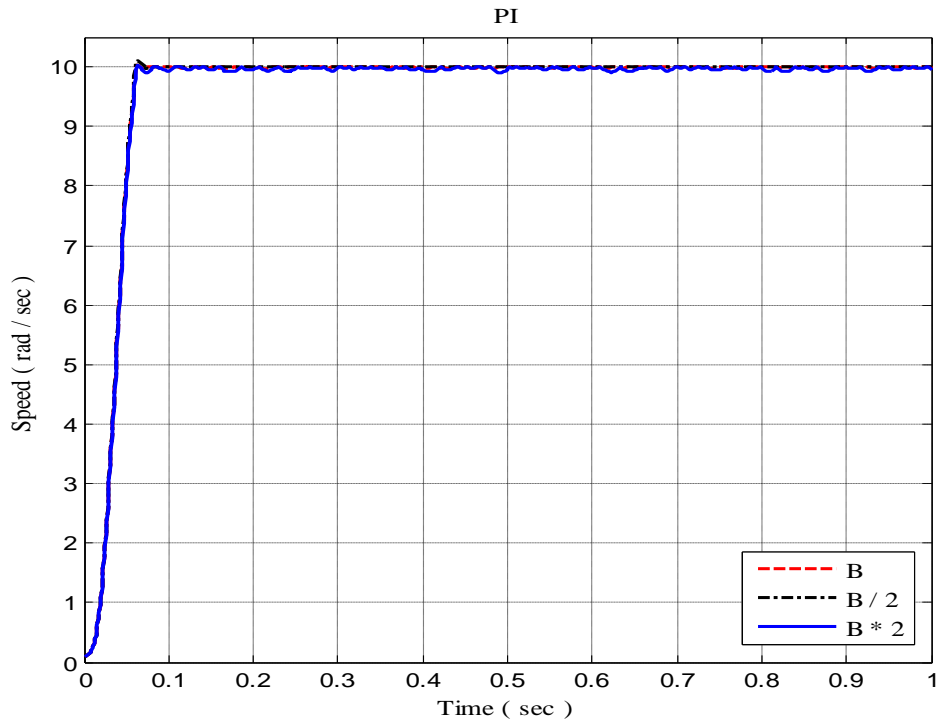


Figure 2.15: Speed response with variations in coefficient of friction B .

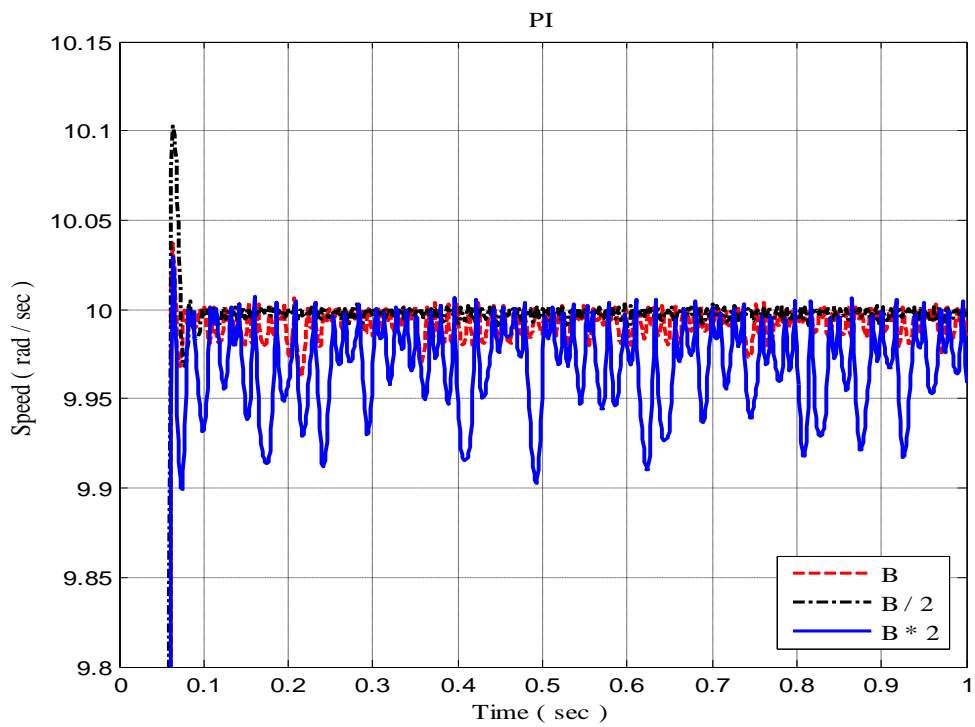


Figure 2.16: A close up view of speed response with changes in B .

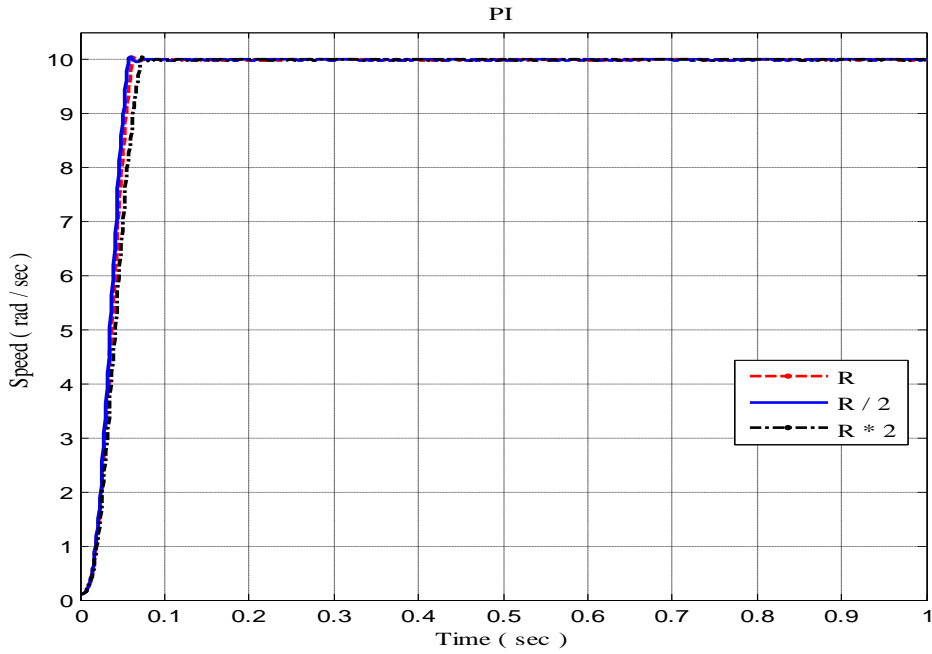


Figure 2.17: Speed response with variations in resistance R .

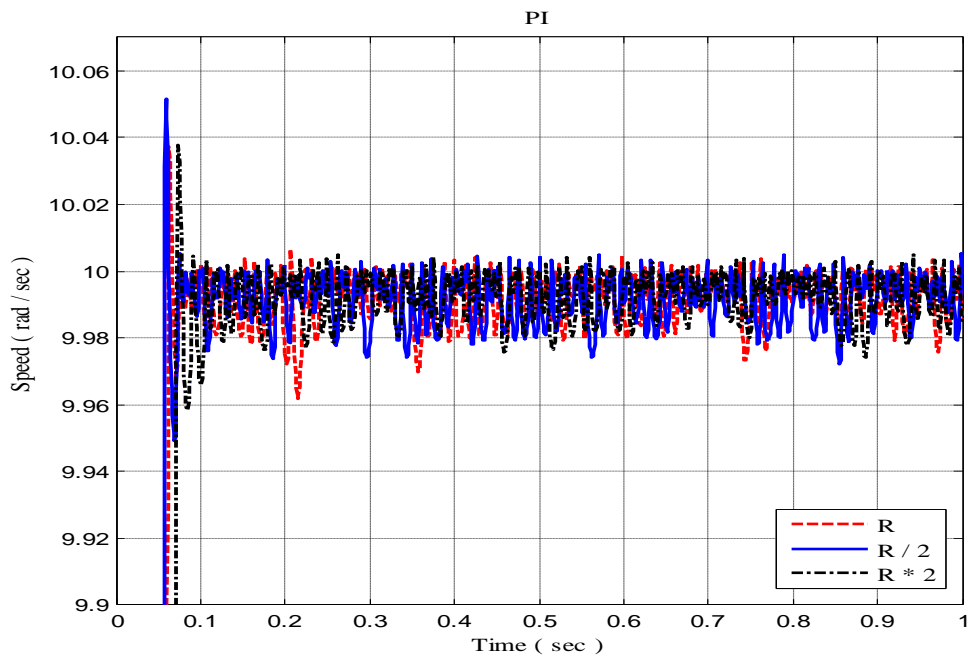


Figure 2.18: A close up view of speed response with changes in R .

It can be seen that conventional PI controller exhibits poor dynamic response. Overshoot and speed ripples are quite significant.

From the above discussion, it can be concluded that PI controller perform well in speed regulation/tracking problem and provide sufficient robustness but this

performance is operating point dependent. When operating point is changed, its performance starts deteriorating. Therefore, there is a need of high performance controller which compensates these problems and requires minimum amount of computations, and provides stability and enough robustness against parameter variations and unknown disturbance.

2.4 Conclusion

After describing the mathematical model of SR motor, a novel commutation scheme was presented for SR motor which, at any time instant, selects only those motor phases for the computation of control law, which can contribute torque of the desired polarity at that instant. This feature helps in achieving the desired speed/position regulation/tracking objective in a power efficient manner as control efforts are applied through selective phases and counterproductive phases are left un-energized. This approach also minimizes the power loss in the motor windings and thus reducing the heat generation within the motor. Using this proposed commutation scheme, a conventional PI controller was designed and its performance was tested against parameter perturbation and unknown disturbances.

Chapter 3

FIRST ORDER SLIDING MODE CONTROL

This chapter provides an overview of basic theory of sliding mode control (SMC) and its design technique. In Section 3.1, some existing techniques about the control of SR motor are discussed. The use of sliding mode on SR motor control is given in Section 3.2. To understand SMC and its use in control applications, few examples are quoted in Section 3.3, Section 3.4 addresses the first order sliding mode controller design (FOSMC) for SR motor and issues of its convergence in detail. Section 3.5 provides the important simulation results for comparison of SMC and designed FOSMC for speed regulation/tracking problems, and some drawbacks of the above mentioned controllers are also discussed in this section. Finally the Section 3.7 highlights the main points of this chapter.

3.1 Existing Techniques for the Control of SR Motor

SR motors are usually operated in magnetic saturation to increase its output torque. Magnetic saturation and mechanical saliencies in SR motors make phase torque a highly non-linear function of phase current and rotor position. Due to advancements in control theory, many nonlinear control techniques such as artificial neural network, feedback linearization, sliding mode, back stepping, fuzzy logic, etc. have been explored in the literature for the control of SR motors. Ref. [41] used finite element method for obtaining dynamic model of SR motor by incorporating flux current rotor position and torque current rotor position values. The model was then used for the development of self tuning fuzzy PI controller with artificial neural network for speed regulation purpose. The designed controller was further tested with other controllers under load and no load conditions. The simulation results presented in their work showed improved performance as compared to fuzzy PI controllers. Ref. [42] used the idea of feedback linearization and proposed speed controller of SR motor using multi phase excitation scheme. The scheme was claimed to be helpful for the reduction of torque ripple and the production of high power. The proposed controller was then compared with conventional PI controller and shown to be robust in presence of

uncertainties and unknown disturbances. Ref. [7] proposed a method using the same technique for controlling speed and torque of SR motor. In their method, a modified state space model was incorporated and generated torque was transformed into transfer function having order one. The main advantage of using this technique was that, the controller could be automatically synthesized and system behaviour remained linear in the working region but for its implementation, a powerful digital processor was required.

Ref. [43] used backstepping approach and developed speed controller for SR motor. Using this approach, feedback control law and Lyapunov based design are considered in controller design. The proposed controller took inputs in the form of rotor position, rotor speed, phase currents and reference speed to estimate the required phase current to keep the motor speed near to the reference speed. The simulation results showed that the proposed controller was better than PI controller in providing fast dynamic response. Ref. [4] developed an adaptive intelligent control based on Lyapunov functions. The proposed technique comprised of two components; the first one approximated the load-torque, error in the moment of inertia and the coefficient of friction, the second component drove the system output to track the desired value. The speed controller did not require exact motor parameters and was shown to be robust against disturbances and uncertainties. Neural network torque estimator was used as a second controller in the proposed technique for torque ripple reduction. A nonlinear robust controller was developed in [44] for speed regulation problem. A model with mutual coupling effects of the phases and their contributions in electromagnetic torque was used. The simulation results indicated that the proposed controller was more robust than PI controller and capable of torque ripples reduction. Ref. [45] presented and implemented the control scheme for four quadrant SR motor. The scheme utilized separate PI controller for phase current, phase torque and speed of the motor. The instantaneous torque was calculated from the look up table on the basis of rotor position and phase current. The results showed that the proposed scheme behaved well under certain operating conditions. Ref. [46] worked on sensorless control of SR motor and developed speed controller based on Lyapunov function. Shaft position and speed were obtained by estimating inductance of the motor. The proposed scheme was then implemented using 32-bit microprocessor and was shown to be robust to unknown disturbances and parameter variations.

Ref. [10] proposed fuzzy logic speed controller for SR motor to improve its dynamic response and robustness. Using this scheme, the need of having exact motor model was not compulsory. In [11], fuzzy logic based control scheme was also reported for speed regulation problem of SR motor by utilizing Gaussian membership function as input and triangular membership function as output . The scheme was employed using DSP board TMS320F281 and was tested under different working conditions. It was shown that the proposed controller was more robust than conventional controllers. Ref. [12] developed fuzzy controllers for SR motor in order to overcome the deficiencies of conventional PID controller in the form of robustness based on small signal model. First controller so called fuzzy compound controller contained the features of both PID and fuzzy control while the other one used fuzzy techniques to tune the controller parameters dynamically. However in this method, the selection of appropriate set of rules is compulsory. For this the designer must have the knowledge about system behavior and fuzzy system so that required membership functions can be selected. In addition, optimization of parameters in membership function is more complex.

Ref. [47] introduced artificial neural network approach with supervised learning for speed control of SR motor. The technique was based on back propagation algorithm in which error and its derivative was taken as input and reference current used as output. After comparing with PI controller, the designed controller showed good dynamic response. In [48], intelligent speed controller was suggested based on emotional learning for SR motor. It did not require the exact model and showed suitable behavior for nonlinear system. They also developed position estimator based on Adaptive Neuro Fuzzy Inference System by taking flux linkage as an input. The proposed scheme was compared with fuzzy logic control at different load conditions and speed, and shown to be superior.

Among the various techniques of SR motor control, only a few of them were about position control problem. Ref. [49] proposed PID controller for position control application. Their work primarily focused on the theoretical concepts about motor shaft position but it did not compensate the large position error near the alignment poles. Ref. [50] introduced partial state feedback technique for position tracking problem of SR motor using rotor position and phase current estimated from nonlinear

observer. The motor was then operated to drive a robotic load. Convergence was confirmed using Lyapunov approach. However the proposed technique requires the complete knowledge of the dynamic system. Ref. [51] suggested a scheme for motion control problem of SR motor for high performance servo drive applications. The key parameter of motor drive system is switching angle which was selected using predetermined look up table. The scheme was implemented using TMS320F2812 DSP card. However controllers required fine tuning as some delay and ripples were observed. Ref. [52] developed a position controller for linear SR motor for high performance application in automation process. They claimed that the proposed controller was robust and performed well in a hostile environment. Ref. [53] did the same work using dSPACE platform. The real time code was generated for PD controller and its parameters were tuned online. It was shown that the scheme was effective and promising as the position error was no more than 0.04 mm. However their work did not account for magnetic saturation which is the important feature of SR motor.

Ref. [54] studied motion control problem of SR motor by exploiting average torque control technique. PI controller for speed and PD controller for position were designed. Controllers' parameters were on line adjusted in accordance with rotor speed and load torque. Good dynamic response and accurate position tracking within the limited range were reported. But these conventional controllers cannot be used for large operational range. Ref. [55] used genetic algorithm to adjust the parameters of PI controller used for speed control of SR motor. The proposed scheme was adaptive and it was demonstrated by simulation results that the proposed genetic PI controller gave excellent performance for all speed range than conventional PI controller. Ref. [56] proposed new scheme based on intelligent control algorithm for motion control problem of SR motor. A neurofuzzy model was taken into account for the design of controller whose parameters were tuned permanently by Emotional Learning Algorithm. Under this scheme, control effort was considerably reduced as indicated by simulation results.

In [9], position control problem using adaptive feedback linearization approach was discussed for three phase SR motor based on parameterized model. Robustness against parameter variations like phase resistance, moment of inertia and external load

was realized using adaptive control. Unfortunately controller parameters updating hold only provided that magnetic saturation would not be taken into account. Ref. [8] derived the nonlinear model of SR motor with all nonlinearities on the basis of differential geometric theories and developed feedback controller for direct drive application. However, the controller synthesis process was complex and also dependent on exact external load model.

Most of the discussed techniques require a lot of knowledge about the dynamic system, such as phase resistance, inductance, flux linkage, inertia, coefficient of friction and external load. Moreover, the controller design and its implementation both are very complex. In a last couple of decades sliding mode technique has gained much popularity and has received considerable attention from control community due to its simple structure, inherent robustness and capability to control nonlinear systems [57]. Since it is nonlinear technique, it works equally well in both linear and nonlinear systems. The structure of the controller is changed in response to the changing variables of the system for achieving optimal control performance in variable structure system [58]. This notion is realized by using high speed switching control law which forces a trajectory of a system to move into a sliding manifold and to stay in that manifold thereafter. The regime of a system in a sliding manifold is called Sliding Mode. In the following section, a brief survey of recent use of sliding mode control for SR Motor is presented.

3.2 Sliding Mode Technique for the Control of SR Motor

First Order Sliding Mode Control (FOSMC) has been successfully applied in control application of SR Motor due to its intrinsic robustness in dealing with nonlinearities and easy implementation. Ref. [13] and Ref. [59-60] have used sliding-mode control for SR motor to control speed but their work did not account for magnetic saturation. Ref. [14] and Ref. [42] took magnetic saturation of the motor into account and developed sliding mode controller for speed regulation problem used in servo applications. The proposed scheme employed only one voltage regulator for all phases making it low cost and then it was implemented on TMS320C50 Processor. After comparing with PI controller, the proposed scheme showed robustness against parameter variations and unknown disturbances. The performance comparison of sliding mode control with PI control for SR motor was also reported in [17]. The

simulation results reflected that the proposed controller was superior to PI controller. Ref. [16] have developed torque controller based on sliding mode technique for SR motor. A switching control voltage was also employed in order to ensure that the torque error lied within the specified bounds. The torque ripples up to the certain limit were minimized by the proposed scheme and was shown to be robust against model inaccuracies and disturbances.

Sliding mode technique had been used to minimize torque ripples and noise in SR motor e.g., [18]. Ref. [5] used a new approach for torque ripples minimization by controlling the sum of square of the phase currents. The approach uses only two current sensors and is independent of digital calculation and exact rotor position. The dynamic model with mutual inductances was derived and sliding mode controller was designed. The controller was capable of removing low frequency oscillations. The proposed controller was then used for speed regulation problem and was shown to be more effective and robust than PI and fuzzy controllers. In [3], a method based on sliding mode control was presented to eliminate the effect of radial and tangential forces which were the sources of noise in SR motor by taking voltage as a control variable. Using this method, the desired smooth torque for each phase was calculated depending upon the selection of sliding surface. The method was simulated and implemented on DSPACE platform and showed good dynamic response. Ref. [21] considered the effect of mutual inductances and magnetic saturation in SR motor and developed its mathematical model which was then used for the design of controllers based on sliding mode technique and feedback linearization. Convergence of speed and phase current was ensured. It was also shown from simulation results that both the controllers were robust to system parameter and load torque variations; speed ripples were reduced to some extent. In [61], a scheme based on sliding mode was incorporated for speed control of SR motor. The rotor position/speed was estimated using wavelet neural network and the estimated values were given to PI controller for finding the desired torque. The torque inverse model which was trained using fuzzy neural network determined the desired phase current for the given desired torque. The current controller based on sliding mode was used to regulate the current. The simulation results showed that, using the proposed scheme, the robustness was improved in addition of torque ripple reduction.

A sliding mode observer based controller was reported in [15] for SR motor. The rotor position was estimated using terminal voltage and current, incorporated for electronic commutation. The estimated states were given to the controller for speed regulation problem. The proposed controller was shown to be robust without requiring any position sensors.

In [62], a robust scheme was suggested for speed control problem of SR motor having any number of phases. The scheme utilized only one current sensor and two sliding mode controllers; one for input power and other for speed regulation and then it was implemented by using 8-bit processor. The simulation results showed good performance of the proposed scheme against nonlinearities of the system and load disturbances. Ref. [20] presented sensorless control scheme based on sliding mode algorithm for SR motor where the implementation problems along with their solutions were addressed. The position was estimated using 2nd order sliding mode observer and estimated value was given to the controller for speed control problem for the entire range. The scheme was shown to be effective and practically applicable at low speed and zero speed.

A comprehensive study of sliding mode, PID and fuzzy logic controllers for SR motor was also reported in [19] for speed regulation problem. Performance was measured in term of speed ripple, overshoot, starting and speed reversal time and torque load capability at different operating points. The simulation results indicated that the performance of sliding mode controller was better than PID and fuzzy logic controllers. A new commutation scheme for SR motor was suggested in [22]. They developed controller based on sliding mode technique for speed regulation and tracking problem. The proposed controller selects only those motor phases which can contribute torque of the desired polarity. In this way the power loss could be reduced considerably as proved by the simulation results.

3.3 Sliding mode control examples

In this section few examples of sliding mode technique will be addressed. First example gives important theoretical concepts about this technique and its design procedure. Second example is for using this technique for stabilizing nonlinear system. Third example is about speed tracking of DC motor.

3.3.1 Example 1

Consider a second order nonlinear system given below

$$\begin{aligned}\dot{x}_1 &= x_2 \\ \dot{x}_2 &= f(x, t) + g(x, t)u\end{aligned}\tag{Eq 3.1}$$

Where

$f(x, t)$ and $g(x, t)$ are nonlinear functions which can be continuous or discontinuous.

and $g(x, t) > 0$

During the reaching phase, it can be observed that x_1 is stable if

$$\dot{x}_1 = -bx_1 \quad , b > 0\tag{Eq 3.2}$$

Taking sliding surface as

$$S = x_2 + bx_1\tag{Eq 3.3}$$

$$\Rightarrow x_2 = -bx_1 + S\tag{Eq 3.4}$$

Above equation is stable only when $S = 0$

Sliding phase dynamics are elaborated by taking time derivative of S

$$\dot{S} = \dot{x}_2 + b\dot{x}_1\tag{Eq 3.5}$$

$$\dot{S} = f(x, t) + g(x, t)u + bx_2\tag{Eq 3.6}$$

3.3.1.1 Convergence analysis

The convergence is analyzed by using the Lyapunov candidate function as

$$V = \frac{1}{2}S^2\tag{Eq 3.7}$$

Taking the time derivative of Lyapunov function following is obtained.

$$\dot{V} = \dot{S}S\tag{Eq 3.8}$$

$$\dot{V} = S(f(x, t) + g(x, t)u + bx_2)\tag{Eq 3.9}$$

A negative definite Lyapunov function derivative guarantees the stability/convergence of states to sliding surface.

\dot{V} is negative definite if

$$f(x,t) + g(x,t)u + bx_2 \begin{cases} < 0 & \text{for } S > 0 \\ = 0 & \text{for } S = 0 \\ > 0 & \text{for } S < 0 \end{cases} \quad (\text{Eq3.10})$$

and stability is guaranteed if

$$u \begin{cases} < \alpha(x) & \text{for } S > 0 \\ = \alpha(x) & \text{for } S = 0 \\ > \alpha(x) & \text{for } S < 0 \end{cases} \quad \text{where} \quad \alpha(x) = -\frac{f(x,t)+bx_2}{g(x,t)} \quad (\text{Eq 3.11})$$

The above condition can be ensured by taking control law as

$$u = \alpha(x) - K_s \text{sign}(S), \text{ where } K_s > 0 \quad (\text{Eq 3.12})$$

3.3.2 Example 2

Consider a simple pendulum described by the following set of equations:

$$\begin{aligned} \dot{x}_1 &= x_2 \\ \dot{x}_2 &= b \sin x_1 + u \end{aligned} \quad (\text{Eq 3.13})$$

Switching surface is taken as

$$S = cx_1 + x_2 \quad (\text{Eq 3.14})$$

and also

$$\begin{aligned} \dot{S} &= c\dot{x}_1 + \dot{x}_2 \\ \dot{S} &= cx_2 + b \sin x_1 + u \end{aligned} \quad (\text{Eq 3.15})$$

For equivalent control, put $\dot{S} = 0$

$$\begin{aligned} cx_2 + b \sin x_1 + u &= 0 \\ \Rightarrow u_{eq} &= -cx_2 - b \sin x_1 \end{aligned} \quad (\text{Eq 3.16})$$

Then sliding mode control law is

$$\begin{aligned} u &= u_{eq} - K \text{sign}(s) \\ u &= -cx_2 - b \sin x_1 - K \text{sign}(s) \end{aligned} \quad (\text{Eq 3.17})$$

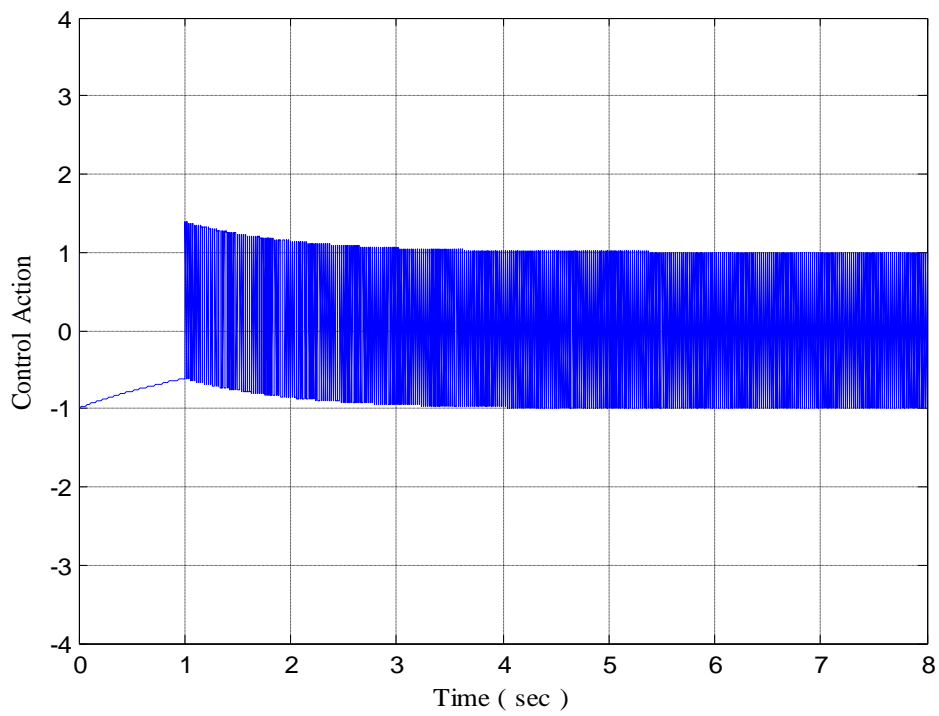


Figure 3.2: Controller effort.

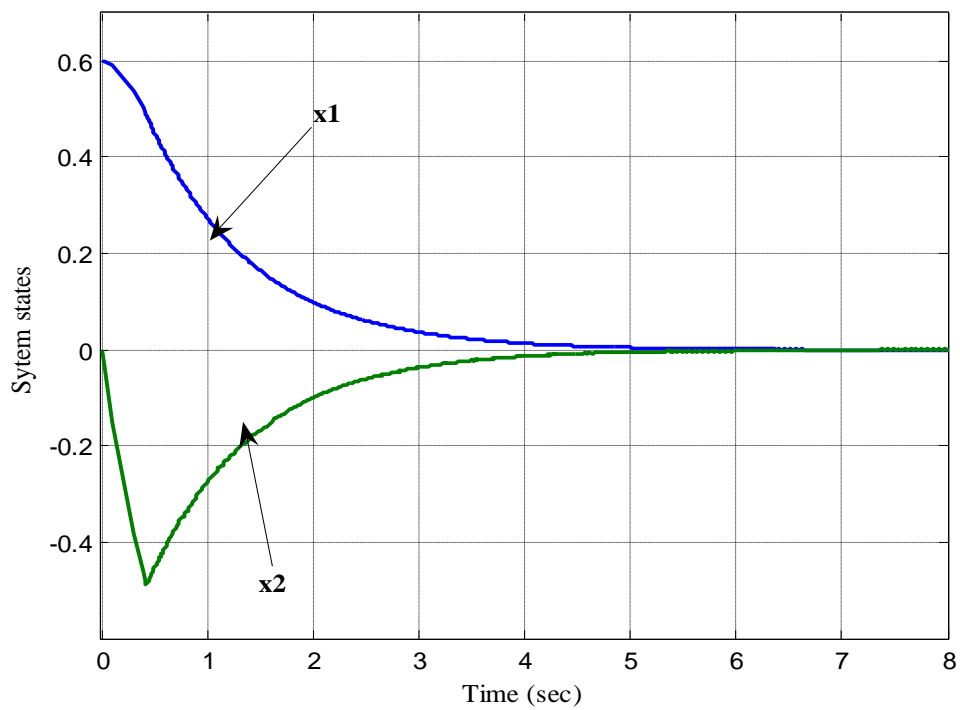


Figure 3.3: System Trajectories.

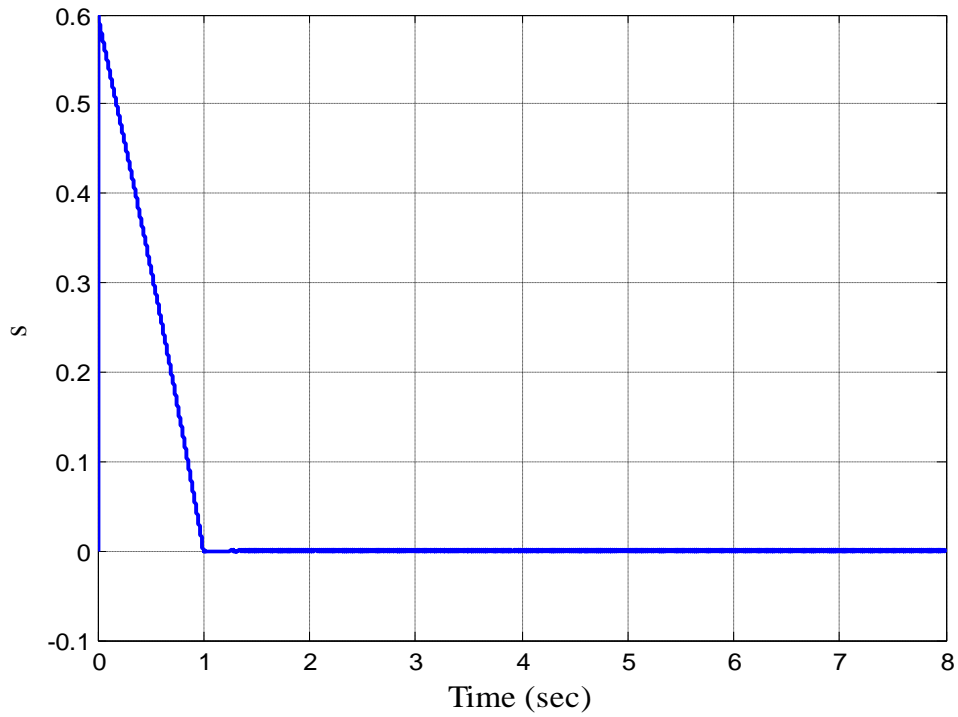


Figure 3.4: Sliding Surface.

Now it is clear from Figure 3.3 that system states converge in finite time. So in conclusion, it can be said that when phase portrait intercepts sliding surface in finite time then it is forced to remain there. Once sliding motion is established, the system acts like a reduced order system, where nonlinearity is totally rejected [63]. After sliding, the system acts as a double integrator system with no effect of nonlinear term. Hence it is called robust controller, because it is not sensitive to plant and control law mismatches.

3.3.3 Example 3

Consider a DC motor with the following dynamics [64]

$$L \frac{di}{dt} + Ri = u - K_e \omega \quad (\text{Eq 3.18})$$

$$j \frac{d\omega}{dt} = K_t i - \tau_l \quad (\text{Eq 3.19})$$

where ω and i are the two states representing shaft speed and armature current respectively. u is the control input and $\tau_l = B\omega$ is the load torque. Motor parameters and their respective nominal values are given in the Table.

Table 4: Parameters of DC Motor.

Parameter	Value
Armature Resistance (R)	0.5 Ω
Armature Inductance (L)	1.0 mH
Back EMF Constant (K_e)	0.001 V/rad
Torque Constant (K_t)	0.008 Nm/A
Coefficient of Friction (B)	0.01 Nm s/rad
Inertia of Motor Rotor & Load (J)	0.001 Kg.m ²

For speed tracking problem, let ω_r be the reference shaft speed and $e = \omega_r - \omega$ be the tracking error. Let the state variables be $x_1 = e$ and $x_2 = \dot{e}$ then error dynamics is defined as

$$\dot{x}_1 = x_2 \quad (Eq\ 3.20)$$

$$\dot{x}_2 = g(x_1, x_2, t) + du \quad (Eq\ 3.21)$$

where

$$g(x_1, x_2, t) = -c_1 x_1 - c_2 x_2 + \ddot{\omega}_r + c_2 \dot{\omega}_r + c_1 \omega_r + \frac{R}{JL} \tau_l + \frac{1}{J} \dot{\tau}_l \quad (Eq\ 3.22)$$

$$c_1 = \frac{K_t K_e}{JL} \quad c_2 = \frac{R}{L} \quad \text{and} \quad d = \frac{K_t}{JL}$$

The sliding surface and control law are designed as

$$s = \lambda x_1 + x_2 \quad (Eq\ 3.23)$$

$$u = \frac{1}{d} (-\lambda x_2 - g(x_1, x_2, t) - K \text{sign}(s)) \quad (Eq\ 3.24)$$

where λ and K are positive constants.

The model was simulated in Matlab-Simulink environment. Simulation results show that the tracking control of DC motor using sliding mode technique is accurate. The speed response is shown in Figure 3.5 and tracking error in speed in Figure 3.6. The controller converges immediately to a very low error (of the order of 10^{-3} rad/s); further reduces to zero in 2-3 seconds and remains zero afterwards throughout the simulation time. The SMC makes the motor follow/track the reference signal well. Figure 3.7 shows the current (Amperes) and Figure 3.8 gives the control effort required in tracking the reference speed signal.

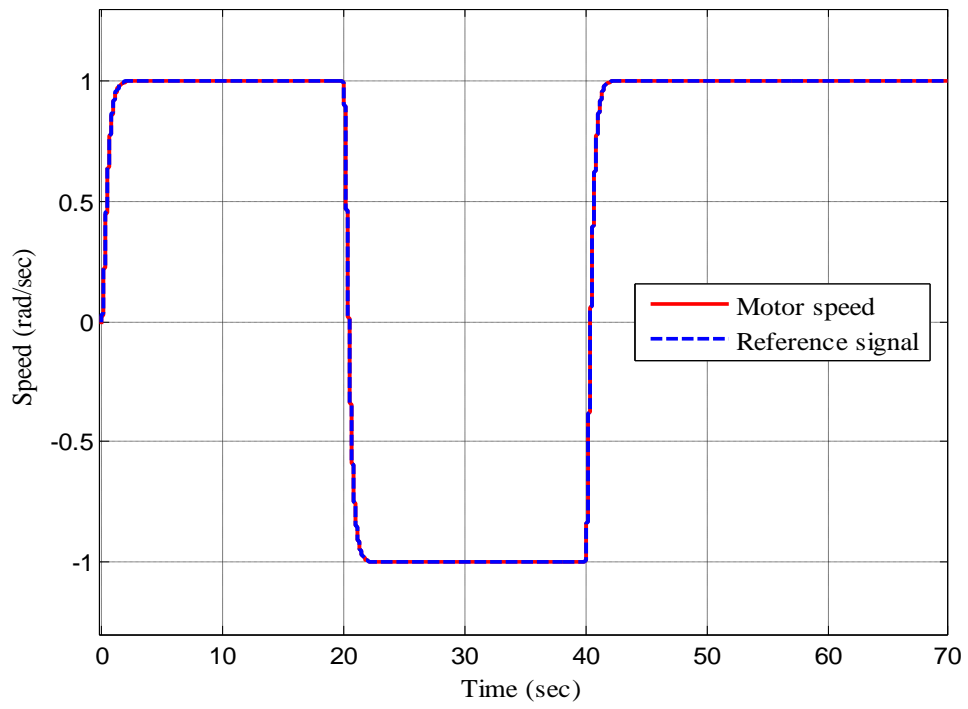


Figure 3.5: Speed response.

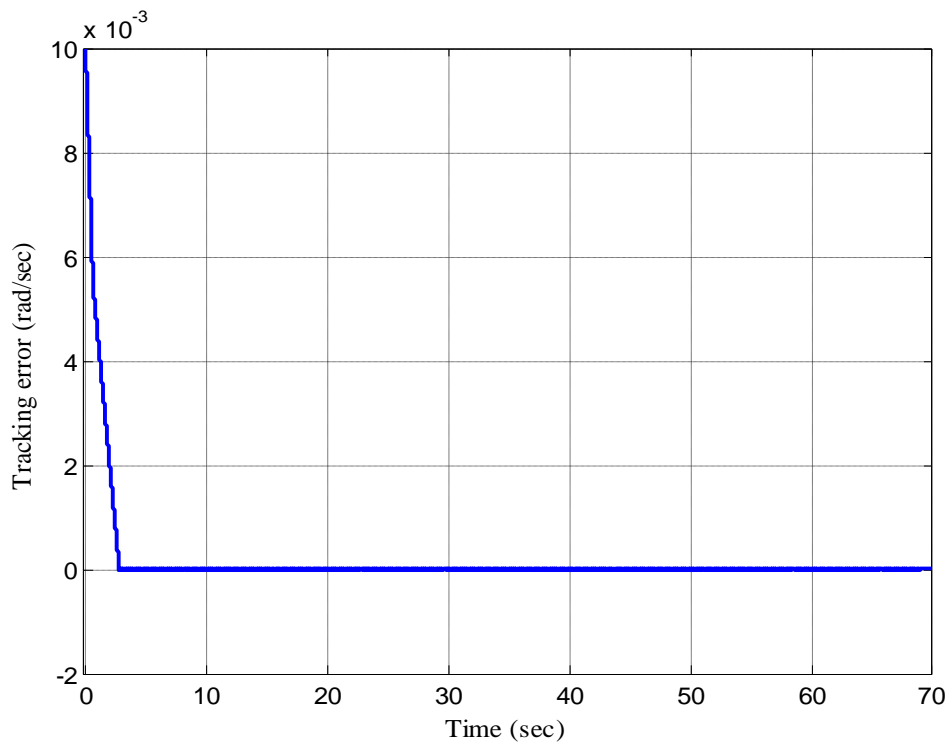


Figure 3.6: Tracking error response.

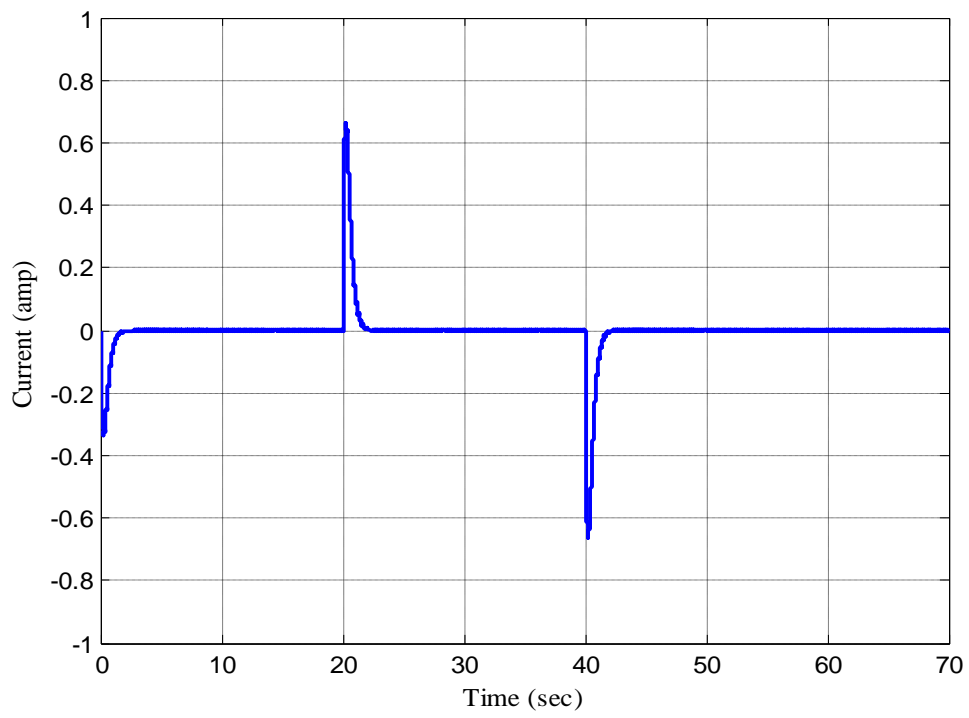


Figure 3.7: Current response.

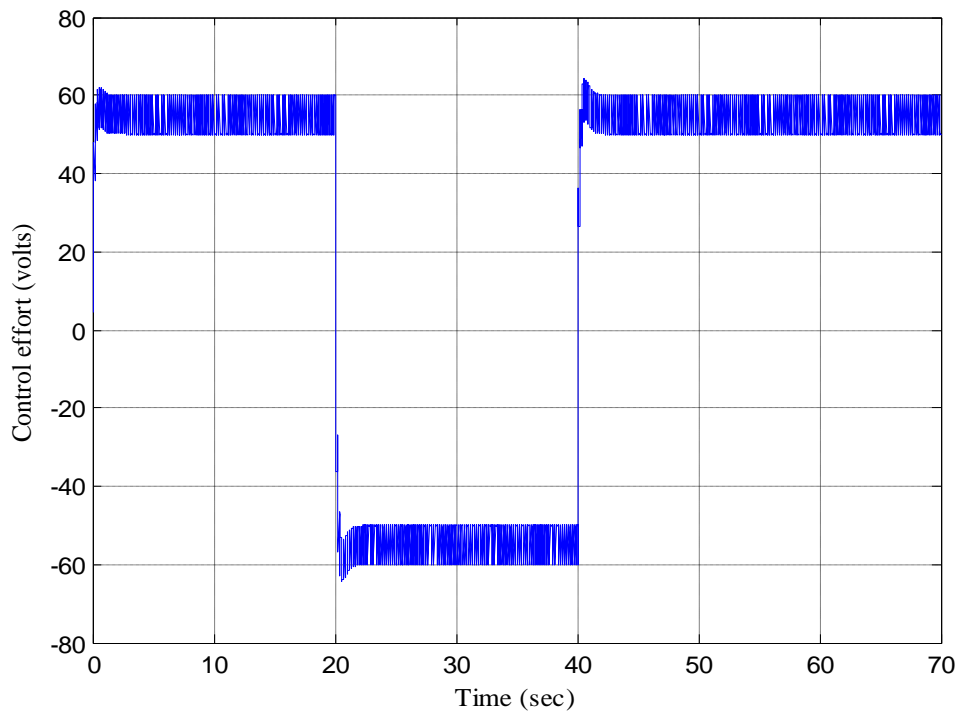


Figure 3.8: Controller effort.

3.4 First Oder Sliding Mode Controller (FOSMC) Design

The design of FOSMC can be achieved into two steps. In first step, switching surface is designed depending upon the error dynamics. In second step, control law is designed in such a way that it should guarantee to steer the system trajectories to the sliding surface. The main advantage of using this technique is, once the system is in sliding phase, it remains insensitive to certain parameter variations and unknown disturbances. In this work, sliding surface proposed by [65] is used.

$$s = \left(\frac{d}{dt} + D \right)^{n-1} e \quad (Eq 3.25)$$

in which D is positive constant, e is the error and n is the system order.

Case-1: For position control problem $n = 3$ and $e(t) = \theta(t) - \theta_{ref}(t)$ is the position error. $\theta_{ref}(t)$ is the desired position. Therefore (Eq 3.25) is rewritten as:

$$s = \left(\frac{d}{dt} + D \right)^2 e \quad (Eq 3.26)$$

$$s = \frac{d^2}{dt^2} e + 2D \frac{d}{dt} e + D^2 e \quad (Eq 3.27)$$

For simplicity, let $2D = D_1$ and $D^2 = D_2$, then (Eq 3.27) can be written as

$$s = \ddot{e} + D_1 \dot{e} + D_2 e \quad (Eq 3.28)$$

Where D_1 and D_2 are strictly positive constants which are to be chosen in such a way that the following (Eq 3.29) is Hurwitz polynomial.

$$p(s) = s^2 + D_1 s + D_2 \quad (Eq 3.29)$$

Now differentiating (Eq 3.28) with respect to time and get

$$\dot{s} = \ddot{\ddot{e}} + D_1 \ddot{\dot{e}} + D_2 \ddot{e} \quad (Eq 3.30)$$

$$\dot{s} = \ddot{\omega}(t) + D_1 \dot{\omega}(t) - \left(\ddot{\theta}_{ref}(t) + D_1 \dot{\theta}_{ref}(t) \right) + D_2 \left(\omega(t) - \dot{\theta}_{ref}(t) \right) \quad (Eq 3.31)$$

Where $\ddot{e} = \ddot{\theta}(t) - \ddot{\theta}_{ref}(t) = \ddot{\omega}(t) - \ddot{\theta}_{ref}(t)$ and $\dot{e} = \dot{\omega}(t) - \dot{\theta}_{ref}(t)$

Case-2: For speed control problem $n = 2$ and $e(t) = \omega(t) - \omega_{ref}(t)$ is the speed error. $\omega_{ref}(t)$ is the desired speed. Therefore (Eq 3.25) is rewritten as:

$$s = \left(\frac{d}{dt} + D \right)^1 e \quad (Eq 3.32)$$

$$s = \dot{e} + D e \quad (\text{Eq 3.33})$$

$$\dot{s} = \ddot{e} + D \dot{e} \quad (\text{Eq 3.34})$$

$$\dot{s} = \ddot{\omega}(t) + D \dot{\omega}(t) - (\ddot{\omega}_{ref}(t) + D \dot{\omega}_{ref}(t)) \quad (\text{Eq 3.35})$$

In order to design control laws for FOSMC, differentiating (Eq 2.11) with respect to time,

$$\ddot{\omega} = \frac{1}{J} \left(\frac{dT_e}{dt} - B \frac{d\omega}{dt} - \frac{dT_L}{dt} \right) \quad (\text{Eq 3.36})$$

$$\ddot{\omega} = \frac{1}{J} \left(\sum_{j=1}^3 \frac{dT_j(\theta, i_j)}{dt} - B \dot{\omega} - \frac{dT_L}{dt} \right) \quad (\text{Eq 3.37})$$

$$\ddot{\omega} = \frac{1}{J} \left(\sum_{j=1}^3 \frac{\partial T_j(\theta, i_j)}{\partial i_j} \frac{di_j}{dt} + \omega \sum_{j=1}^3 \frac{\partial T_j(\theta, i_j)}{\partial \theta} - B \dot{\omega} - \frac{dT_L}{dt} \right) \quad (\text{Eq 3.38})$$

Substituting (Eq 2.12) into (Eq 3.38) leads to:

$$\ddot{\omega} = \frac{1}{J} \left(\sum_{j=1}^3 \frac{\partial T_j(\theta, i_j)}{\partial i_j} \left(\frac{\partial \lambda_j(\theta, i_j)}{\partial i_j} \right)^{-1} \left(u_j - R_j i_j - \omega \frac{\partial \lambda_j(\theta, i_j)}{\partial \theta} \right) + \omega \sum_{j=1}^3 \frac{\partial T_j(\theta, i_j)}{\partial \theta} - B \dot{\omega} - \frac{dT_L}{dt} \right) \quad (\text{Eq 3.39})$$

Which can be written in the following form suitable for the design of our proposed controllers discussed in the following sections:

$$\ddot{\omega} = \frac{1}{J} \left\{ \sum_{j=1}^N \frac{\partial T_j(\theta, i_j)}{\partial i_j} \left(\frac{\partial \lambda_j(\theta, i_j)}{\partial i_j} \right)^{-1} \left(-R_j i_j - \omega \frac{\partial \lambda_j(\theta, i_j)}{\partial \theta} \right) + \omega \sum_{j=1}^N \frac{\partial T_j(\theta, i_j)}{\partial \theta} - B \dot{\omega} - \frac{dT_L}{dt} \right\} + \frac{1}{J} \left\{ \sum_{j=1}^N \frac{\partial T_j(\theta, i_j)}{\partial i_j} \left(\frac{\partial \lambda_j(\theta, i_j)}{\partial i_j} \right)^{-1} u_j \right\} \quad (\text{Eq 3.40})$$

Which can simply be written in a compact form as:

$$\ddot{\omega} = F(\theta, \omega, i, \dot{\omega}, i, B, R, T_L, \dot{T}_L) + G_j(\theta, i_j,)u_j \quad (\text{Eq 3.41})$$

where u represents the input vector comprising of N phase voltages, N represents the number of phases which are being energized at a particular instant to produce net torque and will be determined through the commutation scheme described in the previous chapter. In this particular case $N = 3$, therefore $u = [u_1 \ u_2 \ u_3]^T$ comprising of 3-phase voltages. The scalar function F and vector function G are defined as:

$$F(\theta, \omega, i, \dot{\omega}, i, B, R, T_L, \dot{T}_L) =$$

$$\frac{1}{J} \left\{ \sum_{j=1}^3 \frac{\partial T_j(\theta, i_j)}{\partial i_j} \left(\frac{\partial \lambda_j(\theta, i_j)}{\partial i_j} \right)^{-1} \left(-R_j i_j - \omega \frac{\partial \lambda_j(\theta, i_j)}{\partial \theta} \right) + \omega \sum_{j=1}^3 \frac{\partial T_j(\theta, i_j)}{\partial \theta} - B \dot{\omega} - \frac{dT_L}{dt} \right\} \quad (Eq 3.42)$$

$$G = [G_1(\theta, i_1) \quad G_2(\theta, i_2) \quad G_3(\theta, i_3)]$$

$$= \frac{1}{J} \begin{bmatrix} \left(\frac{\partial T_1(\theta, i_1)}{\partial i_1} \left(\frac{\partial \lambda_1(\theta, i_1)}{\partial i_1} \right)^{-1} \right)^T \\ \left(\frac{\partial T_2(\theta, i_2)}{\partial i_2} \left(\frac{\partial \lambda_2(\theta, i_2)}{\partial i_2} \right)^{-1} \right)^T \\ \left(\frac{\partial T_3(\theta, i_3)}{\partial i_3} \left(\frac{\partial \lambda_3(\theta, i_3)}{\partial i_3} \right)^{-1} \right)^T \end{bmatrix} \quad (Eq 3.43)$$

For simplicity, the explicit dependence of u on time t and F & G vectors on $\theta, \omega, i, \dot{\omega}, \dot{i}, B, R, T_L, \dot{T}_L$ will be omitted in the following sections. Therefore

$$\ddot{\omega} = F + G u \quad (Eq 3.44)$$

Now (Eq 3.31) and (Eq 3.35) can take the form as

$$\dot{s} = F + G u + D_1 \dot{\omega}(t) - \left(\ddot{\theta}_{ref}(t) + D_1 \dot{\theta}_{ref}(t) \right) + D_2 (\omega(t) - \dot{\theta}_{ref}(t)) \quad (Eq 3.45)$$

$$\dot{s} = F + G u + D \dot{\omega}(t) - (\ddot{\omega}_{ref}(t) + D \dot{\omega}_{ref}(t)) \quad (Eq 3.46)$$

An appropriate candidate Lyapunov function is chosen for convergence analysis as $V = \frac{1}{2} s^2$ which leads to

$$\dot{V} = s \dot{s} \quad (Eq 3.47)$$

Now consider the position/speed regulation and speed tracking problem one by one for the design of FOSMC.

3.4.1 Case-1: Regulation Problem

The objective of the regulation problem is to stabilize the motor position / speed at a desired constant value. i.e. $\omega_{ref}(t) = \omega_{ref}$ and $\theta_{ref}(t) = \theta_{ref}$ For proving that the proposed control laws guarantee the constant position/speed requirement, first consider the Proposition 1 and Proposition 2.

Proposition 1: The following control law when applied to the motor will stabilize the position to its desired value when $t \rightarrow \infty$

$$u = [u_1 \quad u_2 \quad u_3]^T = -G^* (F + D_1 \dot{\omega}(t) + D_2 \omega(t) + K \text{sign}(s)) \quad (Eq 3.48)$$

Where K is the gain of FOSMC, and a positive constant number and G^* is a Moore-Penrose pseudoinverse of row vector such that

$$G^* = G^T (GG^T)^{-1}$$

For further details about generalized Moore-Penrose pseudo inverse see [66] and [67].

Proof: For position regulation problem, $\dot{\theta}_{ref}(t) = \ddot{\theta}_{ref}(t) = \ddot{\theta}_{ref}(t) = 0$ then

(Eq 3.45) will be modified as

$$\dot{s} = F + G u + D_1 \dot{\omega}(t) + D_2 \omega(t) \quad (Eq 3.49)$$

Now combining (Eq 3.47) and (Eq 3.49), it becomes as

$$\dot{V} = s(F + G u + D_1 \dot{\omega}(t) + D_2 \omega(t)) \quad (Eq 3.50)$$

Plugging (Eq 3.48) in (Eq 3.50), it comes up with the following equation.

$$\dot{V} = s(F - GG^*(F + D_1 \dot{\omega}(t) + D_2 \omega(t) + K \text{sign}(s)) + D_1 \dot{\omega}(t) + D_2 \omega(t)) \quad (Eq 3.51)$$

$$\dot{V} = s(F - F - D_1 \dot{\omega}(t) - D_2 \omega(t) - K \text{sign}(s) + D_1 \dot{\omega}(t) + D_2 \omega(t)) \quad (Eq 3.52)$$

$$\dot{V} = -K s \text{sign}(s) < 0 \quad (Eq 3.53)$$

From (Eq 3.53), it is easy to see that $\dot{V} < 0$ and would become equal to zero when $s = 0$. This proves that the control law defined in (Eq 3.48) would guarantee that motor will stabilize the position to its desired value when $t \rightarrow \infty$

Proposition 2: The following control law will stabilize the speed to its desired value when $t \rightarrow \infty$

$$u = [u_1 \quad u_2 \quad u_3]^T = -G^*(F + D\dot{\omega}(t) + K \text{sign}(s)) \quad (Eq 3.54)$$

Proof: For speed regulation problem, $\dot{\omega}_{ref}(t) = \ddot{\omega}_{ref}(t) = 0$ then (Eq 3.46) will take the form as

$$\dot{s} = F + G u + D\dot{\omega}(t) \quad (Eq 3.55)$$

Now combining (Eq 3.47) and (Eq 3.55), one can get as

$$\dot{V} = s(F + G u + D\dot{\omega}(t)) \quad (Eq 3.56)$$

Substituting (Eq 3.54) in (Eq 3.56) gives

$$\dot{V} = s(F - G G^*(F + D\dot{\omega}(t) + K\text{sign}(s)) + D\dot{\omega}(t)) \quad (\text{Eq 3.57})$$

$$\dot{V} = s(F - F - D\dot{\omega}(t) - K\text{sign}(s) + D\dot{\omega}(t)) \quad (\text{Eq 3.58})$$

$$\dot{V} = -K s \text{sign}(s) < 0 \quad (\text{Eq 3.59})$$

Now it is clear from (Eq 3.59), $\dot{V} = 0$ only when $s = 0$. This shows that the control law as defined in (Eq 3.54) would guarantee that $\omega(t) \rightarrow \omega_{ref}(t)$ when $t \rightarrow \infty$.

3.4.2 Case-2: Tracking Problem

The aim of tracking problem is to follow the time varying reference signal keeping the tracking error to a minimum. To prove that the proposed control law will follow the reference signal, consider the following Proposition 3.

Proposition 3: The following control law will ensure that the speed will follow the time varying reference signal as $t \rightarrow \infty$.

$$u = [u_1 \quad u_2 \quad u_3]^T = -G^* \left(F + D\dot{\omega}(t) + K\text{sign}(s) - \left(\ddot{\omega}_{ref}(t) + D\dot{\omega}_{ref}(t) \right) \right) \quad (\text{Eq 3.60})$$

Proof: Combining (Eq 3.46) and (Eq 3.47), it comes up with

$$\dot{V} = s(F + G u + D\dot{\omega}(t) - (\ddot{\omega}_{ref}(t) + D\dot{\omega}_{ref}(t))) \quad (\text{Eq 3.61})$$

Substituting (Eq 3.60) in (Eq 3.61) gives

$$\dot{V} = s \left[F - G G^* \left(F + D\dot{\omega}(t) + K\text{sign}(s) - \left(\ddot{\omega}_{ref}(t) + D\dot{\omega}_{ref}(t) \right) \right) + D\dot{\omega}(t) - (\ddot{\omega}_{ref}(t) + D\dot{\omega}_{ref}(t)) \right] \quad (\text{Eq 3.62})$$

$$\dot{V} = s[F - F - D\dot{\omega}(t) - K\text{sign}(s) + \ddot{\omega}_{ref}(t) + D\dot{\omega}_{ref}(t) + D\dot{\omega}(t) - \ddot{\omega}_{ref}(t) - D\dot{\omega}_{ref}(t)] \quad (\text{Eq 3.63})$$

$$\dot{V} = -K s \text{sign}(s) < 0 \quad (\text{Eq 3.64})$$

From (Eq 3.64), it is obvious that $\dot{V} < 0$ and would become zero only when $s = 0$. This ensures that the control law defined in (Eq 3.60) would guarantee the motor speed follows the time-varying reference signal in the limit. Now from the above propositions, it is clear that

1. V is positive definite
2. \dot{V} is negative definite

Therefore it is concluded that the control laws would guarantee the speed and position converge to the desired values as $t \rightarrow \infty$.

3.5 Simulation Results of FOSMC using Proposed Commutation scheme

A lot of work has been done on speed control problem using sliding mode technique, but no such work exists for position control problem. We selected SMC using conventional scheme [24] for comparison purpose with FOSMC, designed in the above section using proposed commutation scheme explained in chapter 2 for speed regulation case.

3.5.1 Comparison of Speed Response of FOSMC and SMC to A Step Command

Figure 3.9 shows the response of SMC and FOSMC when motor is directed to move with a speed of 10 rad/s. It is clear that FOSMC reaches the desired speed more rapidly than the conventional SMC, in spite of using the same gain and parameter values. The performance of FOSMC is better than SMC.

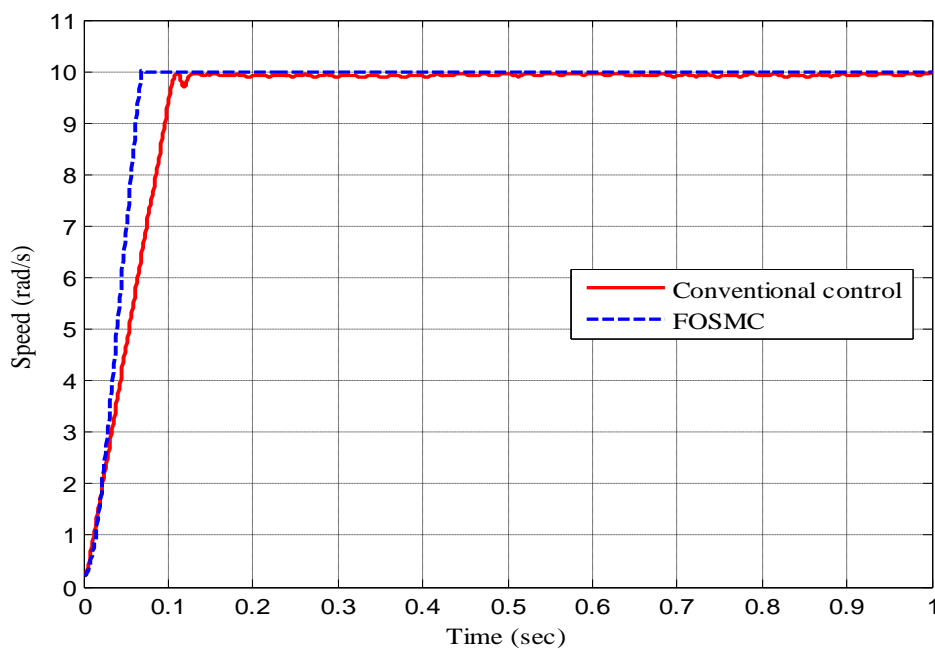


Figure 3.9: Speed response of SMC and FOSMC to a step command.

3.5.2 Comparison between FOSMC and SMC With Respect To Power Loss, Input Phase Voltages and Torques in Speed Regulation Problem

Figures 3.10-3.13 give a performance comparison test between conventional scheme based SMC and proposed commutation scheme based FOSMC when motor is commanded to achieve the desired speed of 10 rad/s. Power loss in conventional design is 85KW but in FOSMC, it is just 19 KW which is clearly visible from Figure 3.10. Power loss is computed by the formula, $Power\ Loss = i^2R$. This power saving is due to the commutation scheme which is employed in FOSMC. Figures 3.11-3.13 depict the basic reasons behind this power saving.

To analyze the behavior closely, a plot of initial stage of steady state response for voltages/currents is drawn in Figures 3.11-3.12. It is noted that in FOSMC; at most two phases are selected at any instant for excitation with lesser voltage values that results in lesser amounts of currents. On the other hand, in conventional design more than one phase is energized with maximum voltage values. Therefore maximum currents are produced in conventional design which results in maximum individual torques in motor phases, but the net torque which is produced in conventional design is less as compared to the net torque produced in FOSMC. Therefore a lot of power is wasted in conventional design.

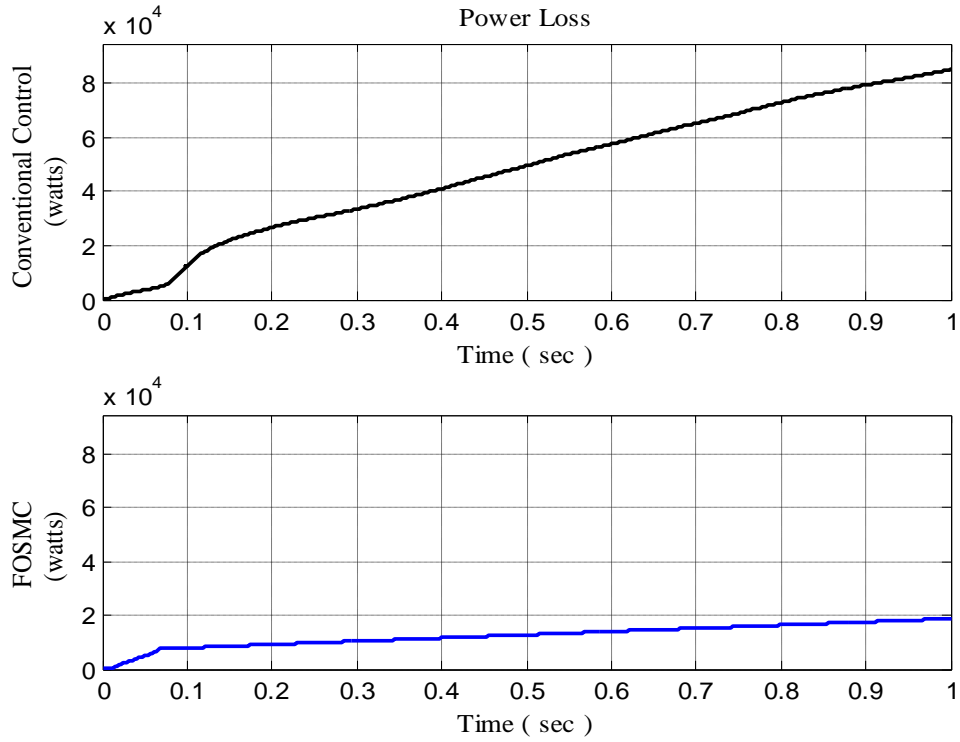


Figure 3.10: Power loss in SMC and FOSMC during the entire simulation period of one second.

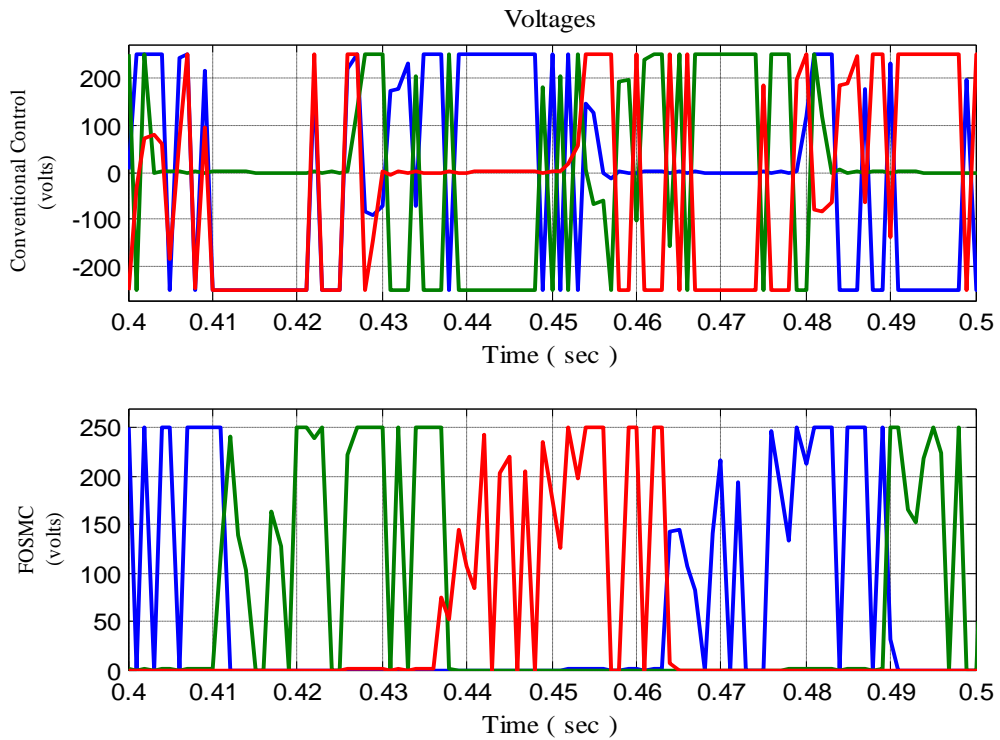


Figure 3.11: 3-phase voltages during initial stage of steady state response.

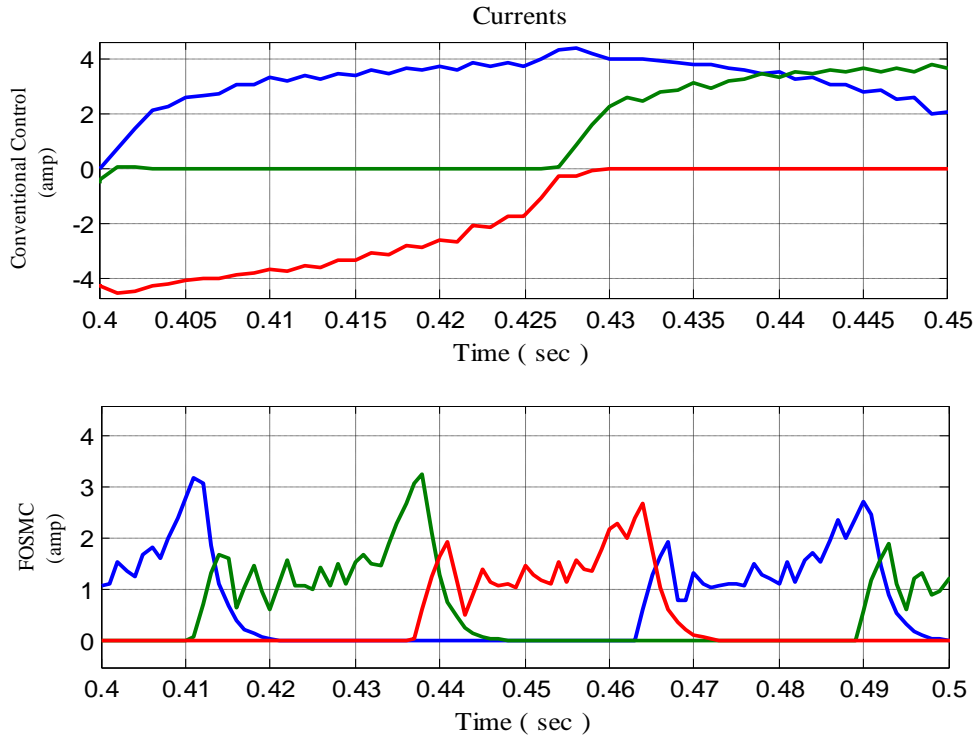


Figure 3.12: 3-phase current during initial stage of steady state response.

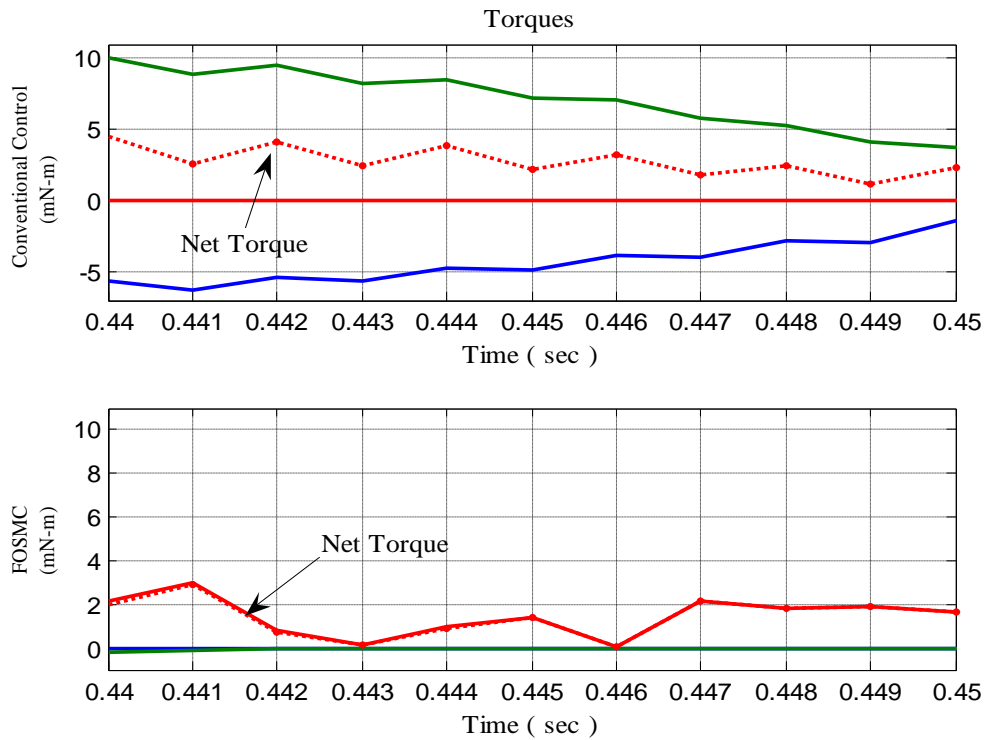


Figure 3.13: Torques during initial stage of steady state response.

3.5.3 Comparison of Speed Response of FOSMC and SMC to a Sinusoidal Signal.

Figure 3.14 shows the motor response of SMC and FOSMC to a sinusoidal signal. It is clear that tracking response of proposed commutation scheme based FOSMC is far better than conventional scheme based SMC. The conventional scheme based SMC gave a 5% error in tracking which is visible at the peaks of signal while the FOSMC reduces this error to almost zero, tracking the sinusoidal signal accurately.

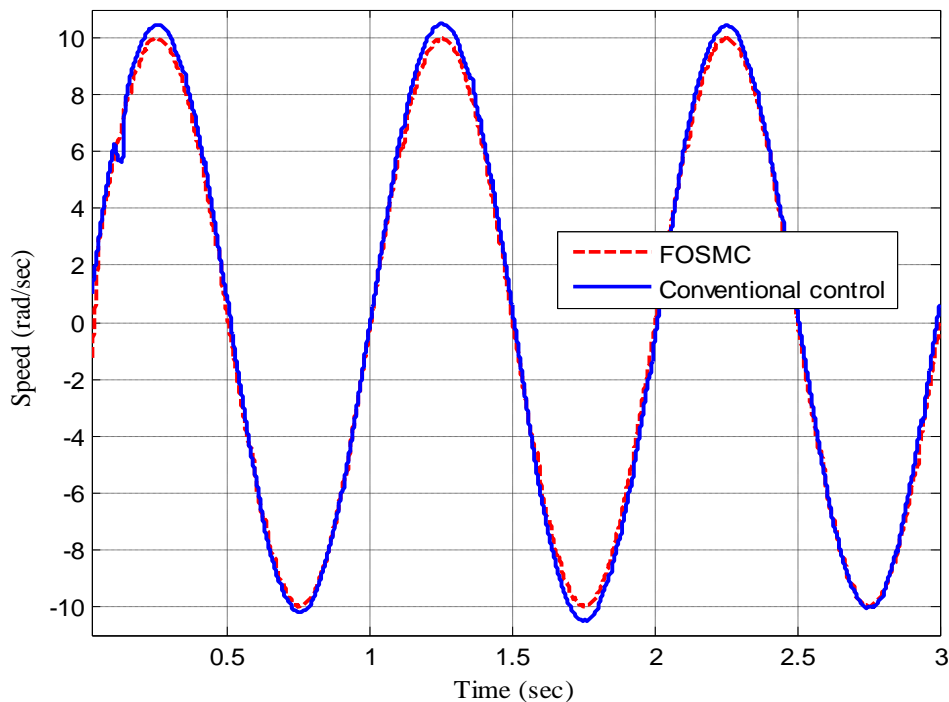


Figure 3.14: Speed response of FOSMC and SMC against sinusoidal signal.

3.5.4 Position Response of FOSMC to A Step Command.

Figure 3.15 illustrates the step response of FOSMC when motor is directed from 0.1 radian to attain a desired position of 30 radians. Figure 3.16 gives its respective error plot. As shown in figure the motor achieves the target position within 2 seconds which confirms FOSMC good dynamic response.

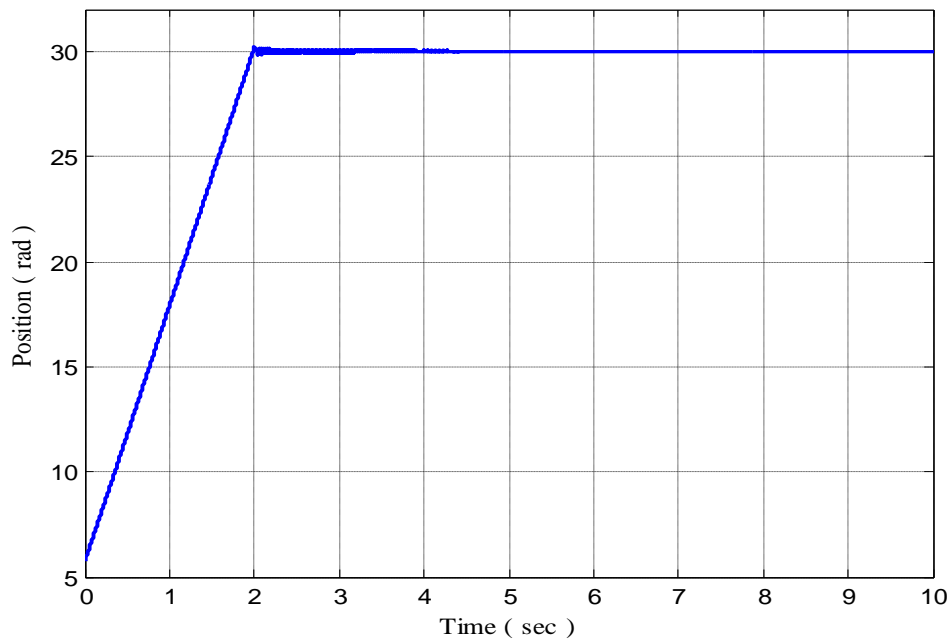


Figure 3.15: Position response of FOSMC to a step command.

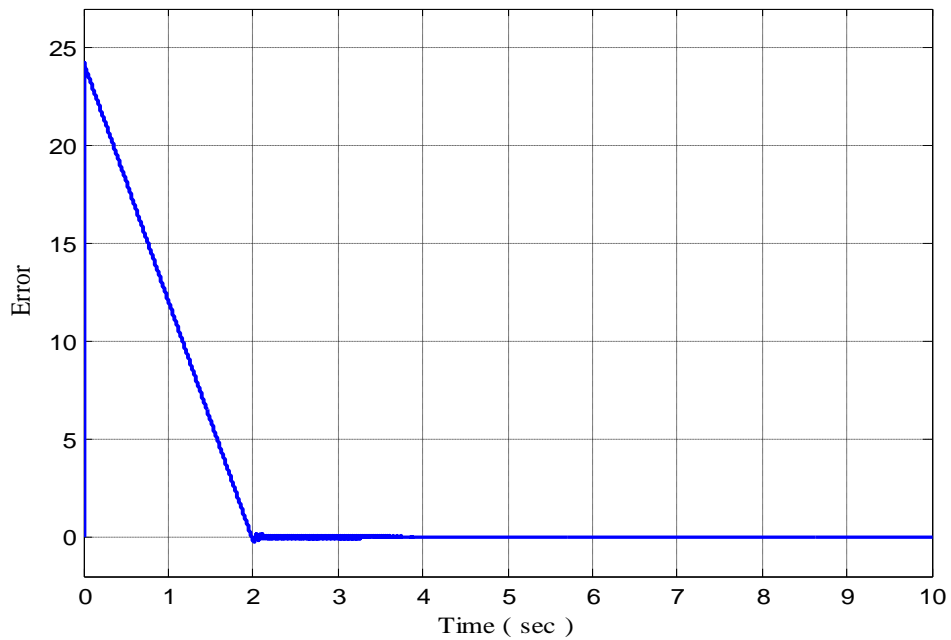


Figure 3.16: Error plot of position response of FOSMC to a step command.

3.6 Drawbacks of Conventional SMC and FOSMC

The main drawback in conventional SMC and proposed commutation scheme based FOSMC is that they exhibit chattering. Chattering is undesirable for electro-mechanical system because it invokes high frequency dynamics which can cause

system instability. If the plots drawn in Figure 3.9 and Figure 3.15 are sketched closely, it comes to our knowledge that chattering is highly concerned with the above controllers' performance. A lot of research has been done on chattering reduction. Higher order sliding mode technique is one of the solutions of chattering removal.

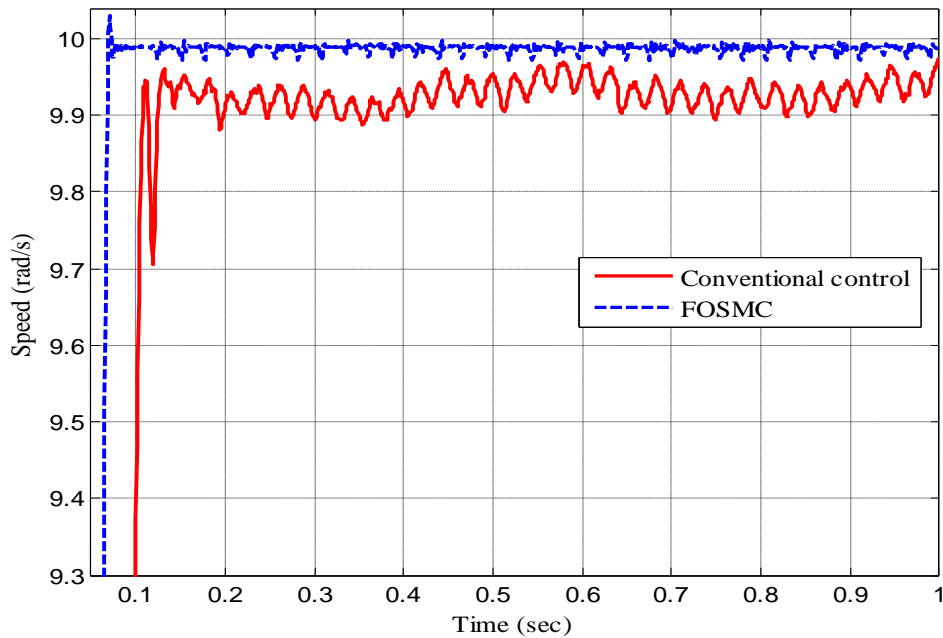


Figure 3.17: A close-up of speed response of conventional SMC and FOSMC to a step command.

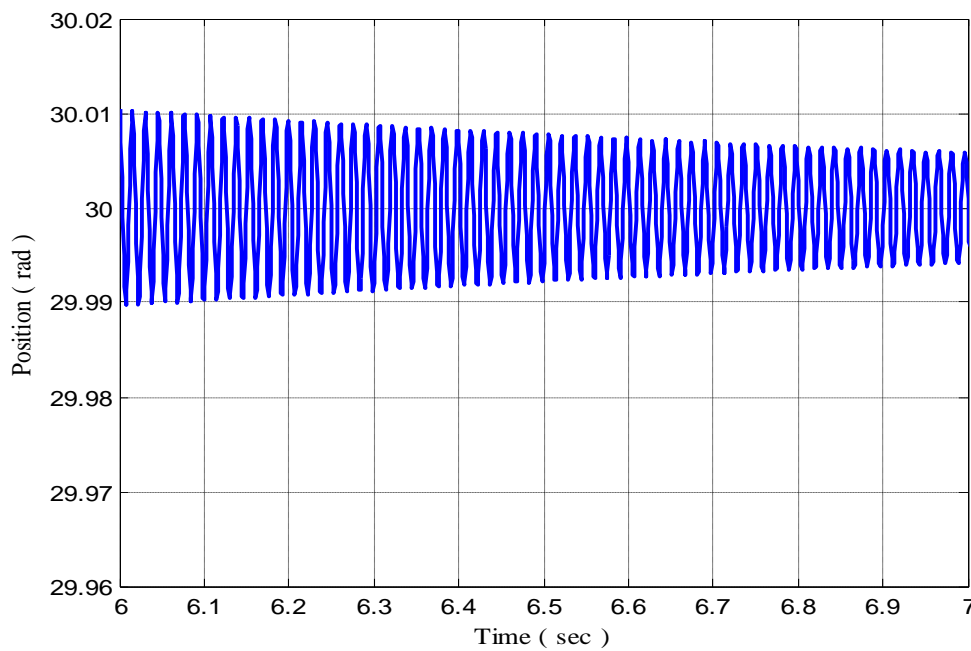


Figure 3.18: A close-up of steady state position response of FOSMC to a step command.

3.7 Conclusion

SR motor is highly nonlinear machine due to its nonlinear characteristics. Many nonlinear techniques have been developed so far for the control of SR motor. Most of the techniques require a lot of knowledge about the dynamic system, such as phase resistance, inductance, flux linkage, inertia, coefficient of friction and external load. Moreover, the controller design and its implementation are very complex. Sliding mode technique has gained much popularity and has received considerable attention from control community due to its simple structure, inherent robustness and easy implementation. Due to these reasons, the use of SMC for SR motor has been adopted. Also the motor control is inherently discrete in nature, the use of sliding mode technique is ideal in these type of applications.

The designed FOSMC with proposed commutation scheme was simulated and compared with conventional scheme based SMC for speed regulation/tracking problem. FOSMC saves power consumption and its performance is far better than SMC. But sliding mode technique causes undesirable chattering. Higher order sliding mode is one of the solutions of chattering reduction.

Chapter 4

HIGHER-ORDER SLIDING-MODE CONTROL

In this chapter higher order sliding mode (HOSM) technique is discussed. Section 4.1 gives its background. HOSM technique is discussed in Section 4.2. Importance of super twisting algorithm is described in Section 4.3. An example is taken in order to demonstrate the performance of SOSMC over FOSMC. In Section 4.4, important results are given for comparison of conventional SMC, FOSMC and SOSMC over power loss, amount of voltage, and torques for speed/position regulation problem. Concluding remarks are made in Section 4.5.

4.1 Background

The inherent problem of chattering in conventional sliding mode control is dangerous for electro-mechanical system because it excites unmodelled dynamics that makes system unstable. Various approaches have been proposed to avoid undesirable chattering phenomenon. One of the possible solutions is boundary layer solution where saturation function is used to approximate the sign function term in the sliding surface [23, 68]. With the advancement of this approach, many types of saturation functions have been introduced i.e. [69]. The basic idea behind this approach is the replacement of discontinuous switching function with continuous function depending upon the thickness of the boundary layer. As a result, the system trajectories are restricted to a small vicinity of the sliding surface. The main drawback of using this technique is, the system behavior may not be identified within the small vicinity of the boundary layer and it is not guaranteed that the system trajectories in the same vicinity will converge to zero. Moreover this technique causes steady state error.

Another solution to suppress chattering is the use of dynamic sliding mode control [24]. The basic idea in this approach is that the dynamic sliding surface is incorporated to produce dynamic feedback. The dynamic surface is either control dependant or control independent. Actually DSMC provides an extra dynamics which can be treated as compensators and forms the augmented system after combining with

the sliding system [70]. These compensators are very helpful for obtaining desired response and improving system stability. However this method cannot be applied to all types of nonlinear systems.

Ref. [71] introduced integral sliding mode control as another chattering reduction tool and employed on induction motor for speed estimation process using current control scheme for decoupling but it is applicable only in the presence of synchronous current control strategy. A new approach for chattering reduction so called dynamic integral sliding mode control (DISMC) was presented in [72] for uncertain MIMO systems. The proposed approach merged the best features of DSMC and integral sliding mode control (ISMC) into DISMC. The basic idea behind this approach was to develop sliding mode without establishing reaching phase. As a result, the robustness of the process against parametric uncertainties and unknown disturbance could be improved from the beginning.

Researcher also combined sliding mode control (SMC) with other control techniques to implement controllers suitable for various engineering applications. For example in [73], [74] etc. sliding mode control was integrated with fuzzy logic control to develop so called fuzzy sliding mode controller (FSMC). FSMC had been found in literature for the control of various electric motors [75-77]. One of the advantages of FSMC is its insensitivity to the controlling system's parameters without the need for exact mathematical models of the controlling systems [78-79]. Using this approach, switching function could be used directly as a fuzzy logic control input for the motor and fuzzy logic rule could be minimized without taking number of state variables into account. Ref. [80-84] developed FSMC for SR motor for speed regulation problem using triangular membership function, the max-min reasoning method, and the center of gravity defuzzification method. Parameters of the equivalent control law were designed by fuzzy inference mechanism. It was observed that the proposed technique could handle modeling uncertainties, parameter variations, torque ripples, acoustic noise and unknown disturbances due to switching gain change. But this technique required more complex process to design controller than conventional SMC.

Another method to attenuate chattering was the use of higher order sliding mode (HOSM) control. HOSM had been successfully applied for a variety of engineering applications, i.e. [85-88]. Ref. [89] developed HOSM observer for nonlinear model

using real twisting algorithm. The proposed technique was capable of estimating more than one parameter from a single dynamic equation. The estimated parameters were then used to cater for unmodelled dynamic, model inaccuracies of the actual system. It was claimed that these estimated parameters can also be incorporated for controller design and fault diagnosis problem and also for monitoring conditions of an automotive systems. Ref. [90-91] designed HOSM controller based on super twisting algorithm for speed control problems of a diesel generator and compared its performance with conventional controllers against load changes, fuel consumption, speed band etc. The simulation results showed high efficiency and good robustness of the proposed design. Ref. [92-94] worked on permanent magnet synchronous motor and stepper motor and proposed a new technique, so called observer based controller using HOSM approach. The proposed technique eliminated the need of mechanical sensors. The motor parameters magnetic flux, angular velocity, stator phase current and load torque were estimated by the observer and were given to the controller for speed tracking problem. The stability was insured by using Lyapunov approach. The given results proved the effectiveness of the proposed technique. In [95], a new commutation scheme was incorporated with HOSM controller using super twisting algorithm for speed regulation/ tracking problems of SR motor. The commutation scheme selected only those motor phases for the commutation of control laws at any instant which can contribute torque of the desired polarity. This approach also minimizes the power loss in the motor windings thus reducing the heat generation within the motor. In order to highlight the advantages of second order sliding mode controller (SOSMC), a classical First-Order Sliding-Mode controller (FOSMC) was also developed and applied to the same system. The comparison of the two schemes shows much reduced chattering in case of SOSMC. The performance of the proposed SOSMC controller for speed regulation was also compared with that of another sliding mode speed controller published in the literature. The simulation results showed that SOSMC is more effective in terms of accuracy and reduced amount of chattering than First-order sliding-mode controller (FOSMC). To see the performance of HOSM controller clearly, a test was conducted in [96] at different system parameters and unknown disturbances. It was found that HOSM has outperformed the conventional controllers with respect to chattering reduction and robustness.

4.2 Higher Order Sliding Mode

The higher-order sliding-mode (HOSM) technique generalized the basic sliding-mode idea by incorporating higher-order derivatives of the sliding variable. The inclusion of higher-order derivatives, while maintaining the same robustness and performance as that of the conventional sliding-mode, led to a reduction in the undesirable chattering effect inherent in the sliding-mode technique [97]. The n th order sliding mode is defined by the equalities $s = \dot{s} = \ddot{s} = \dots = s^{(n-1)} = 0$. The sliding order is determined from the number of continuous derivatives of sliding variable in the neighbourhood of sliding mode. As the sliding order increases, the dimension of the sliding manifold decreases, this results in chattering reduction in the neighbourhood of sliding manifold.

Among HOSM controllers, second order sliding mode controller is very popular. The reason of its popularity is its implementation which is easy.

4.3 Second order sliding mode algorithms

To design second order sliding mode, a number of algorithms are available in the literature in which twisting, super twisting, sub optimal and drift [98] are common. Now these algorithms are discussed one by one.

4.3.1 Twisting Algorithm

By considering local coordinates $y_1 = s$ and $y_2 = \dot{s}$, the SOSMC problem is the same as the finite time stabilization problem for uncertain second-order systems having a relative degree 1 [99-100].

$$\dot{y}_1 = y_2$$

$$\dot{y}_2 = \phi(t, x) + \gamma(t, x)\dot{u} \quad (Eq 4.1)$$

Here $y_2(t)$ is immeasurable but the sign is possibly known. $\phi(t, x)$ and $\gamma(t, x)$ are uncertain functions such that

$$\Phi > 0, |\phi| \leq \Phi, 0 < \Gamma_m \leq \gamma \leq \Gamma_M \quad (Eq 4.2)$$

The main feature of this algorithm is the twisting behavior around the origin as depicted in Figure 4.1. The trajectories converge to the origin after performing infinite

number of rotations. The vibration magnitude and rotation time decrease in geometric progression. The control law is defined as [99]

$$\dot{u}(t) = \begin{cases} -u & \text{if } |u| > 1 \\ -V_m \text{sign}(y_1) & \text{if } y_1 y_2 \leq 0; |u| \leq 1 \\ -V_M \text{sign}(y_1) & \text{if } y_1 y_2 > 0; |u| \leq 1 \end{cases} \quad (\text{Eq 4.3})$$

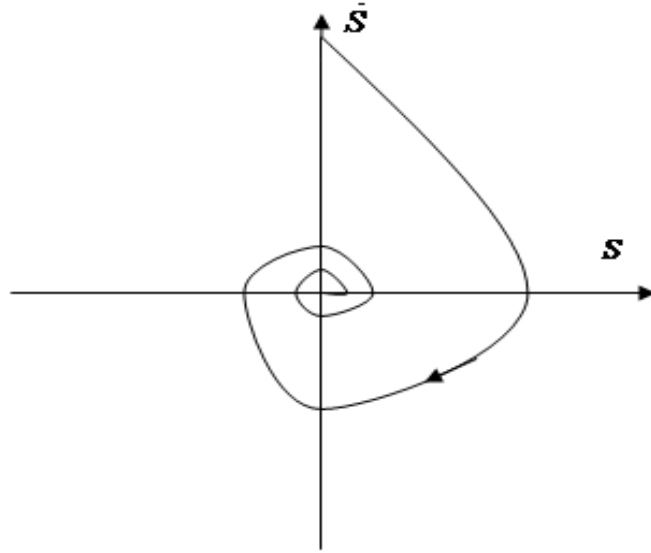


Figure 4.1: Phase trajectory of twisting algorithm.

The corresponding sufficient conditions for the finite time convergence are given below

$$V_M > V_m$$

$$V_m > \frac{4\Gamma_M}{s_0}$$

$$V_m > \frac{\Phi}{\Gamma_M}$$

$$\Gamma_m V_M - \Phi > \Gamma_M V_m + \Phi \quad (\text{Eq 4.4})$$

Where V_m and V_M are proper positive constants such that $V_M > V_m$ and V_M/V_m is sufficiently large. The above equations of controller can be used for relative degree 1 systems, for relative degree 2 systems, the following controller can be used.

$$u(t) = \begin{cases} -V_m \text{sign}(y_1) & \text{if } y_1 y_2 \leq 0 \\ -V_M \text{sign}(y_1) & \text{if } y_1 y_2 > 0 \end{cases} \quad (\text{Eq 4.5})$$

4.3.2 Sub-Optimal Algorithm

This algorithm represents sub-optimal feedback realization for a time-optimal control for a double integrator system [99]. By considering relative degree 2, the auxiliary system can be defined as

$$\begin{aligned} \dot{y}_1 &= y_2 \\ \dot{y}_2 &= \phi(t, x) + \gamma(t, x)\dot{u} \end{aligned} \quad (\text{Eq 4.6})$$

Using this algorithm, the system trajectories are restricted within limit parabolic arcs including origin [99,101]. In this algorithm both twisting and leaping behaviors are possible as shown in Figure 4.2.

$$\begin{aligned} v(t) &= -\alpha(t)V_M \text{sign}\left(y_1(t) - \frac{1}{2}y_{1M}\right) \\ \alpha(t) &= \begin{cases} \alpha^* & \text{if } \left[y_1(t) - \frac{1}{2}y_{1M}\right][y_{1M} - y_1(t)] > 0 \\ 1 & \text{if } \left[y_1(t) - \frac{1}{2}y_{1M}\right][y_{1M} - y_1(t)] \leq 0 \end{cases} \end{aligned} \quad (\text{Eq 4.7})$$

Where y_{1M} is the final singular value of the function $y_1(t)$.

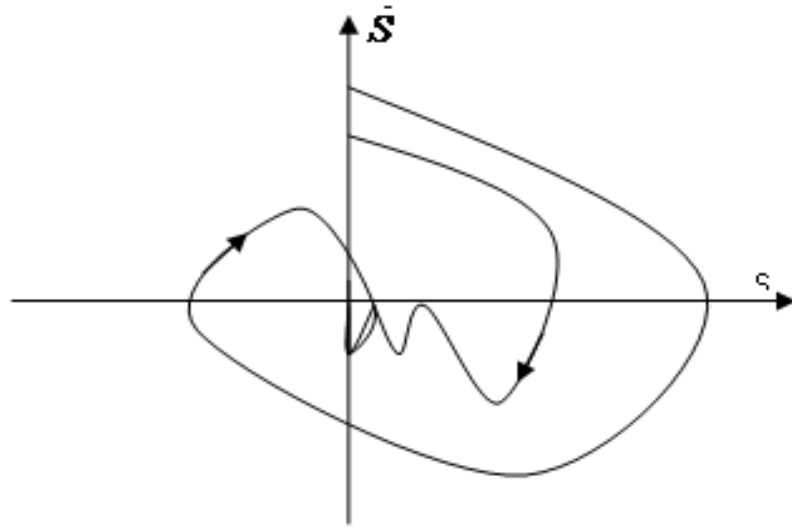


Figure 4.2: Phase trajectories of sub-optimal algorithm.

The corresponding sufficient conditions for the finite-time convergence are as follows [99,101]

$$\alpha^* \in]0,1] \cap \left(0, \frac{3\Gamma_m}{\Gamma_M}\right)$$

$$V_M > \max\left(\frac{\Phi}{\alpha^* \Gamma_m}, \frac{4\Phi}{3\Gamma_m - \alpha^* \Gamma_M}\right) \quad (Eq 4.8)$$

4.3.3 Drift Algorithm

In drift algorithm the system trajectories are moved to the 2nd order sliding mode while keeping \dot{s} small. In other words trajectories are forced to move towards the origin along y_1 -axis. The phase trajectories of this algorithm on 2-sliding manifold are characterized by loops having constant sign of sliding variable y_1 as shown in Figure 4.3.

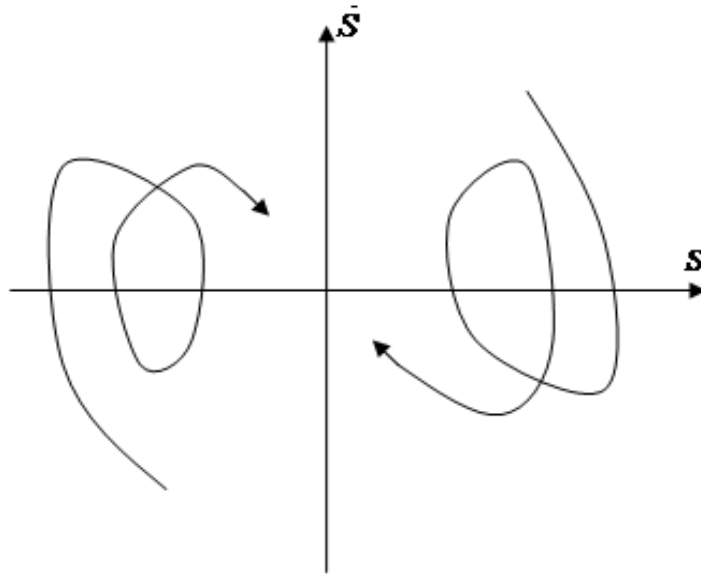


Figure 4.3: Phase trajectories of drift algorithm.

The control algorithm for the case of relative degree 1 is defined as follows [99]

$$\dot{u} = \begin{cases} -u & \text{if } |u| > 1 \\ -V_m \text{sign}(\Delta y_{1i}) & \text{if } y_1 \Delta y_{1i} \leq 0; |u| \leq 1 \\ -V_M \text{sign}(\Delta y_{1i}) & \text{if } y_1 \Delta y_{1i} > 0; |u| \leq 1 \end{cases} \quad (Eq 4.9)$$

Where V_m and V_M are proper positive constants such that $V_m < V_M$ and V_M/V_m is sufficiently large, also $\Delta y_{1i} = y_1(t_i) - y_1(t_i - \tau)$, $t \in [t_i - t_{i+1}]$. For relative degree 2, the control law is modified as shown below.

$$\dot{u} = \begin{cases} -V_m \text{sign}(\Delta y_{1i}) & \text{if } y_1 \Delta y_{1i} \leq 0 \\ -V_M \text{sign}(\Delta y_{1i}) & \text{if } y_1 \Delta y_{1i} > 0 \end{cases} \quad (\text{Eq4.10})$$

4.3.4 Super-Twisting Algorithm

Super-Twisting Algorithm has been employed for the systems having relative degree one for the purpose of chattering reduction. Since an n th-order sliding-mode controller requires the information about $s, \dot{s}, \ddot{s} \dots s^{(n-1)}$ in order to keep $s = 0$, therefore the knowledge about the values of higher-order derivatives of the sliding variable seemed to be a constraining requirement. However, this apparent restriction could be avoided by the use of this algorithm that does not require this extra piece of information. The algorithm ensures that system trajectories twist around the origin in the phase portrait as shown in the Figure 4.4. Another advantage of this algorithm is that it is not sensitive to sampling time. Another advantage of this algorithm is its insensitivity to sampling time.

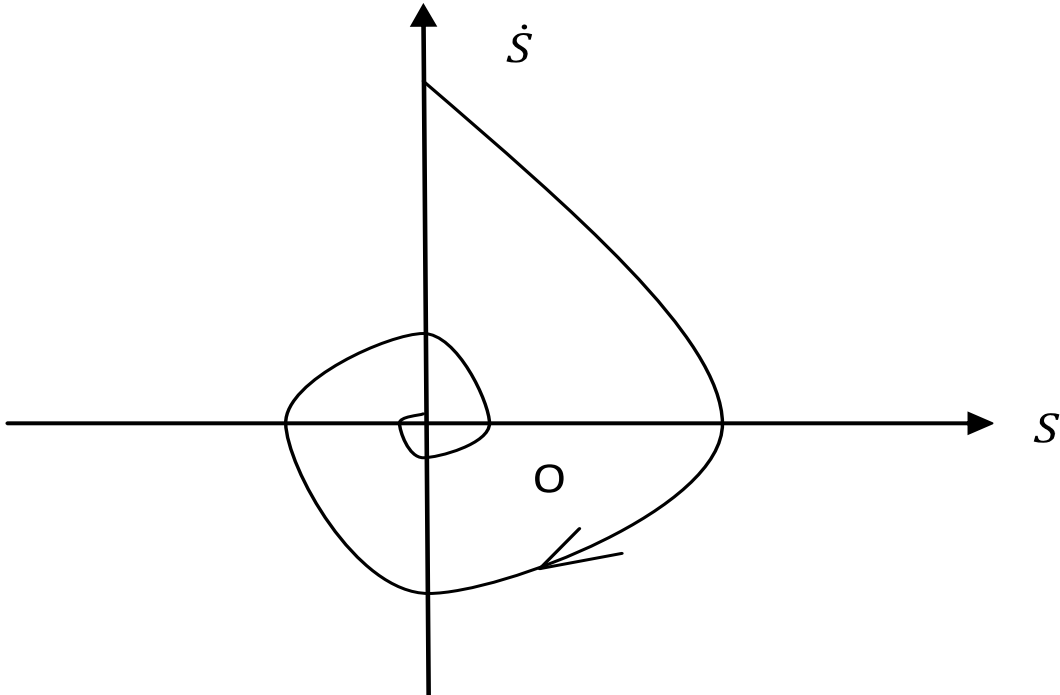


Figure 4.4: Evolution of Switching Surface during the super twisting controller action; minimizing the error between reference signal and desired output.

Super twisting algorithm (STA) had been successfully applied and implemented on various engineering and non engineering applications. In [102], STA was incorporated in order to achieve robust and chattering free control for diabetic patient to regulate blood glucose concentration level. The simulation results showed good performance against meal disturbances and make it a suitable candidate for insulin pump design. Ref. [103] used STA for altitude tracking of four rotors helicopter. The simulation results showed that the proposed scheme performed well for stabilization, robustness and tracking, in addition of chattering reduction.

In [85], STA based controller was designed using proposed dynamic model of nuclear research reactor for tracking problems. The experimental results showed that the control scheme was robust against different disturbance levels and uncertainties in addition of chattering reduction. Ref. [104] applied STA on induction motor to achieve chattering free and decoupled control over motor speed and flux by incorporating stator phase resistance, rotor speed and load torque estimators. STA was also found in [105] for chattering removal in output regulation problem of the same system. The proposed algorithm improved the accuracy as well as dynamic response of the system. In [106], the performance of STA was tested with other algorithm, so called twisting algorithm on dc drive under uncertain parameters and load conditions. It was claimed that STA is best suited for real experiments subject to certain conditions. The STA based sliding mode observer was also investigated in [107] for sensorless speed control of permanent magnet synchronous motor. The simulation results showed that the proposed scheme behaved well at low speed and was robust.

The super twisting algorithm had the advantage over other algorithms in that it did not demand the time derivatives of sliding variable. The control law used in this algorithm was composed of two terms. The first term u_a was defined in term of discontinuous time derivative whereas the second term u_b was a continuous function of sliding variable [98,108].

$$u = u_a + u_b \quad (Eq\ 4.11)$$

$$\dot{u}_a = \begin{cases} -u & \text{when } |u| > 1 \\ -K \text{ sign}(s) & \text{when } |u| \leq 1 \end{cases} \quad (Eq\ 4.12)$$

$$u_b = \begin{cases} -\lambda |s_0|^\xi \text{ sign}(s) & \text{when } |s| > s_0 \\ -\lambda |s|^\xi \text{ sign}(s) & \text{when } |s| \leq s_0 \end{cases} \quad (Eq\ 4.13)$$

The super twisting algorithm converged in finite time and the corresponding sufficient conditions were:

$$K > \frac{\Phi}{\Gamma_m}, \lambda^2 \geq \frac{4\Phi}{\Gamma_m^2} \frac{\Gamma_M(K+\Phi)}{\Gamma_m(K-\Phi)}, 0 < \xi \leq 0.5 \quad (\text{Eq 4.14})$$

where $K, \lambda, s_0, \Phi, \Gamma_m, \Gamma_M$ are some positive constants. When controlled system was linearly dependent on u , the control law could be simplified as:

$$u = -\lambda|s|^\xi \text{sign}(s) + u_a \quad (\text{Eq 4.15})$$

$$\dot{u}_a = -K \text{sign}(s) \quad (\text{Eq 4.16})$$

When $\xi = 1$ then this algorithm converges to the origin exponentially.

4.3.5 Example

To elaborate the significance of 2nd order sliding mode over 1st order sliding mode, the following 3rd order nonlinear system [32] is considered for stabilization problem.

$$\left. \begin{aligned} \dot{x}_1(t) &= x_2(t) \\ \dot{x}_2(t) &= x_3(t) \\ \dot{x}_3(t) &= F(X, t) + G(X, t) u(t) \end{aligned} \right\} \quad (\text{Eq 4.17})$$

Where

$$F(X, t) = 3 e^{x_1} + 5x_2 \sin(20t + x_1) \cos(x_2^2 + x_3^2) \quad (\text{Eq 4.18})$$

$$G(X, t) = 3 + \sin(3t + x_1 + x_2) \quad (\text{Eq 4.19})$$

$$|F(X, t)| \leq 3 e^{x_1} + 5|x_2| \quad \text{and} \quad 3 \leq |G(X, t)| \leq 4$$

It is assumed that the state vector is completely measurable and control objective is to asymptotically stabilize the states to zero with initial conditions $x(0) = [2 \ 2 \ 2]$.

The sliding surface and control law using FOSMC are designed as

$$s(x(t)) = x_3(t) + 8x_2(t) + 16x_1(t) \quad (\text{Eq 4.20})$$

$$u(t) = -U(x(t)) \text{sign}(s) \quad (\text{Eq 4.21})$$

$$\text{Where} \quad U(x(t)) = 1.5e^{x_1} + 4.5|x_2(t)| + 2|x_3(t)| + 5 \quad (\text{Eq 4.22})$$

The sliding surface and control law using SOSMC are designed as

$$s(x(t)) = x_2(t) + 4x_1(t) \quad (\text{Eq 4.23})$$

$$u(t) = \begin{cases} -\frac{h}{\Gamma_m} \Psi_0(t) \text{sign}[y_1(t) - y_1(0)] & 0 \leq t \leq T_{M_1} \quad h > 1 \\ -\mathcal{L}(t) V_{M_k} \text{sign} \left[y_1(t) - \frac{1}{2} y_{1M_k} \right] & T_{M_k} \leq t \leq T_{M_{k+1}} \quad k = 1, 2, \dots \end{cases} \quad (\text{Eq 4.24})$$

where

$$y_1 = s, \quad y_2 = \dot{s} \quad \text{and}$$

$$\Psi_0(t) = F_{1M}[\|\hat{x}(t)\|] + (C_{n-2} + q_f) Y_{10M} \quad (\text{Eq 4.25})$$

$$F_{1M}[\|\hat{x}(t)\|] = F(\|\hat{x}(t)\|) + \left(\sum_{j=1}^{n-3} C_j + (C_{n-2} + q_f) \sum_{j=1}^{n-2} C_j \right) \|\hat{x}(t)\| \quad (\text{Eq 4.26})$$

$$Y_{10M} = x_{no_{MAX}} + \sum_{j=1}^{n-3} C_j x_{j+1}(0) \quad (\text{Eq 4.27})$$

$$V_{M_k} = \zeta \gamma^* \Psi_k \quad \zeta > 1 \quad k = 1, 2, \dots \quad (\text{Eq 4.28})$$

$$\Psi_k = F_{1M}[\|\hat{x}(t)\|_{M_k}] + \frac{1}{2} d_k^2 + d_k \sqrt{4F_M[\|\hat{x}(t)\|_{M_k}] + d_k^2} \quad (\text{Eq 4.29})$$

$$d_k = \left| y_{1M_k} \right| (C_{n-2} + q_f) \sqrt{\mathcal{L}^* \Gamma_M \zeta \gamma^* + 1} \quad (\text{Eq 4.30})$$

$$\|\hat{x}(t)\|_{M_k} = q_x \|\hat{x}(T_{M_k})\| + q_y y_{1M_k} \quad (\text{Eq 4.31})$$

$$\mathcal{L}(t) = \begin{cases} \mathcal{L}^* & \text{if } \left[y_1(t) - \frac{1}{2} y_{1M_k} \right] [y_{1M_k} - y_1(t)] > 0 \\ 1 & \text{if otherwise} \end{cases} \quad (\text{Eq 4.32})$$

$$\mathcal{L}^* \in]0, 1] \cap \left(0, \frac{3\Gamma_m}{\Gamma_M} \right)$$

$$\gamma^* = \max \left(\frac{\Phi}{\mathcal{L}^* \Gamma_m}, \frac{4\Phi}{3\Gamma_m - \mathcal{L}^* \Gamma_M} \right)$$

Now after simulating the system given in (Eq 4.17), Figures 4.5-4.6 show the phase portrait of FOSMC and SOSMC where as the controller efforts are indicated by Figures 4.7-4.8.

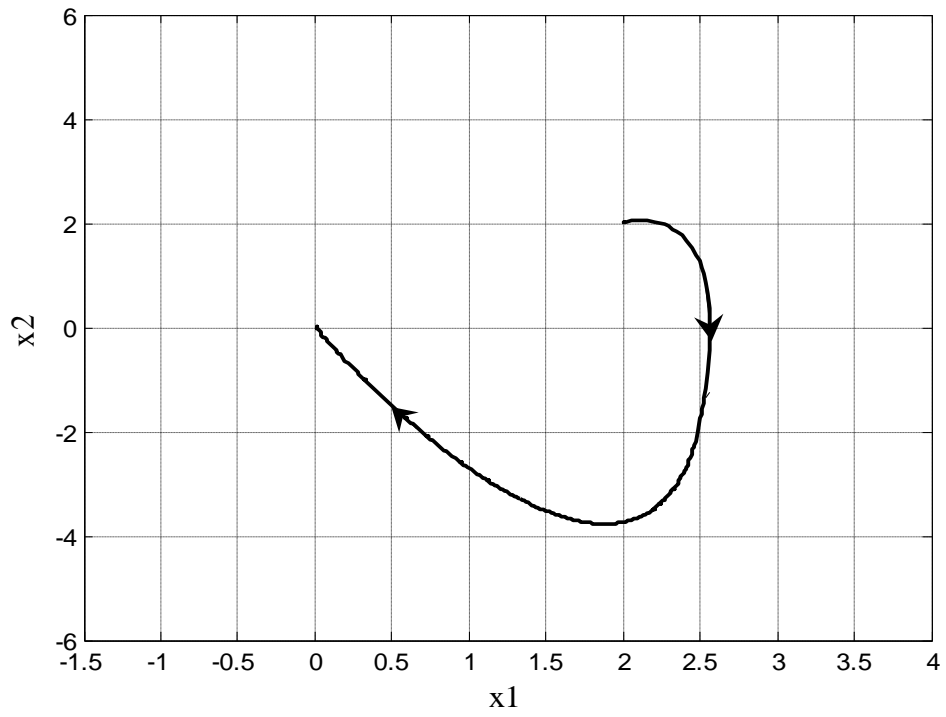


Figure 4.5: Phase portrait using FOSMC.

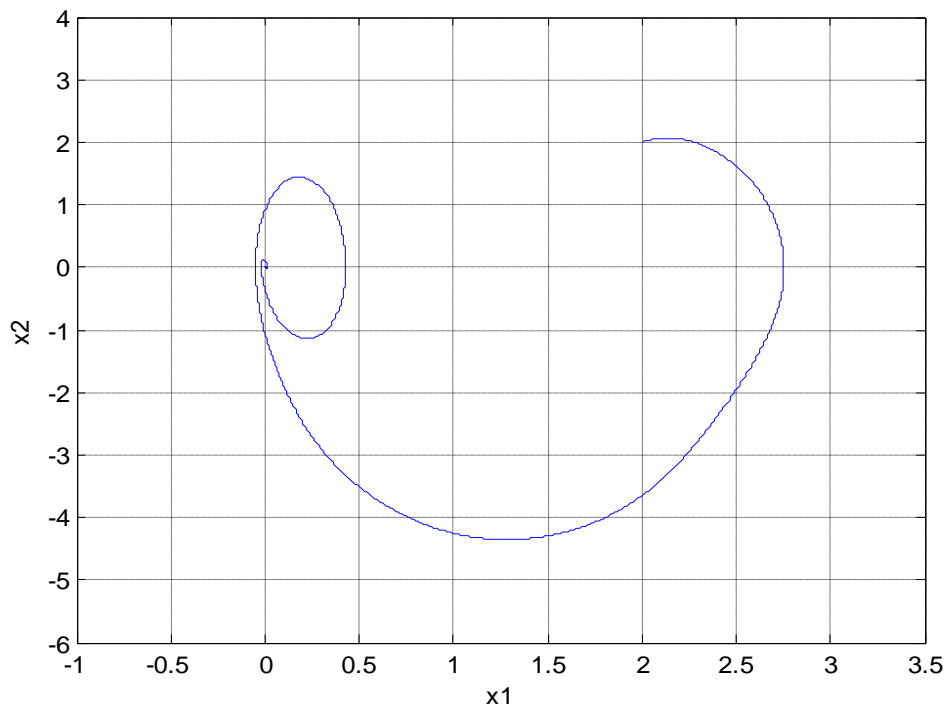


Figure 4.6: Phase portrait using SOSMC.

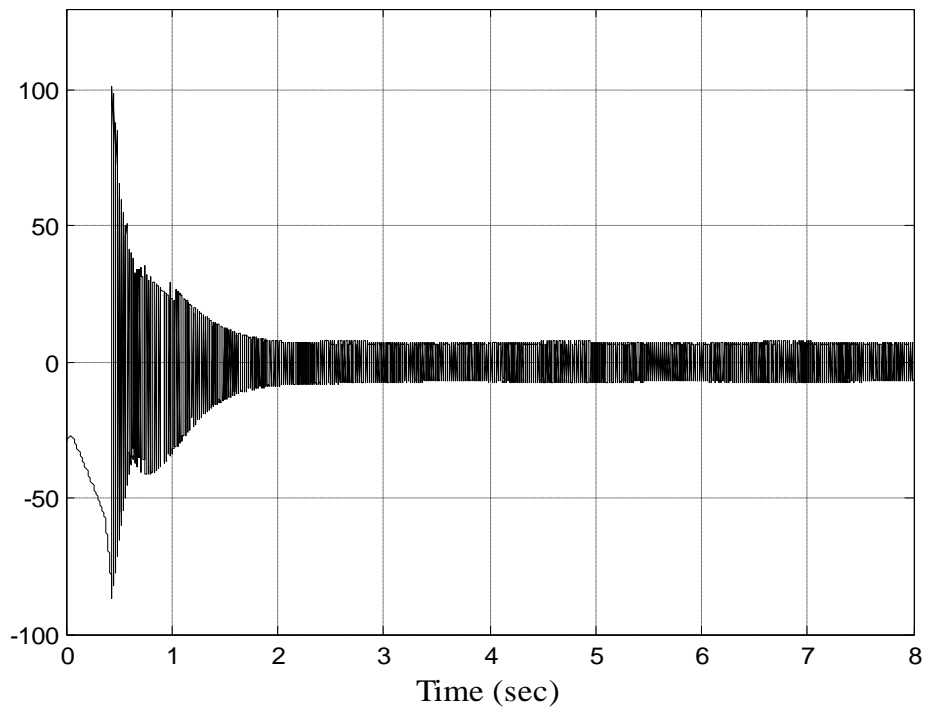


Figure 4.7: Controller effort using FOSMC.

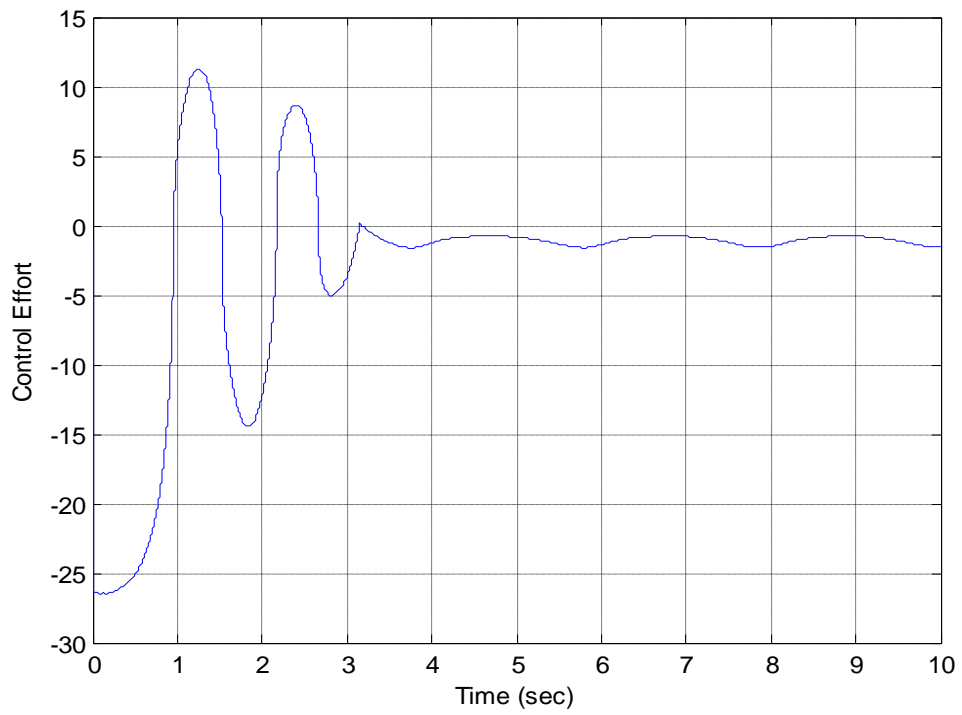


Figure 4.8: Controller effort using SOSMC.

It can be seen that SOSMC has reduced the control effort significantly as compared to FOSMC. Figures 4.9-4.10 demonstrate the system states of both the controllers.

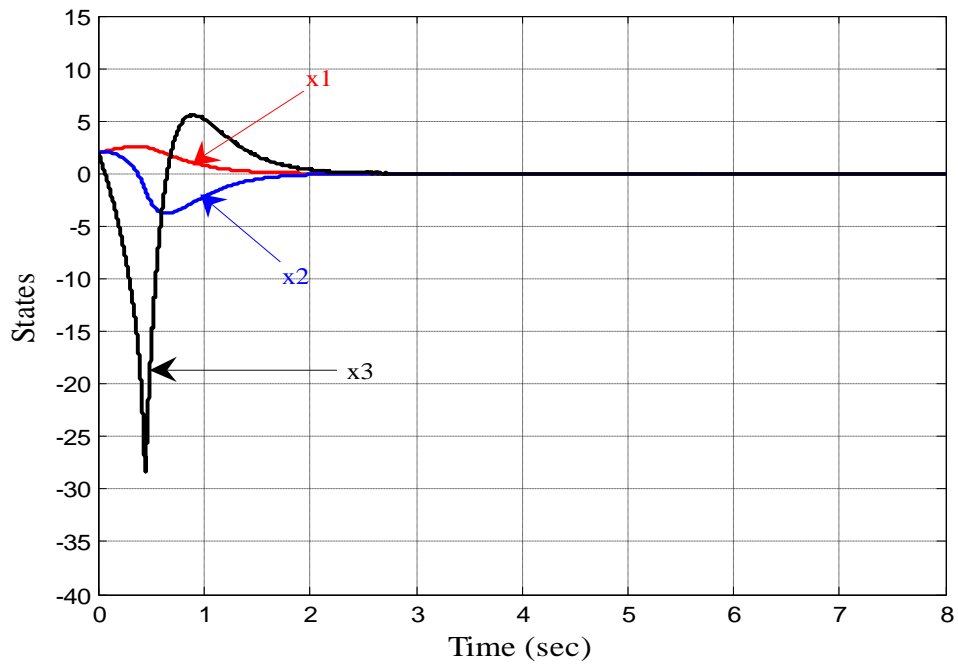


Figure 4.9: System trajectories using FOSMC.

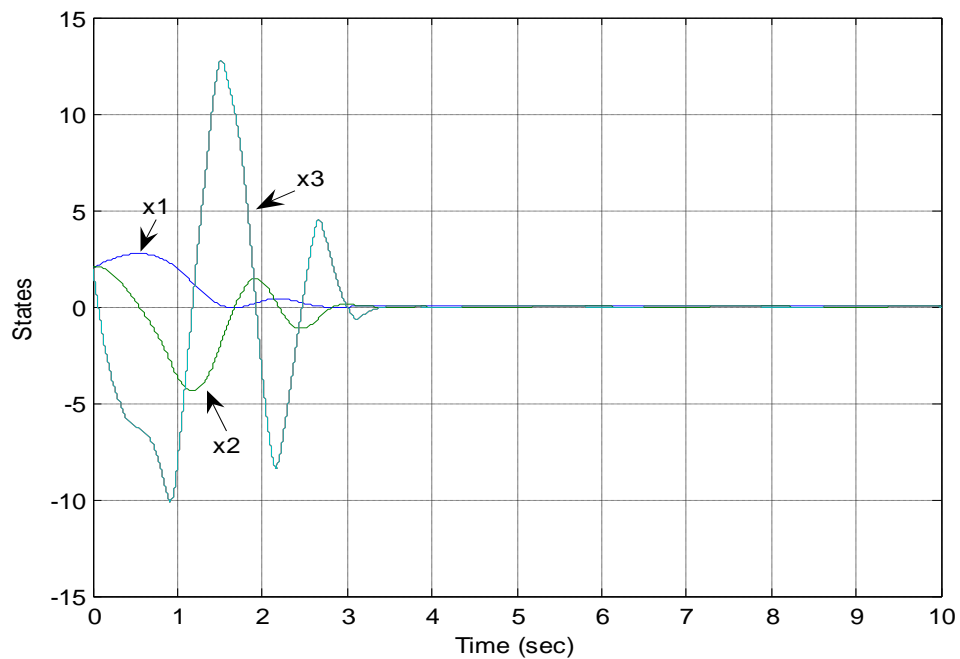


Figure 4.10: System trajectories using SOSMC.

It is clear that response of first and second state is almost the same in both FOSMC and SOSMC. However in third state, transient effect is observed. The sliding surfaces used in FOSMC and SOSMC are given in Figure 4.11.

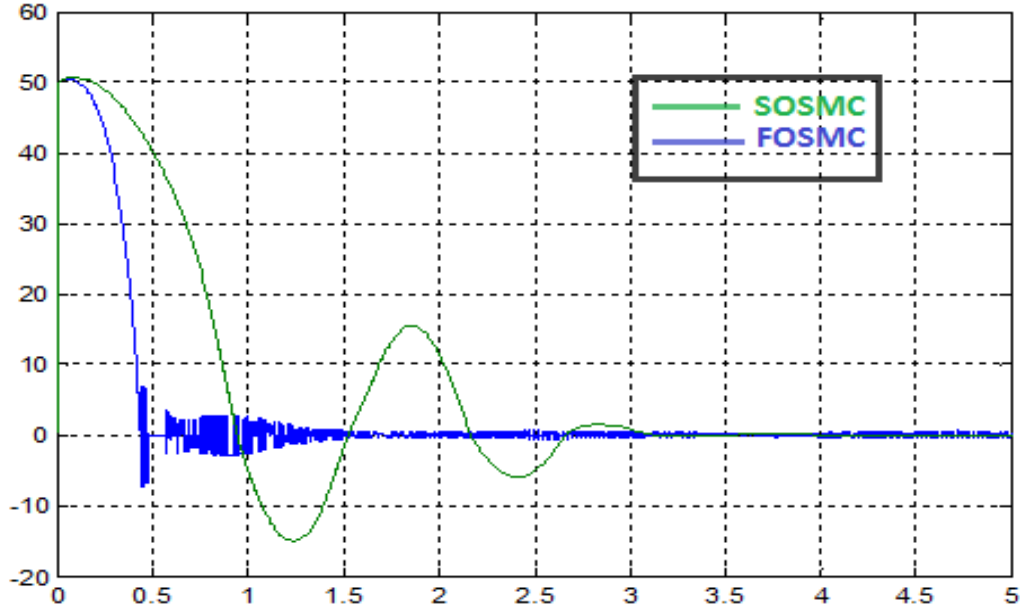


Figure 4.11: Sliding surfaces of FOSMC and SOSMC

Now it is very much clear that more chattering is observed in FOSMC. Hence it is evident that SOSMC not only reduced the control effort extensively but also diminished the chattering effect.

Now the Second Order Sliding Mode Control (SOSMC) for SR motor using Super-Twisting algorithm is designed as follows.

The control law takes the following form for speed regulation case:

$$u = [u_1 \quad u_2 \quad u_3]^T = -G^* (F + D\dot{\omega}(t) + \lambda |s|^{0.5} \text{sign}(s)) + u_a \quad (\text{Eq 4.33})$$

$$\dot{u}_a = -K \text{sign}(s) \quad (\text{Eq 4.34})$$

and for speed tracking problem

$$u = [u_1 \quad u_2 \quad u_3]^T = -G^* \left(F + D\dot{\omega}(t) + \lambda |s|^{0.5} \text{sign}(s) - \left(\ddot{\omega}_{ref}(t) + D\dot{\omega}_{ref}(t) \right) \right) + u_a \quad (\text{Eq 4.35})$$

$$\dot{u}_a = -K \text{sign}(s) \quad (\text{Eq 4.36})$$

and for position regulation problem,

$$u = [u_1 \quad u_2 \quad u_3]^T = -G^* (F + D_1 \dot{\omega}(t) + D_2 \omega(t) + \lambda |s|^{0.5} \text{sign}(s)) + u_a \quad (\text{Eq 4.37})$$

$$\dot{u}_a = -K \text{sign}(s) \quad (\text{Eq 4.38})$$

Where D_1, D_2 and D are positive constants and $G^* = G^T (GG^T)^{-1}$

Note: - The value obtained from integration of \dot{u}_a is a single scalar and will be added to each element of vector.

4.4 Simulation Results of HOSM Using STA and Commutation Scheme

The effectiveness of the proposed controllers is evaluated through simulations carried out using MATLAB/SIMULINK software. The parameters of SR motor used for simulations are given in Table 1, Chapter 2. The schematic of driver circuit used to drive the motor phases is shown in Figure 4.12, which uses only one leg of the H-bridge as our proposed controllers require only positive phase voltage.

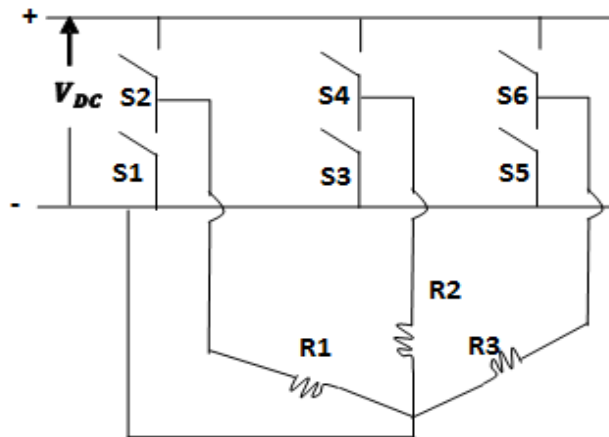


Figure 4.12: Driver circuit used for energizing motor phases.

The FOSMC and SOSMC designed in Section 3.4 and 4.3 along with the commutation scheme developed in Section 2.3 are applied for speed regulation, speed tracking as well as position regulation problems. For comparison purpose, sliding

mode controller of [24] is also implemented. Simulation results are presented in Figures 4.13-4.36. A number of advantageous features of FOSMC and SOSMC with the designed commutation scheme are elaborated and compared to the conventional control where all phases are excited, the latter can also be seen for example in [24] and [22].

4.4.1 Comparison of Speed Response of FOSMC and SOSMC to A Step Command

Figure 4.13 compares the outputs of FOSM & SOSM controllers developed in this work with that of another sliding-mode controller reported in [24] for the case where the motor is commanded to operate at 10 rad/s from its stand still position. It can be observed that the motor speed converges to the desired value more quickly for the proposed commutation scheme based FOSM and SOSM controllers. Figures 4.14-4.17 show a performance test for FOSMC and SOSMC for a reference speed of 10 rad/s. To observe the performance of both controllers deeply, we have taken up some close up view of the plots. It can be visualized from Figure 4.14 and Figure 4.16 that FOSMC shows higher magnitude of chattering than SOSMC. The same results are verified for a motor speed of 20 rad/s in next simulation tests shown in Figure 4.17 and Figure 4.18 where as control efforts are shown in Figures 4.19-4.20.

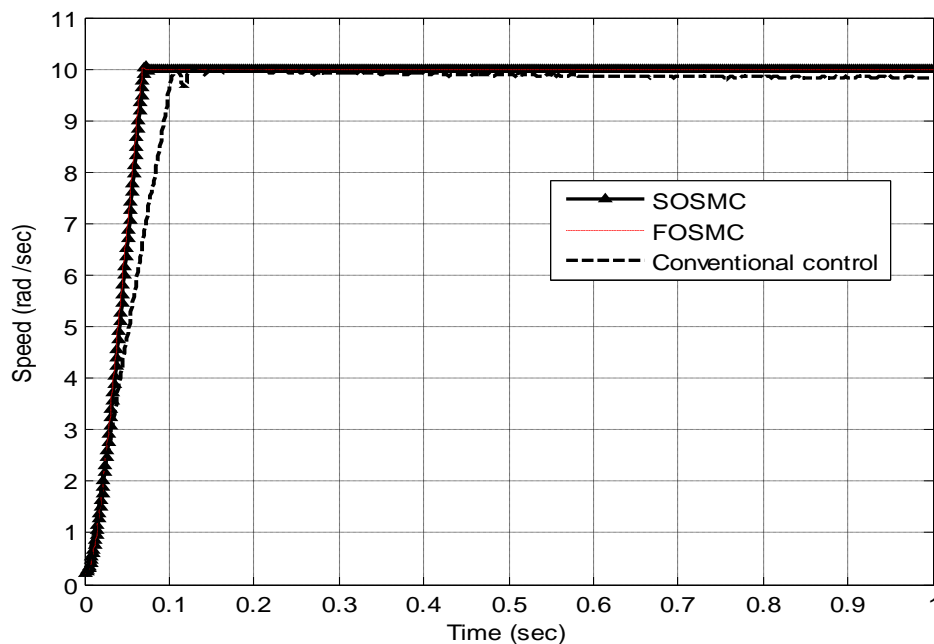


Figure 4.13: Speed response of FOSMC and SOSMC to a step command.

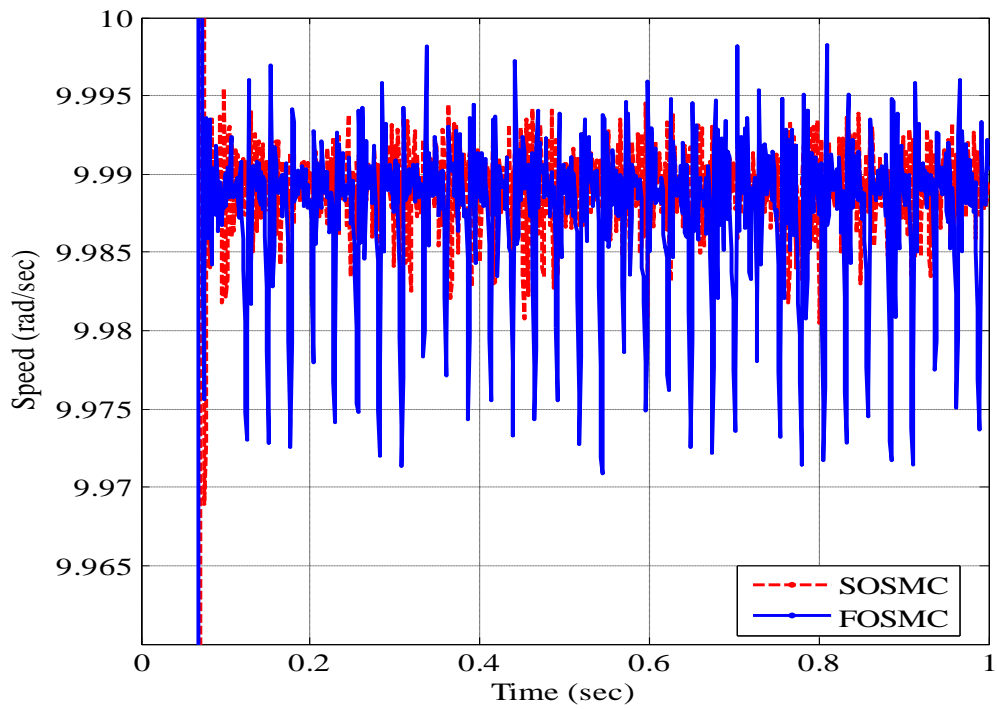


Figure 4.14: A Close-up View of Response of both FOSMC and SOSMC to a step command. The high magnitude of chattering signal of FOSMC is clearly noticeable.

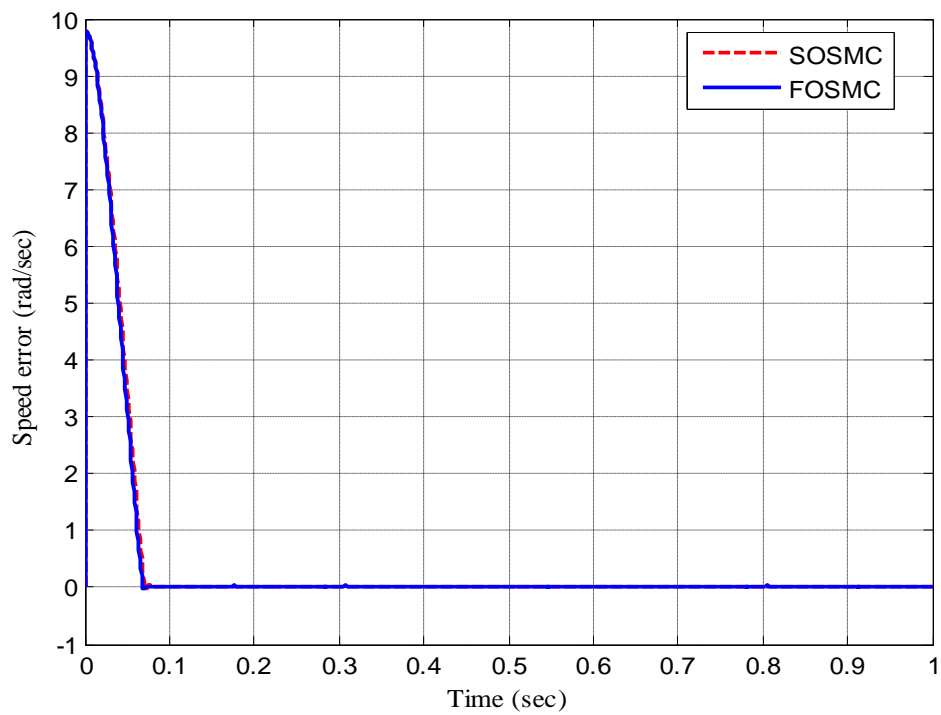


Figure 4.15: Error plot of Speed Response of FOSMC and SOSMC to a step command.

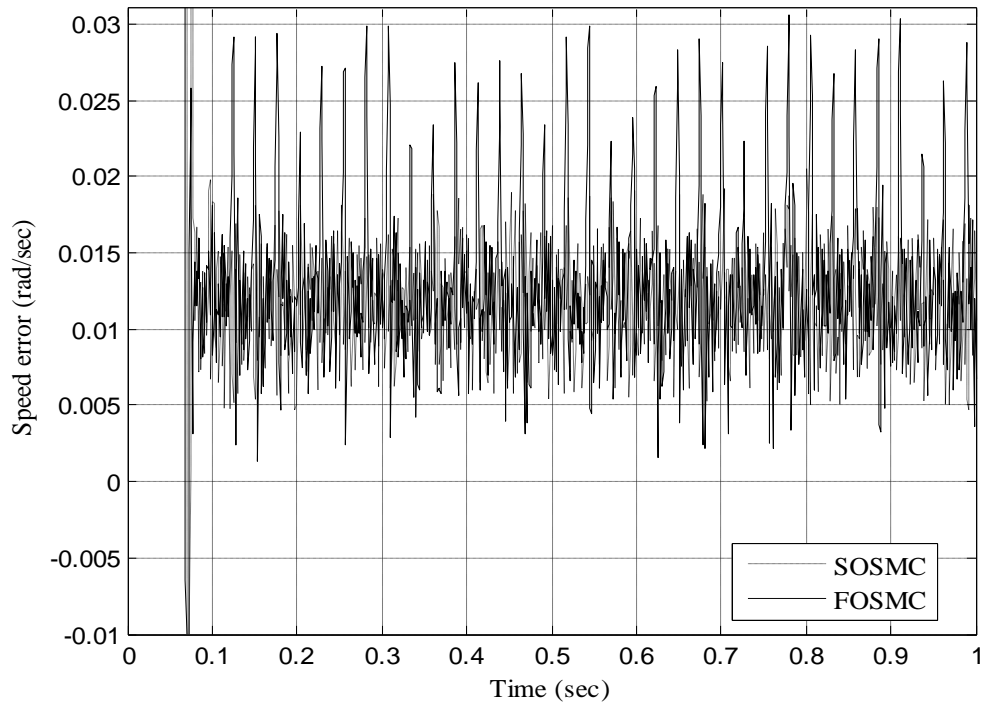


Figure 4.16: A Close-up View of Error plot of Speed Response for FOSMC and SOSMC to a step command. The reduced amount of error magnitude is clearly visible.

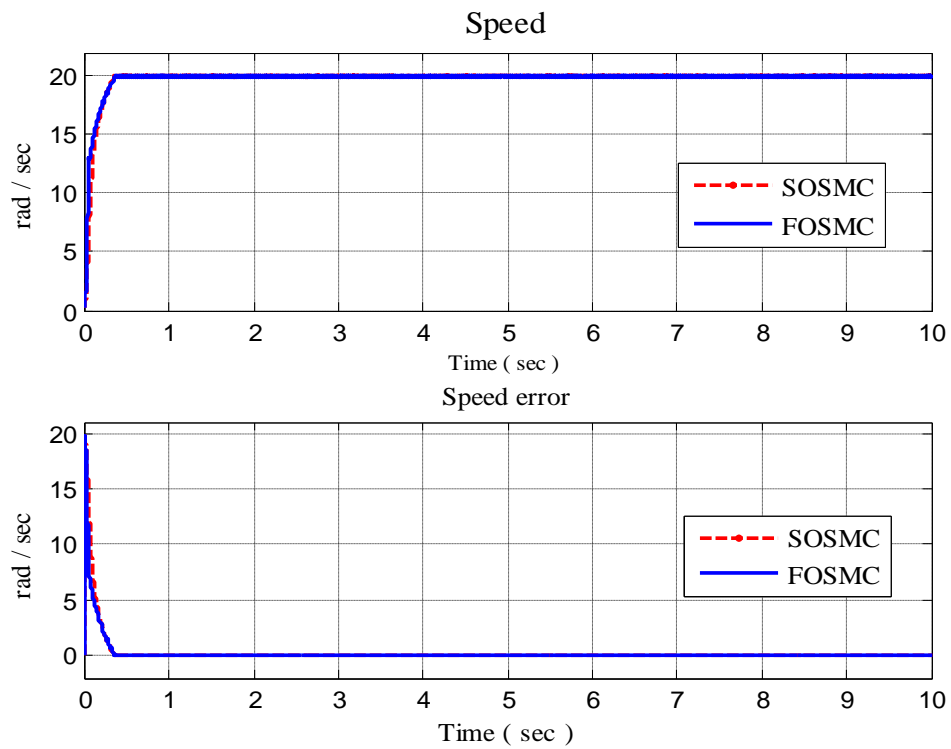


Figure 4.17: Speed Response and Speed error plot of FOSMC and SOSMC to a step command for a relative speed of 20 rad/s.

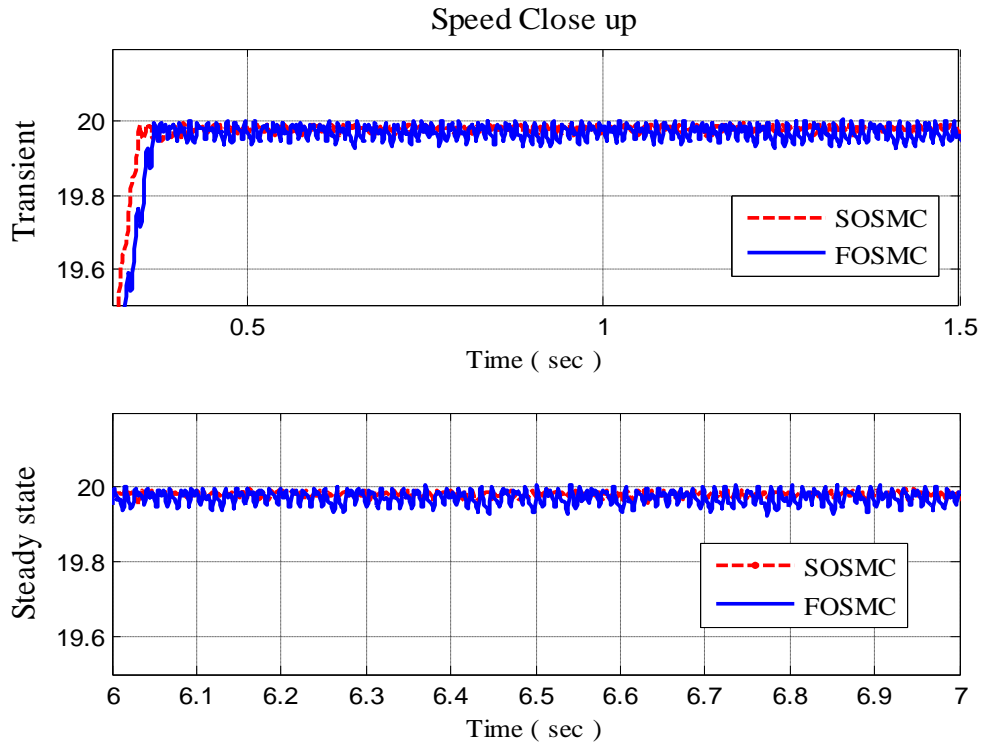


Figure 4.18: A close up view of Speed Response of both FOSMC and SOSMC to a step command in the starting and steady state regions. The high magnitude of chattering signal of FOSMC is clearly visible.

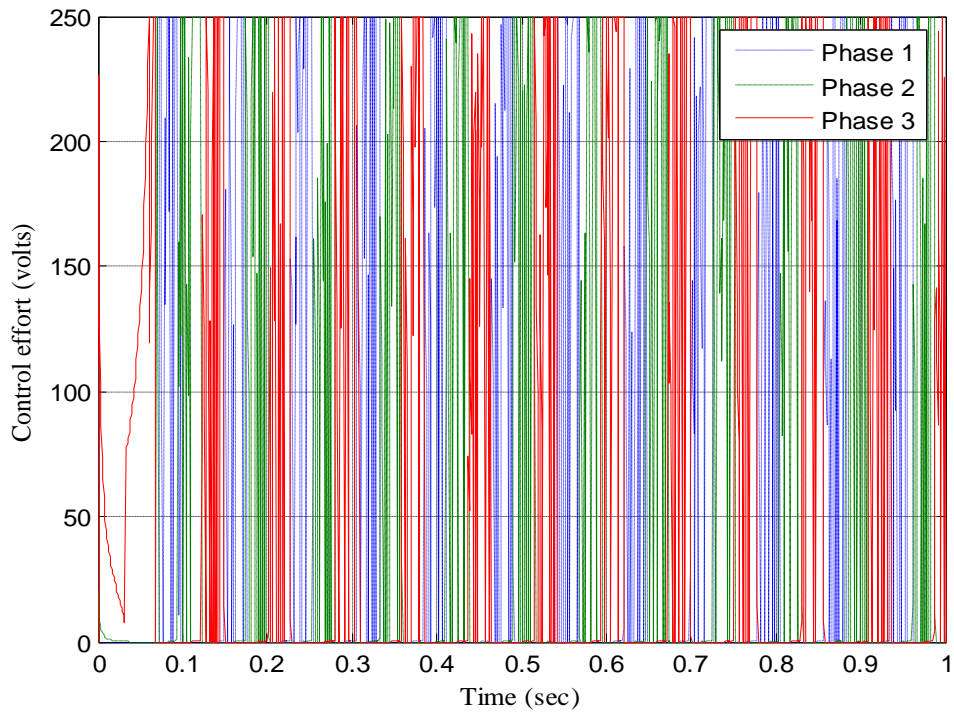


Figure 4.19: Control effort using FOSMC.

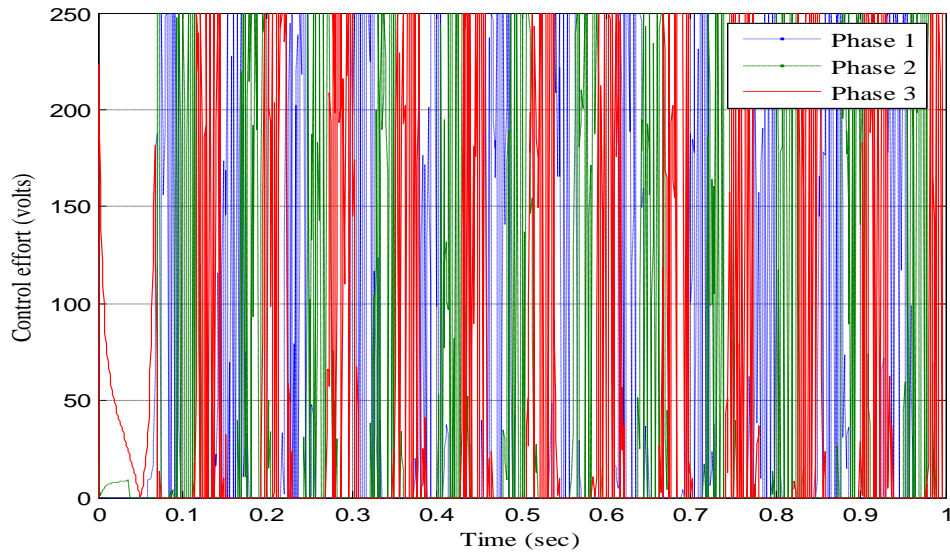


Figure 4.20: Control effort using SOSMC.

4.4.2 Comparison of Position Response of FOSMC and SOSMC to A Step Command

The response of controllers is shown in Figure 4.21 when SR motor is commanded from initial position 0.2 radian to attain a reference position 30 radians. Figure 4.23 gives the respective position error and, Figure 4.22 and Figure 4.24 are their close ups.

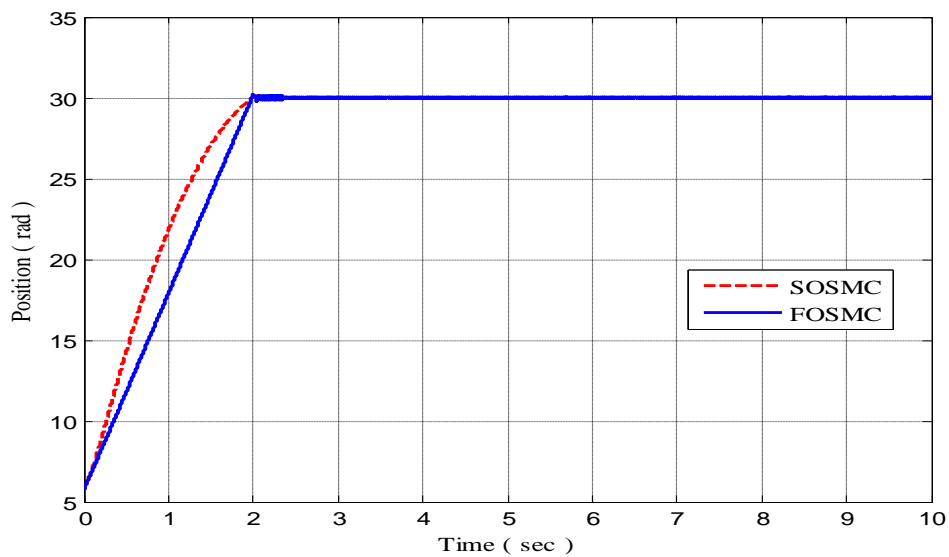


Figure 4.21: Position response of FOSMC and SOSMC to a step command.

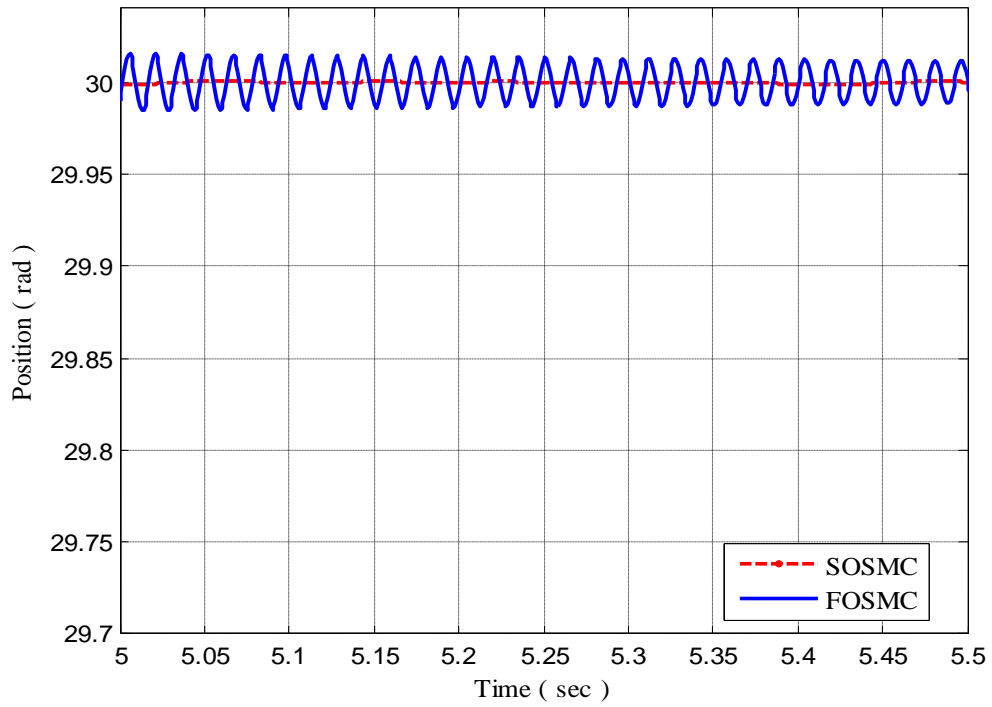


Figure 4.22: A close-up view of responses of both FOSMC and SOSMC to a step command. The high magnitude of chattering signal of FOSMC is clearly noticeable.

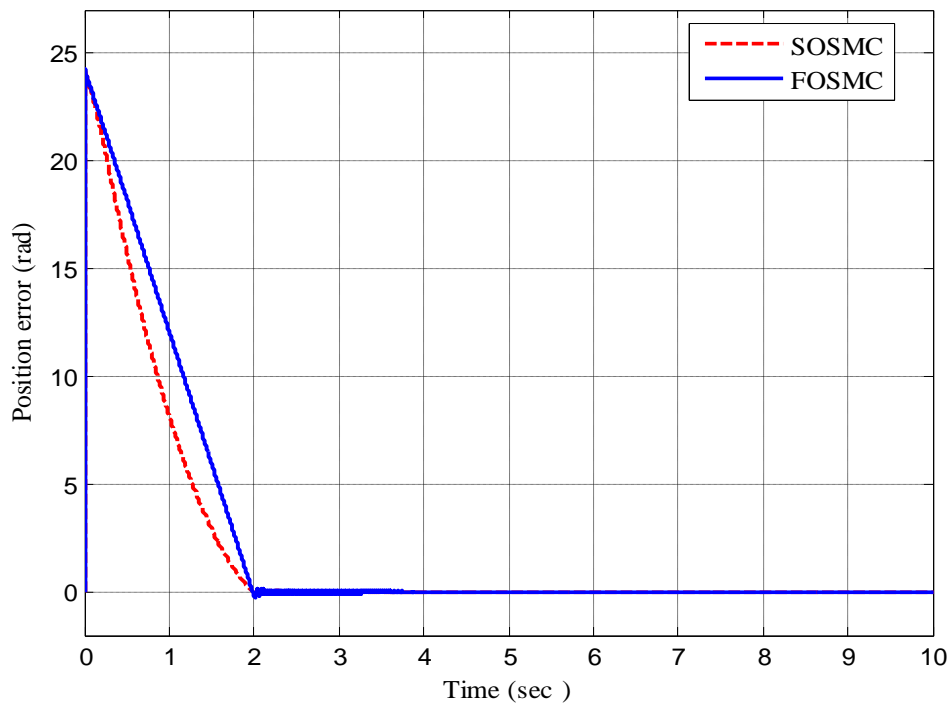


Figure 4.23: Error plot of position responses of FOSMC and SOSMC to a step command.

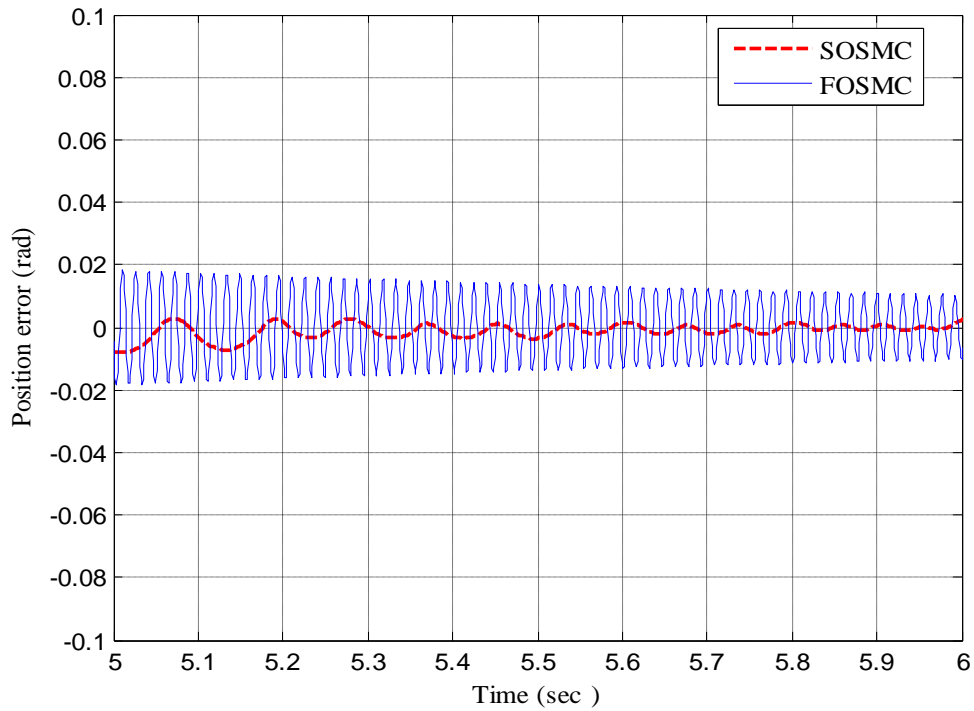


Figure 4.24: A close-up view of error plot of position responses for FOSMC and SOSMC to a step command in initial stage of steady state.

From these Figures, it is shown that motor position converges to its reference position within 2 seconds. It is also clear from Figure 4.22 that FOSMC is producing higher magnitude of chattering than the proposed controller SOSMC. Figure 4.24 also supports this statement.

4.4.3 Comparison between FOSMC and SOSMC With Respect to Power Loss, Input Phase Voltages and Torques in Speed Regulation Problem

A comparison of power loss in motor phases during operation is shown in Figure 4.25. Power loss in conventional design is about 85 kW whereas even the FOSMC which suffers from the same level of chattering has much reduced power loss, i.e. only 19 KW.

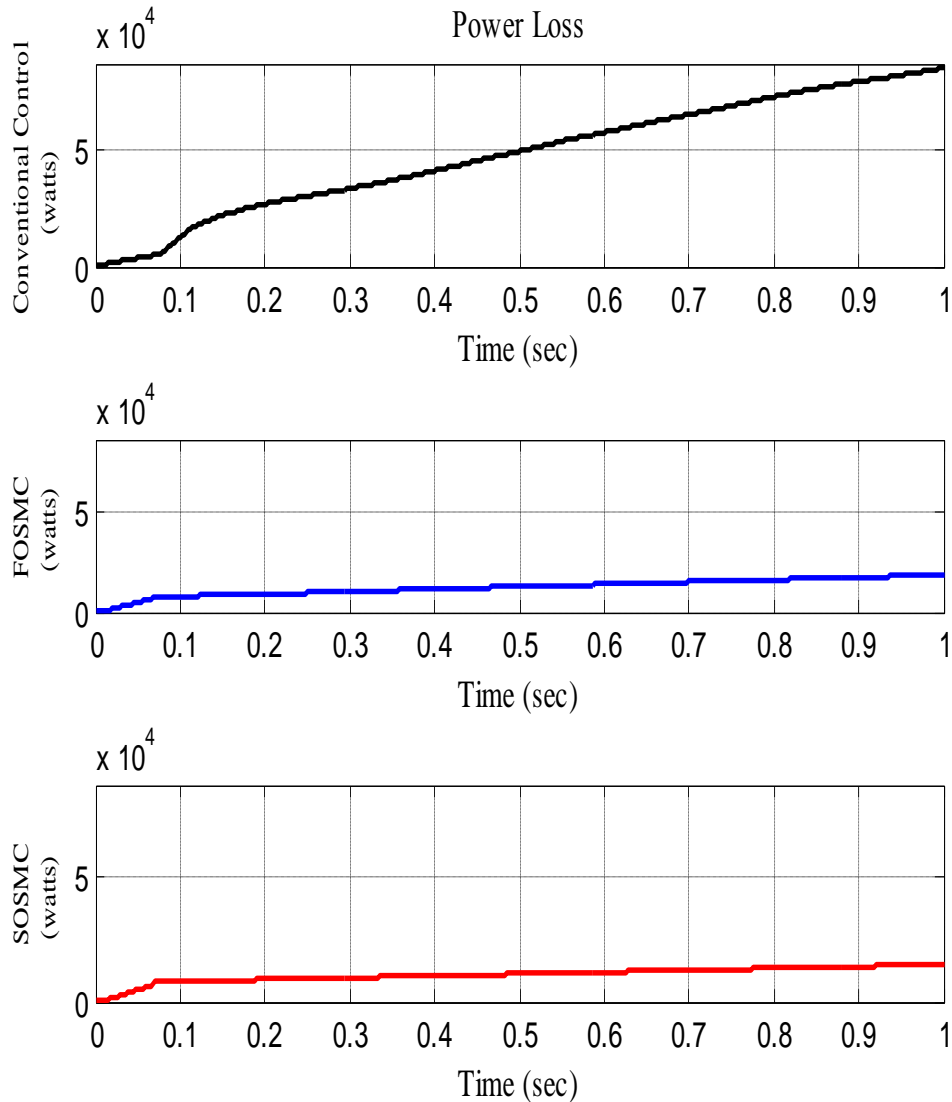


Figure 4.25: Power loss in Conventional Design is about 85 kW. Using FOSMC it is about 19 KW. Using SOSMC it even lowers to about 15 kW.

This power saving can be mainly attributed to the commutation scheme employed in FOSMC. SOSMC with its reduced level of chattering reduces the power loss further to 15 kW which confirms the effectiveness of the proposed design. Figure 4.26 and Figure 4.27 highlight the main reason behind this power savings (area under the curve, which is less for SOSMC).

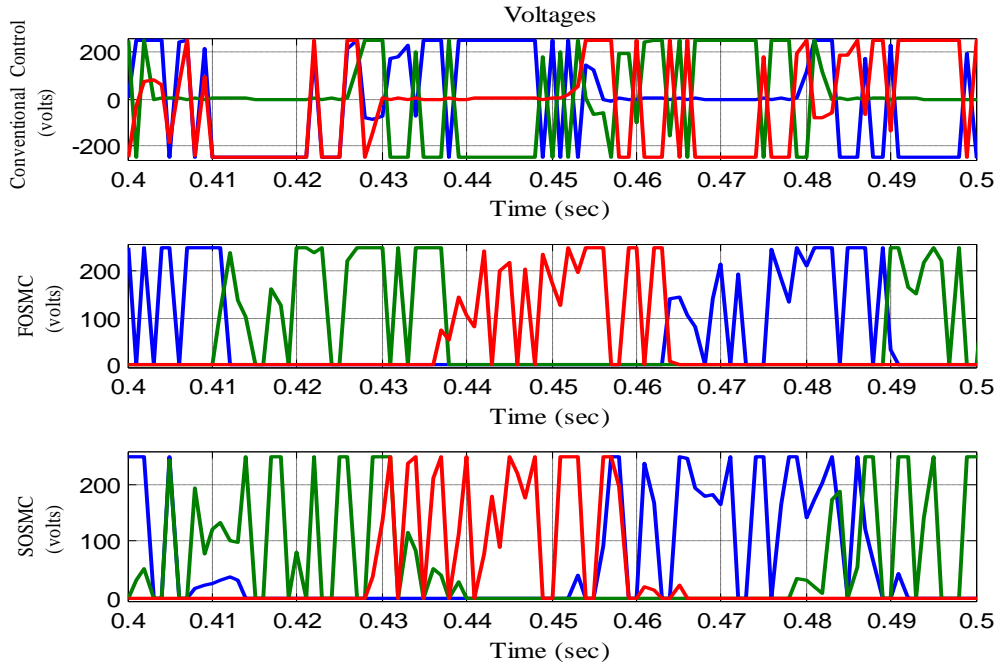


Figure 4.26: 3-phase voltages during initial stage of steady state response.

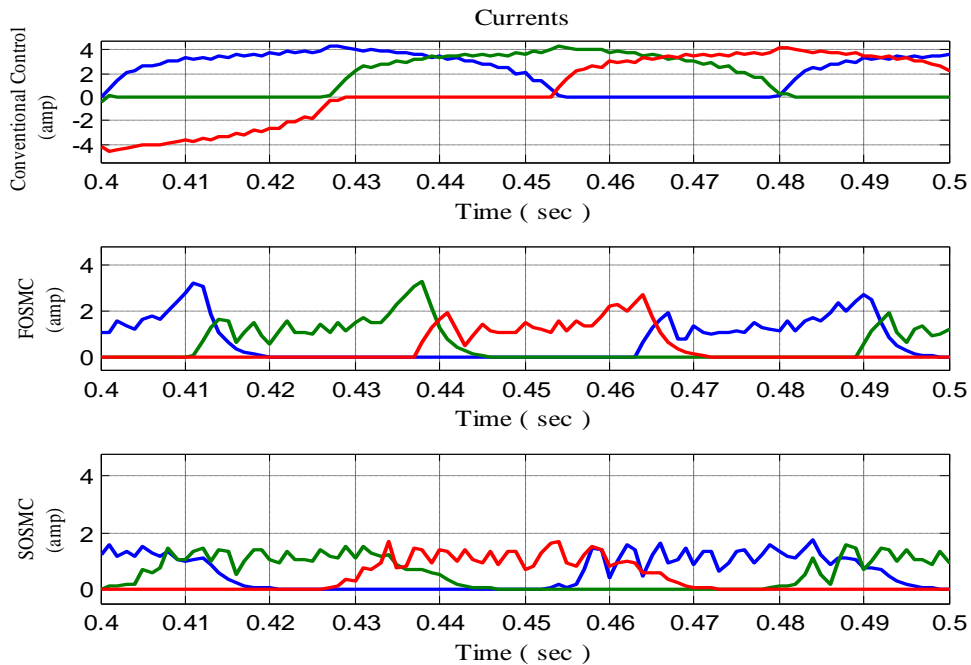


Figure 4.27: 3-phase currents during initial stage of steady state response.

The three phase voltages during initial stage of steady state operation are shown in Figure 4.26. It is well clear from these figures that in commutation based controllers, only one or two motor phases are selected for generation of control efforts at any given instant of time. The conventional design, on the other hand, energizes all the three phases simultaneously and applies bipolar voltages to motor phases. A closer

focus on the time interval 0.44 - 0.45 sec is of particular interest. It shows that even in those cases where apparently only two of the three phases are being energized by the conventional sliding-mode controller, the controller has selected wrong phases for the generation of control efforts. Despite that maximum voltages are being applied to the two phases resulting in large phase currents, the torques produced by the two phases are cancelling each other. This results in much reduced net motor torque as compared to the torques produced by each phase independently.

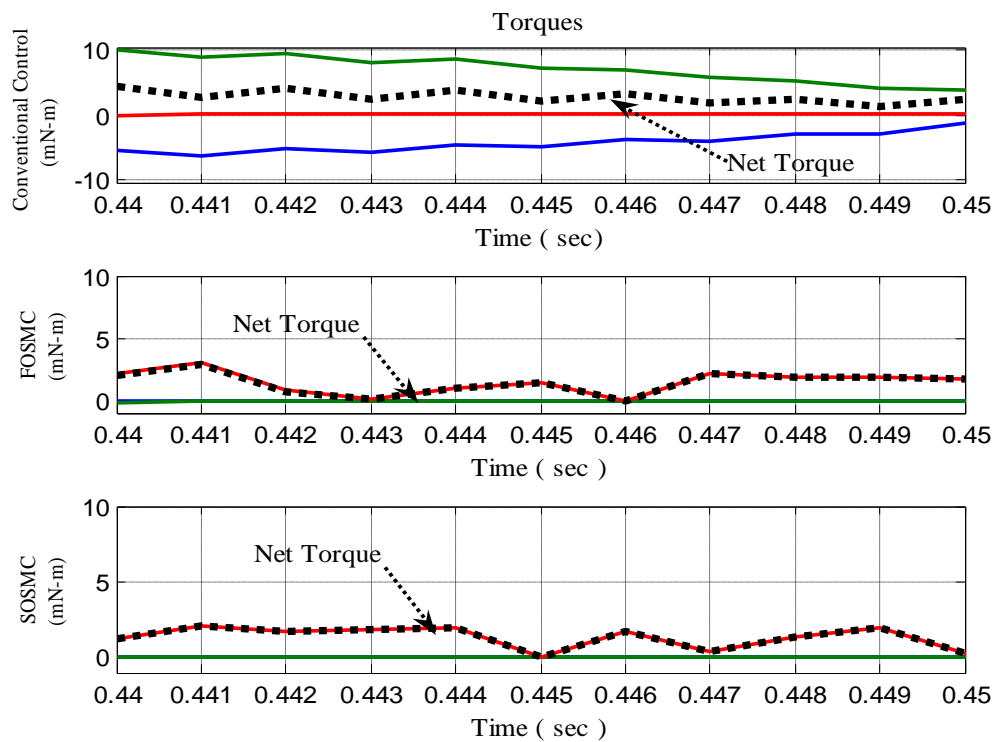


Figure 4.28: Torques during initial stage of steady state response.

This amounts to wastage of efforts and also results in increased power loss in motor windings. The commutation based FOSMC and SOSMC use only unipolar voltages with reduced voltage levels thus resulting in lower phase currents. As a result, proposed controllers (FOSMC and HOSMC) produce lesser individual torques of the same polarities which add up to give a higher net torque. The torques produced by three individual phases and net torque are shown in Figure 4.28 which verify the above statement.

4.4.4 Comparison between FOSMC and SOSMC With Respect to Power Loss, Input Phase Voltages and Torques in Position Regulation Problem

Figure 4.29 and Figure 4.30 represent the three phase input voltages when motor is directed to attain the desired position of 30 radians. It can be observed from these Figures that SOSMC saves the power consumption as the phase voltage values in SOSMC are low due to less area under the curve.

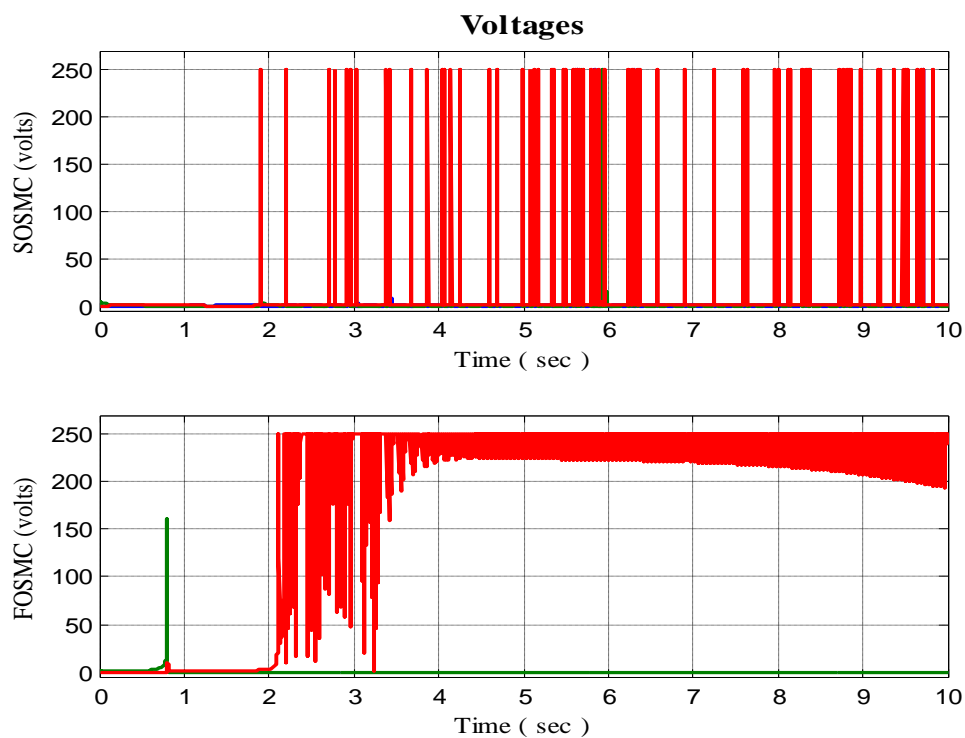


Figure 4.29: Phase voltages during simulated period for a simulation run of 10 seconds when motor is directed to obtain a desired position 30 radian

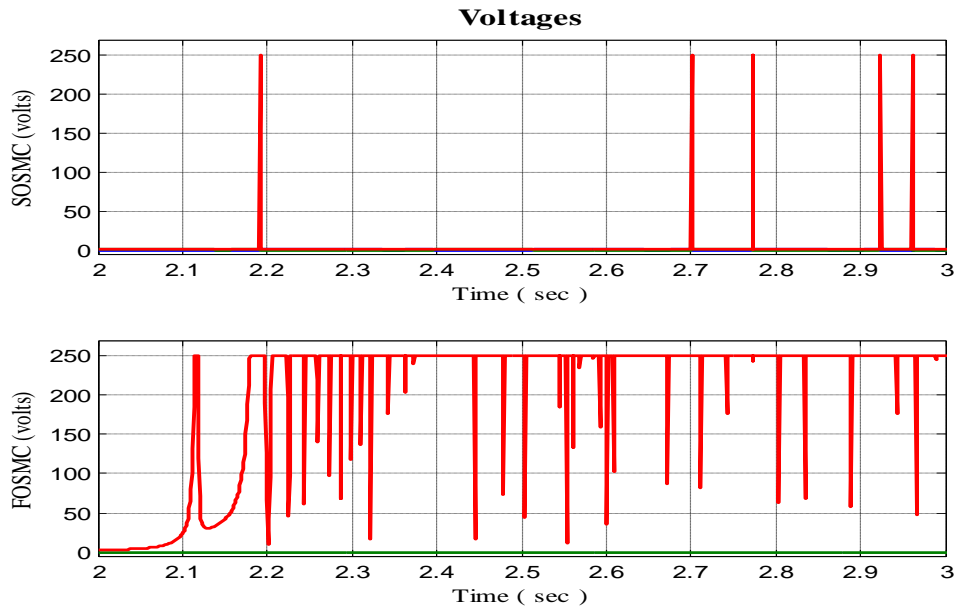


Figure 4.30: Phase voltages during transient response seconds when motor is directed to obtain a desired position 30 radian.

A comparison of power loss in motor phases in position regulation problem is also carried out in Figure 4.31 at transient state. Figure 4.32 represents the respective 3-phase currents. Individual torques and net torque is given in Figure 4.33. Power Loss in FOSMC is about 0.66 KW where as in SOSMC; it is just 0.34 KW which also confirms the effectiveness of the proposed design.

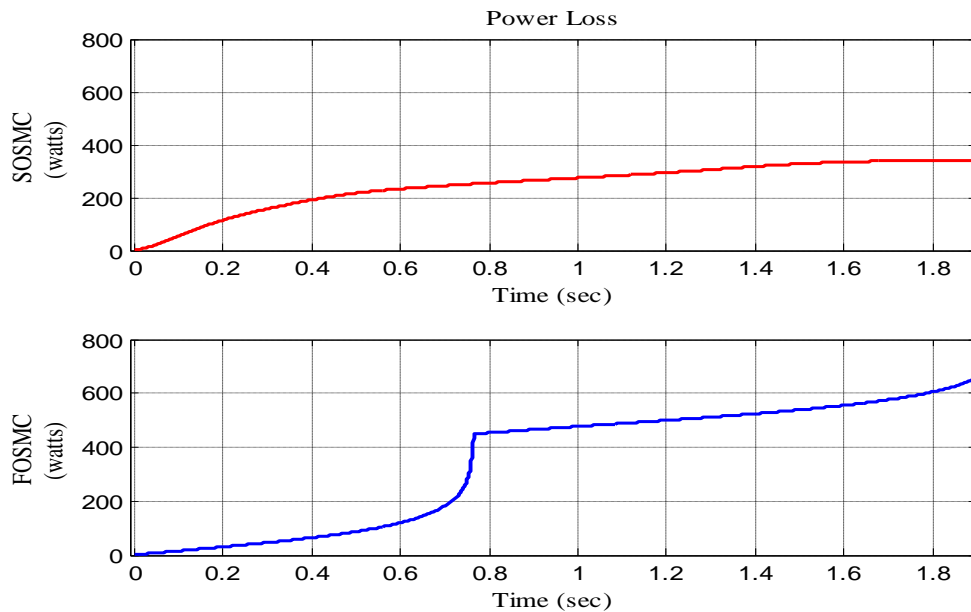


Figure 4.31: Power Loss during transient state when SR motor is commanded to attain a desired position 30 radian.

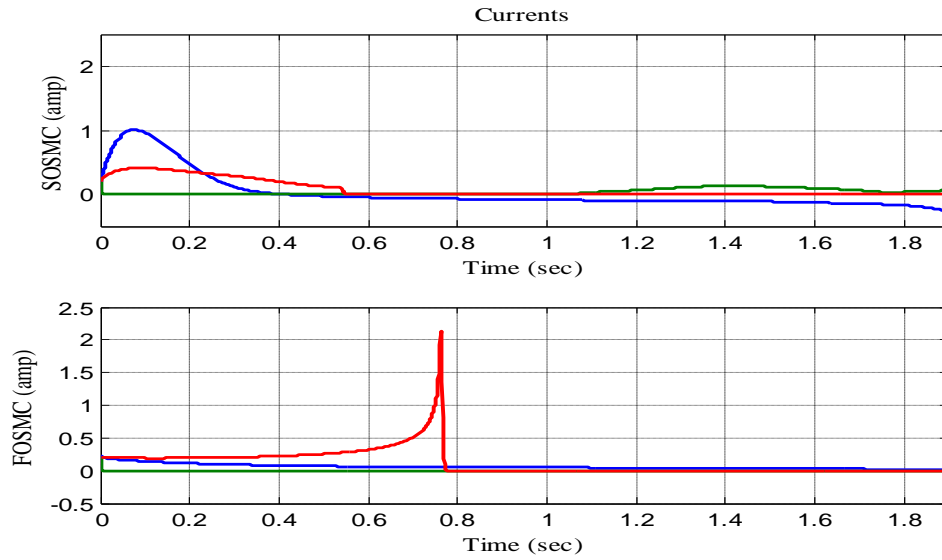


Figure 4.32: Power Loss during transient state when SR motor is commanded to attain a desired position 30 radian..

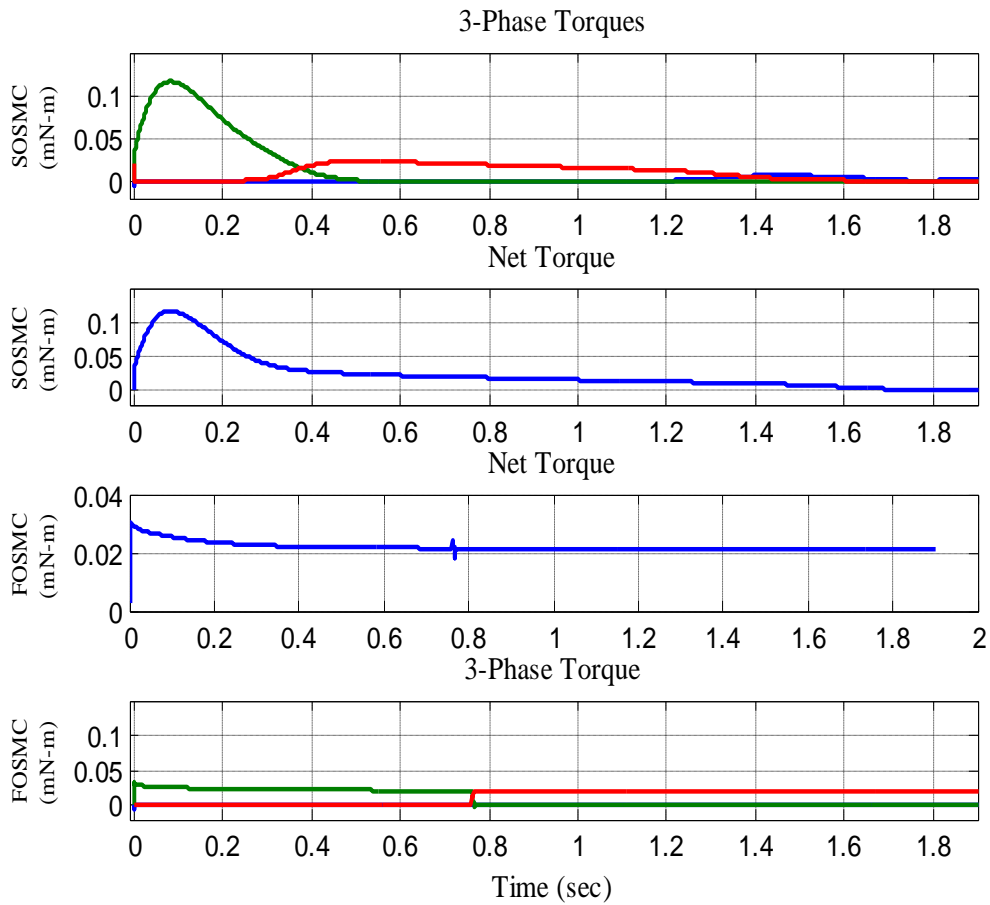


Figure 4.33: 3-Phase Torque and Net Torque during transient state when SR motor is commanded to attain a desired position 30 radian.

4.4.5 Comparison of Speed Response of FOSMC and SOSMC to A Sinusoidal Signal

Tracking performance of FOSMC and SOSMC can be reflected from Figure 4.34 where sinusoidal signal is selected for comparison test. Figure 4.35 gives clear picture of what is happening at the different points of one sinusoidal cycle and Figure 4.36 gives the speed error of both the controllers.

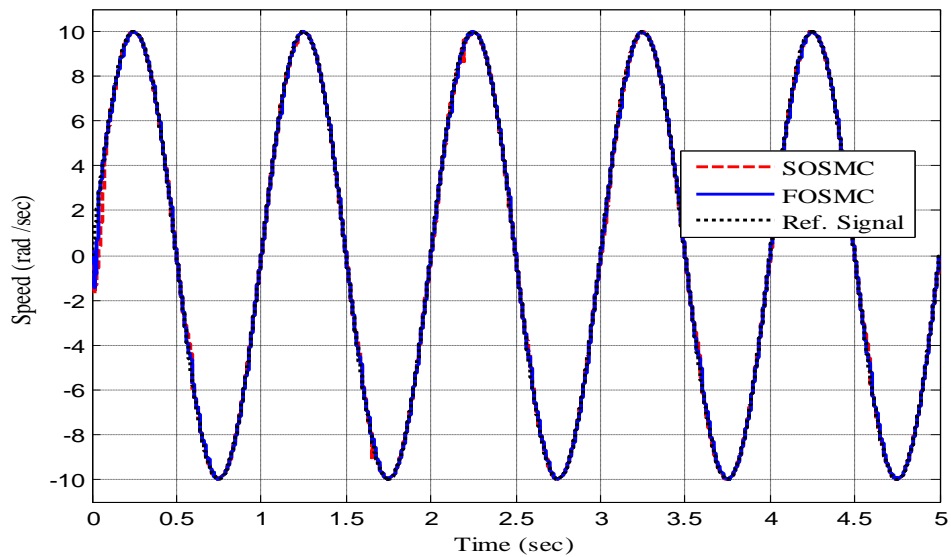


Figure 4.34: Speed response of proposed design for sinusoidal signal .

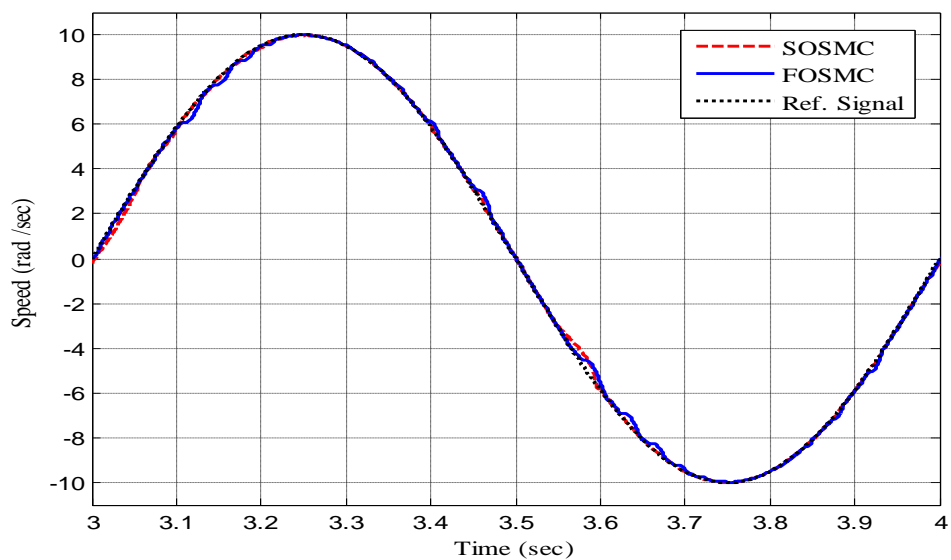


Figure 4.35: A Close-up of Speed response of proposed design for sinusoidal signal.

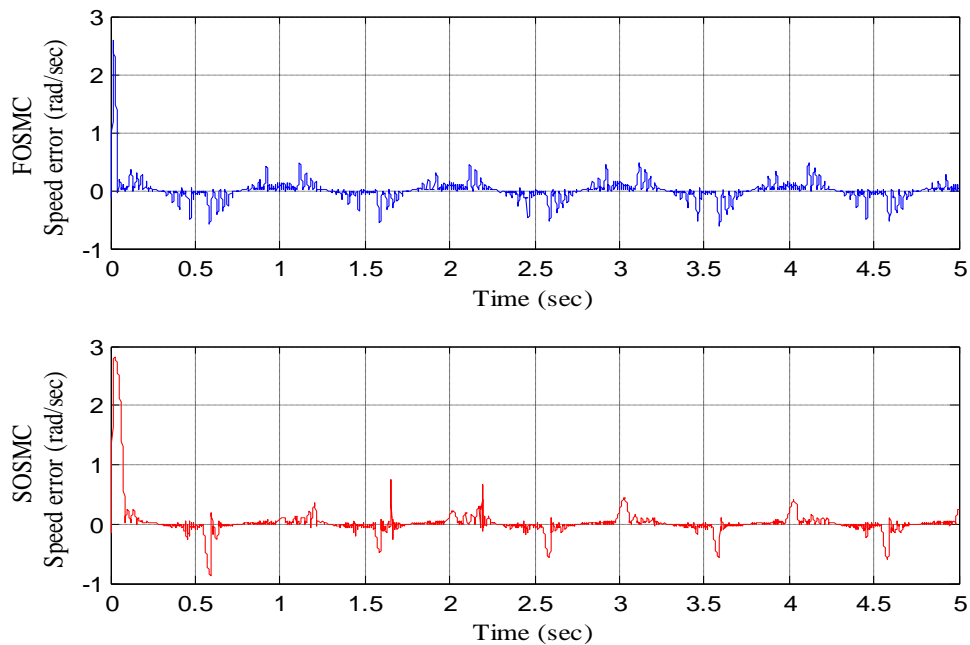


Figure 4.36: Error response using FOSMC and SOSMC.

It is clear from Figure 4.36 that FOSMC is showing higher magnitude of chattering, while SOSMC is producing smaller spikes whenever sinusoid crosses the datum (zero) line. It is a well documented fact that high frequency or high magnitude of chattering of a sliding control is dangerous when an implementation is done and an actuator has to obey a sliding/ switching control command. Therefore, it is established that SOSMC is producing better overall results for SR motor control.

The results of these simulations clearly indicate that commutation scheme based sliding-mode controllers developed in this thesis show promising results. These results are good enough to establish the fidelity of both designs in tracking as well as regulation applications. A selection out of these two schemes would depend upon a number of factors, some of which are highlighted below:

- The magnitude of error a designer can safely tolerate.
- The effect of chattering on the actuator action.
- The actuator safety while dealing with chattering in the actuation signal.
- The natural frequency of actuator, and the frequency and magnitude of chattering, etc.

4.5 Conclusion

FOSMC and SOSMC were simulated for speed regulation, speed tracking and position regulation problems using proposed commutation scheme described in Chapter 2. Chattering in conventional sliding mode control is dangerous for electro-mechanical system because it excites unmodelled dynamics that makes system unstable. HOSM is one of the solutions of chattering removal in addition of robustness and order reduction. Moreover it can also be stated that the proposed controller SOSMC can only be used for chattering reduction as well as for power saving. This feature is especially very important for SR motor control, due to reduced chattering; wear and tear problem of actuators is reduced.

Chapter 5

ROBUSTNESS OF THE PROPOSED CONTROL

This chapter deals with robustness, the important characteristic of the proposed controllers. The significant results are elaborated through simulation study. In Sections 5.1-5.2, performance of the proposed controllers SOSMC is tested and compared with FOSMC against parameter variation such as moment of inertia, coefficient of friction, resistance and external disturbances. Figures 5.1-5.19 are sketched for this purpose. Section 5.3 concludes the chapter.

5.1 Robustness

High performance applications demand that the proposed design should be robust against parameter variations and external disturbances. In case of SR motor, the most common external disturbance is load torque. The motor is assumed to operate under no torque load with a speed of 10 radian/sec. Motor is also commanded to achieve a desired position of 30 radians from its standstill position. To test the performance of the proposed controllers, we also apply the same change on FOSMC for comparison purpose.

5.1.1 Robustness against External Load

Figures 5.1-5.7 show the motor response when a sudden change in torque load is occurred. We would see its impact on speed as well as on position application.

5.1.1.1 Comparison of Speed Responses of SR Motor with Sudden Change in Torque Load

Figure 5.1 depicts the response when a sudden change in torque load from 0 to 2 N-m at $t = 0.5$ second is applied and then again removed at $t = 0.6$ second when motor was running at 10 rad/sec. It is evident from the Figure 5.2 that FOSMC exhibits a large amount of chattering during this time interval 0.5-0.6 second, whereas SOSMC does not allow a bigger dip and keeps the motor closer to its desired speed. However both controllers produce negligible amount of overshoot and steady state error.

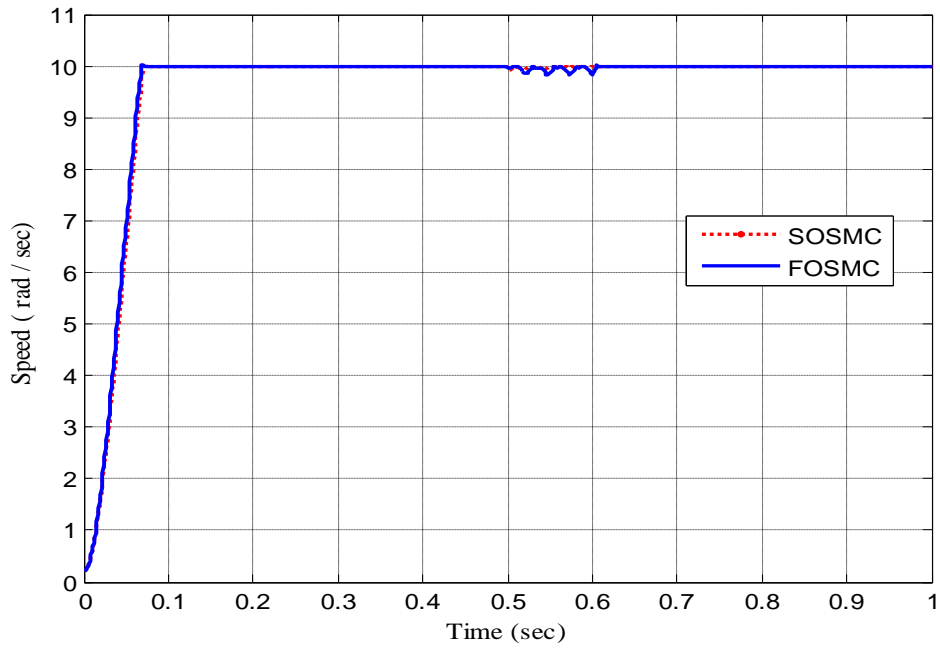


Figure 5.1: Speed response of SR motor with sudden change in torque load.

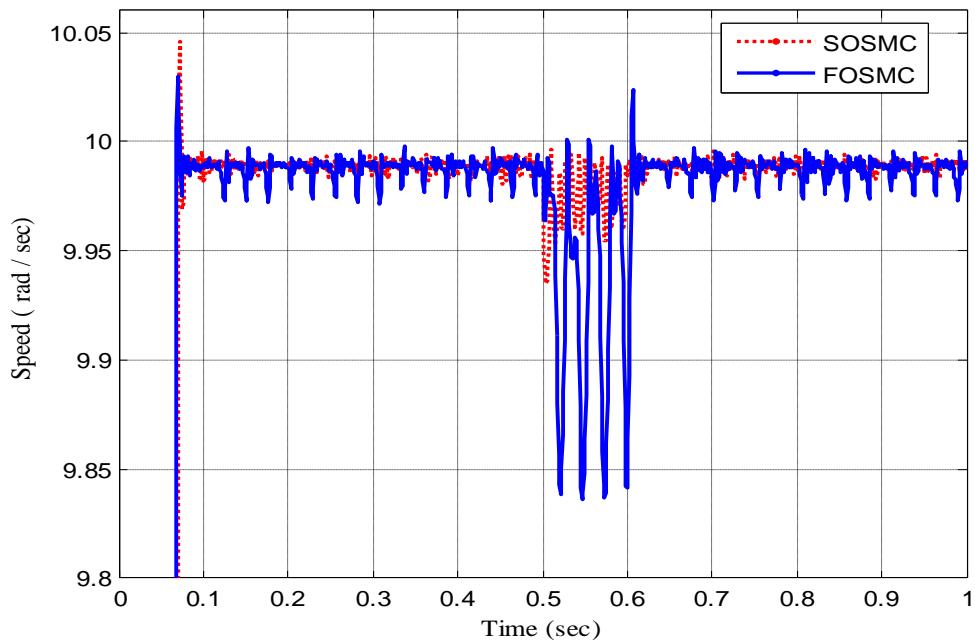


Figure 5.2: A close-up view of Figure 5.1 with sudden change in Torque Load.

The same results are verified for a motor speed of 25 rad/s and 30 rad/s in the next simulation tests shown in Figures 5.3-5.4, when a sudden change in torque load from

0 to 3 N-m is applied during the intervals $t=2.0$ to $t=2.1$, $t=3.0$ to $t=3.1$ and $t=4.0$ to $t=4.1$ seconds and Figure 5.31 when motor is suddenly subjected to a disturbance in the form of a sudden external load of 2 N-m and 4 N-m. A comparison of the robustness of both FOSMC and super twisting SOSMC controllers is immediately evident from the plots.

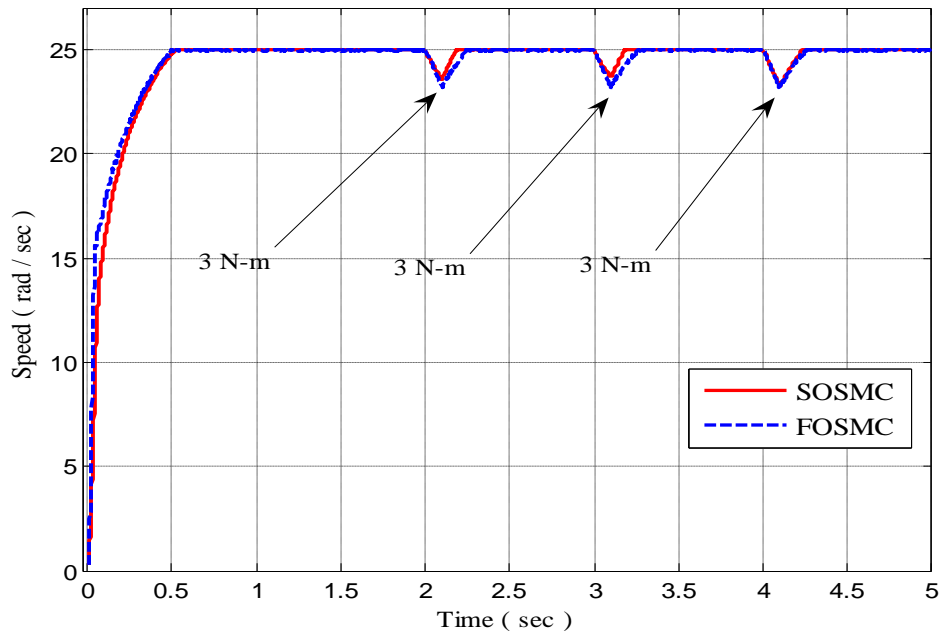


Figure 5.3: Speed response of SR motor with sudden change in torque load.

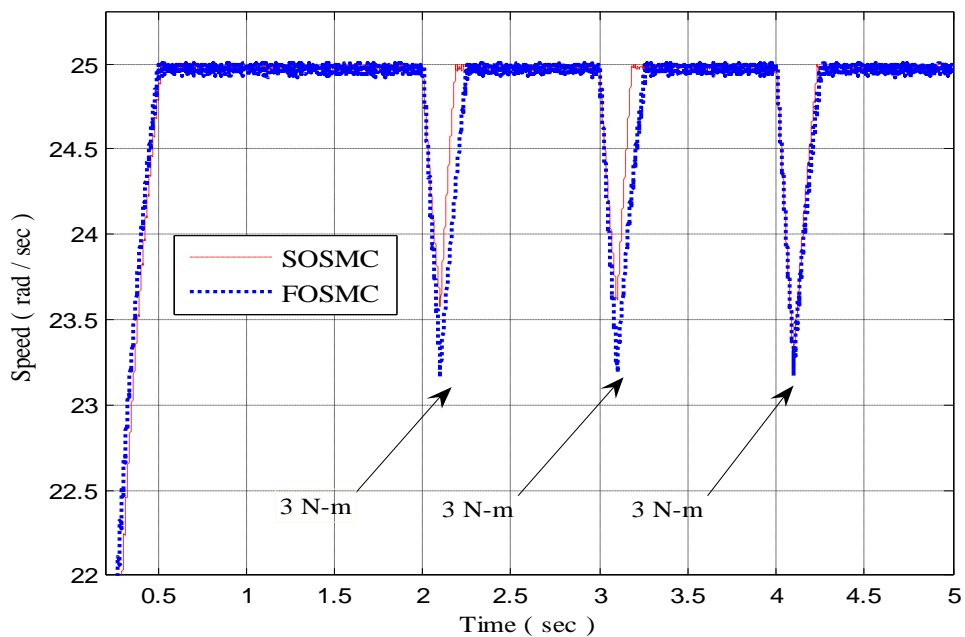


Figure 5.4: A close-up view of Figure 5.3 with sudden change in Torque Load.

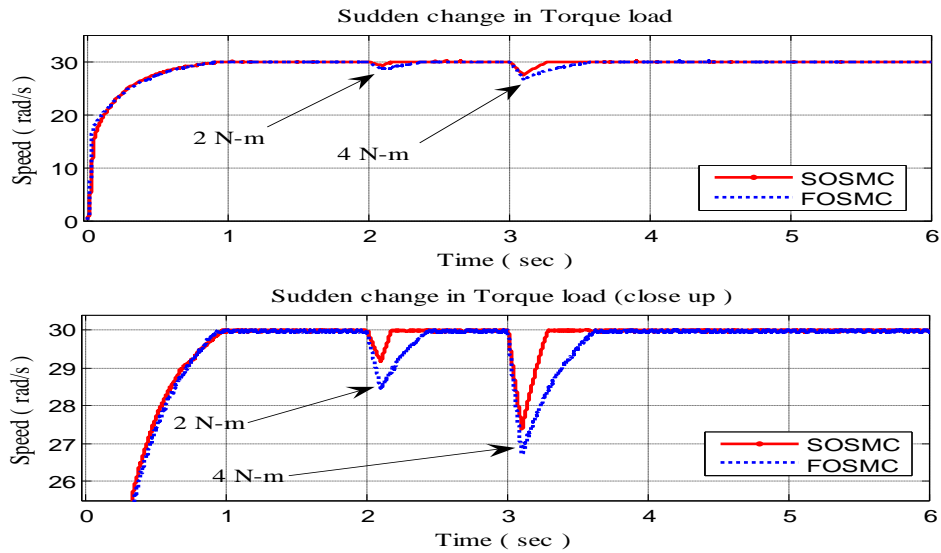


Figure 5.5: Speed response during sudden change in torque load .

It can be seen that the higher order sliding mode controller (SOSMC) is more robust than the FOSMC and outperforms it in maintaining the motor speed against the suddenly applied external load.

5.1.1.2 Comparison of Position Responses of SR Motor with Sudden Change in Torque Load

The same sudden change in torque load during the time interval $t=5$ sec to $t=5.5$ sec is investigated in Figure 5.6 when motor was approaching the desired position of 30 radians.

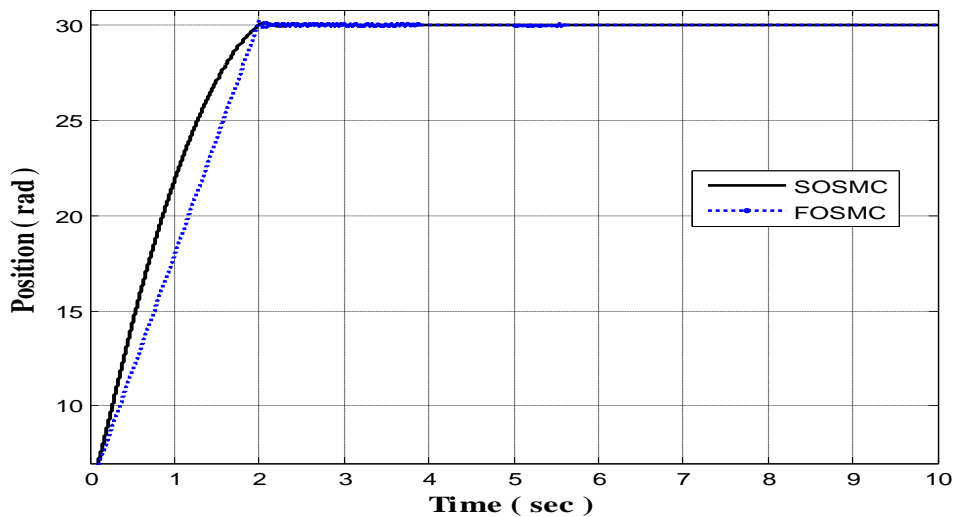


Figure 5.6: Position response of SR motor with sudden change in torque load.

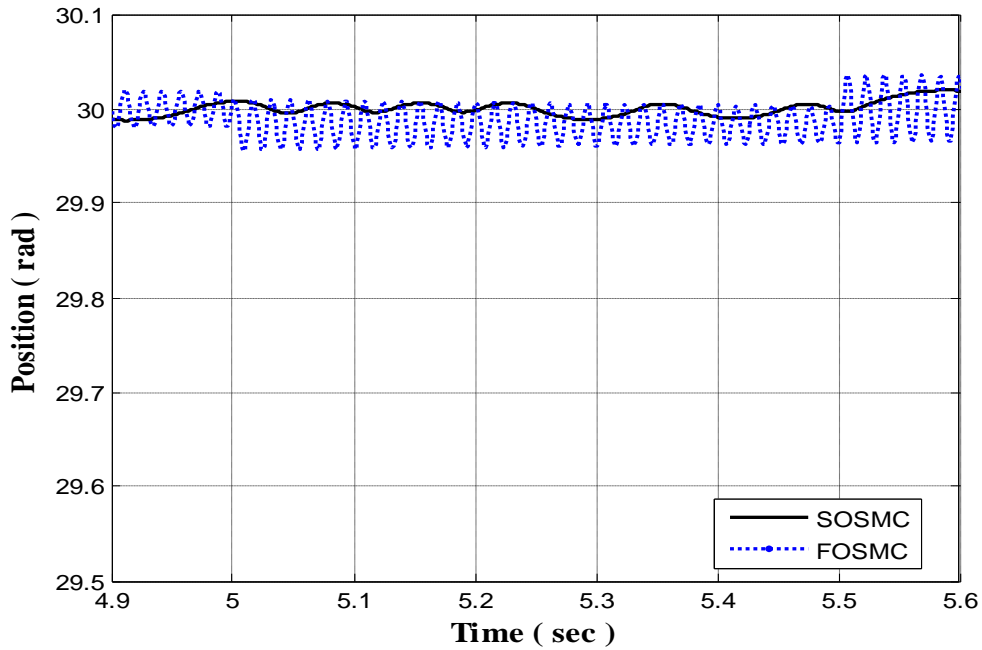


Figure 5.7: A close-up view of Figure 5.6 with sudden change in Torque Load.

It is very much clear from Figure 5.7 that the performance of SOSMC is far better than FOSMC.

5.2 Robustness against Parameters Variation

Next, the robustness of controllers is compared on parametric variations. The responses of synthesized controllers are investigated against changes in moment of inertia J , which could be due to engagement of load; stator phase resistance R , which could vary due to temperature variations in winding during operation [109] and coefficient of viscous friction B as a model uncertainty, since this parameter is usually provided by the manufacturer of mechanical components of motor, and may not be accurate when the motor parts are assembled into a complete and operational SR motor assembly. Therefore, it is difficult to find its exact value, and is usually estimated [110]. Changes in moment of inertia J , stator resistance R and coefficient of friction B are analyzed through simulations. In these simulation experiments, one parameter is allowed to change at one time during one experiment; the other parameters are kept constant.

5.2.1 Comparison of Speed/Position Responses of SR Motor with Changes in J

Figures 5.8-5.11 demonstrate the motor response when changes in moment of inertia are carried out. Moment of inertia is first decreased by 50% and then increased by 100% from its original value.

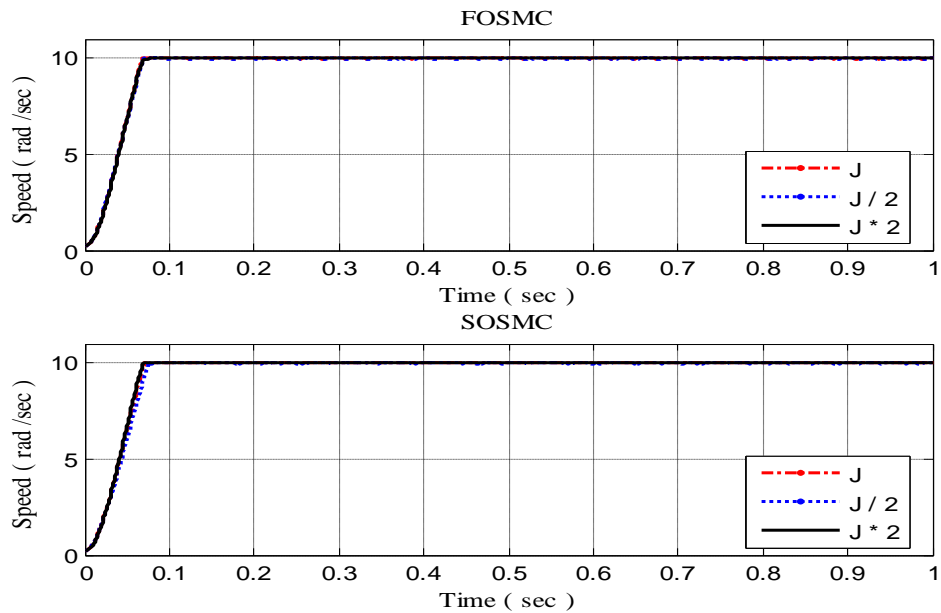


Figure 5.8: Speed response of SR motor with sudden changes in J.

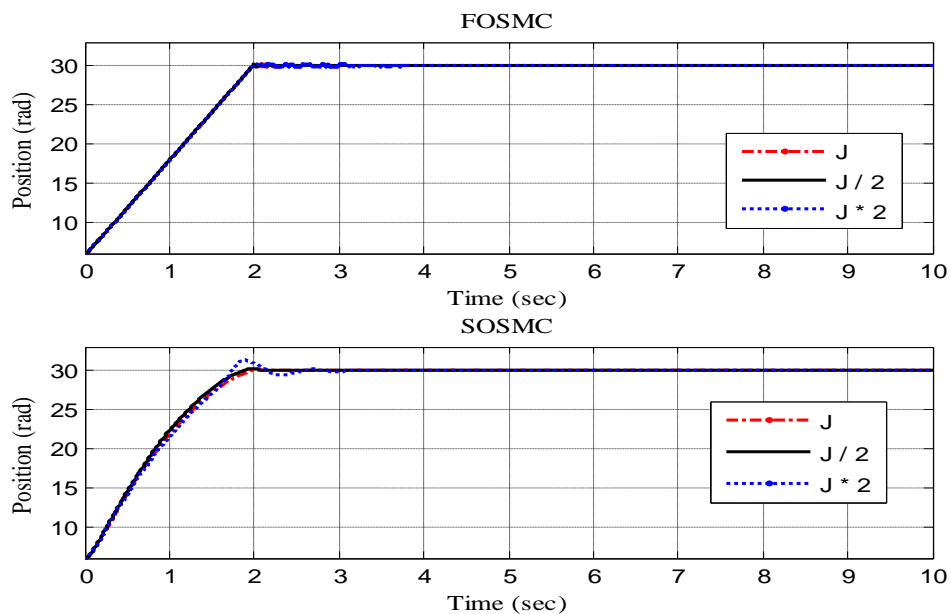


Figure 5.9: Position response of SR motor with sudden changes in J.

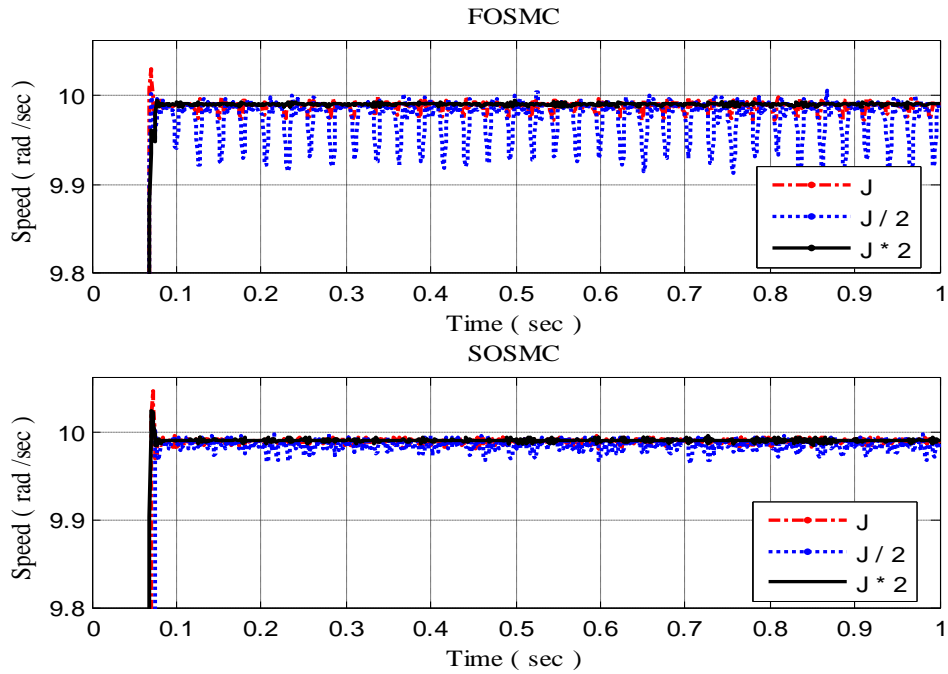


Figure 5.10: A close up view of Figure 5.8 with sudden changes in J.

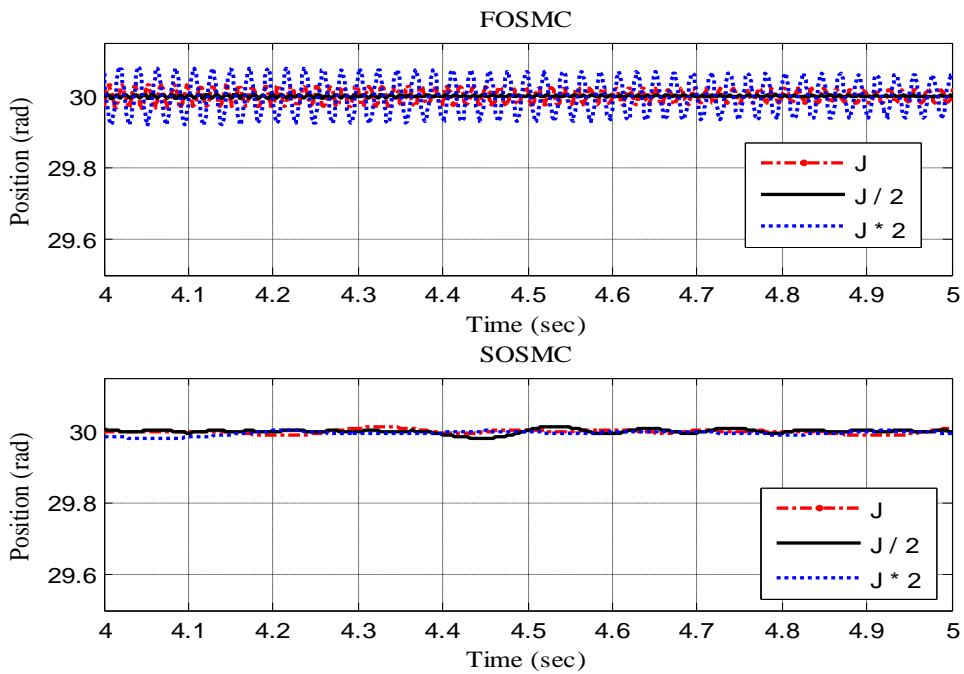


Figure 5.11: Close up view of position response of controllers during initial stage of steady state against sudden change in J.

As can be seen from Figure 5.10 and Figure 5.11, the speed/position response of FOSMC is, however, excellent but it suffers from the chattering effect; which is an undesirable phenomena. An increase of moment of inertia (J) causes some overshoot

in the proposed controller SOSMC. The decrease of moment of inertia gives good performance however it slows down the dynamic response of the system.

5.2.2 Comparison of Speed/Position Responses of SR Motor with Changes in B

The consequences of the same changes in coefficient of friction (B) are taken into account in Figures 5.12-5.15. It can be realized that speed/position response of SOSMC does not have any effect with increment or decrement of coefficient of friction. On the otherhand, the performance of FOSMC in speed regulation problem is affected at transient stage but in position regulation problem, it causes more chattering when coefficient of friction is decreased by 50%.

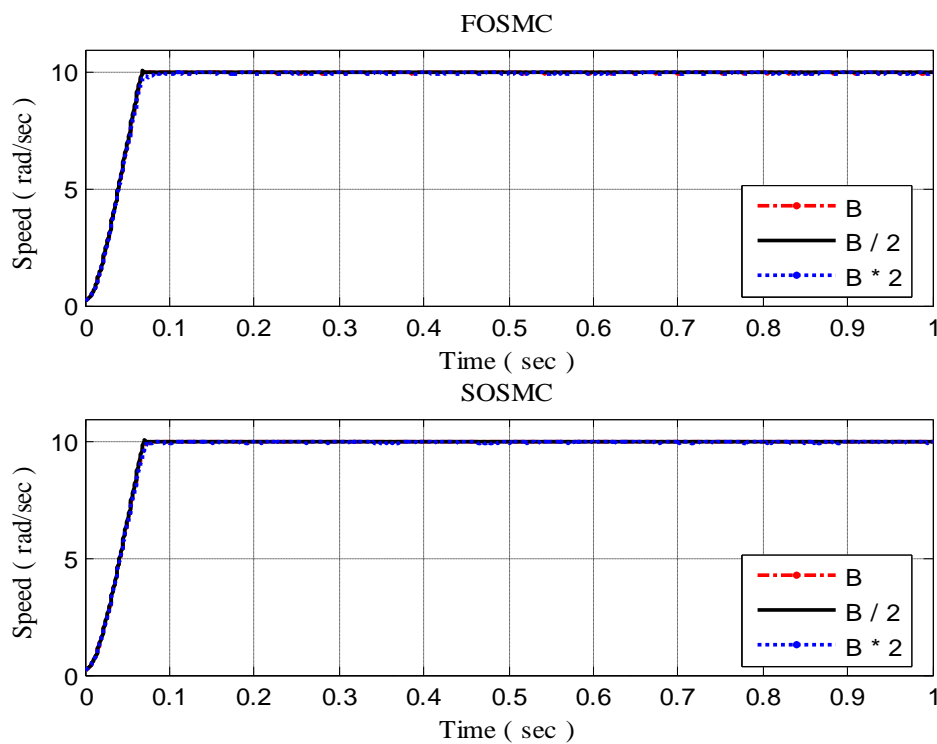


Figure 5.12: Speed response of SR motor with sudden changes in B.

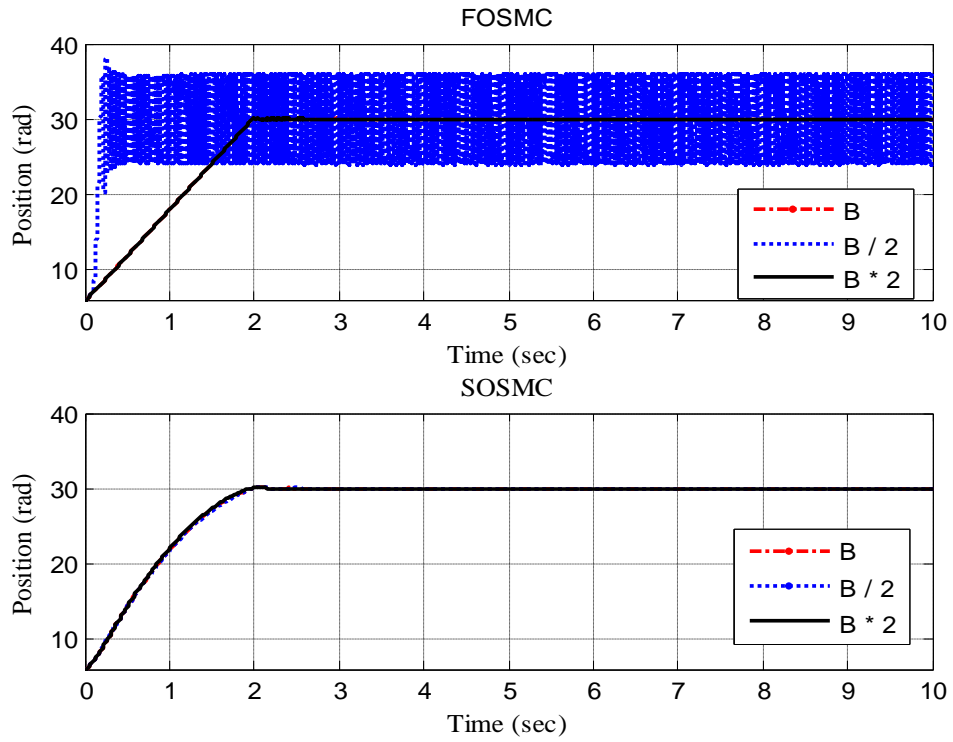


Figure 5.13: Position response of SR motor with changes in B.

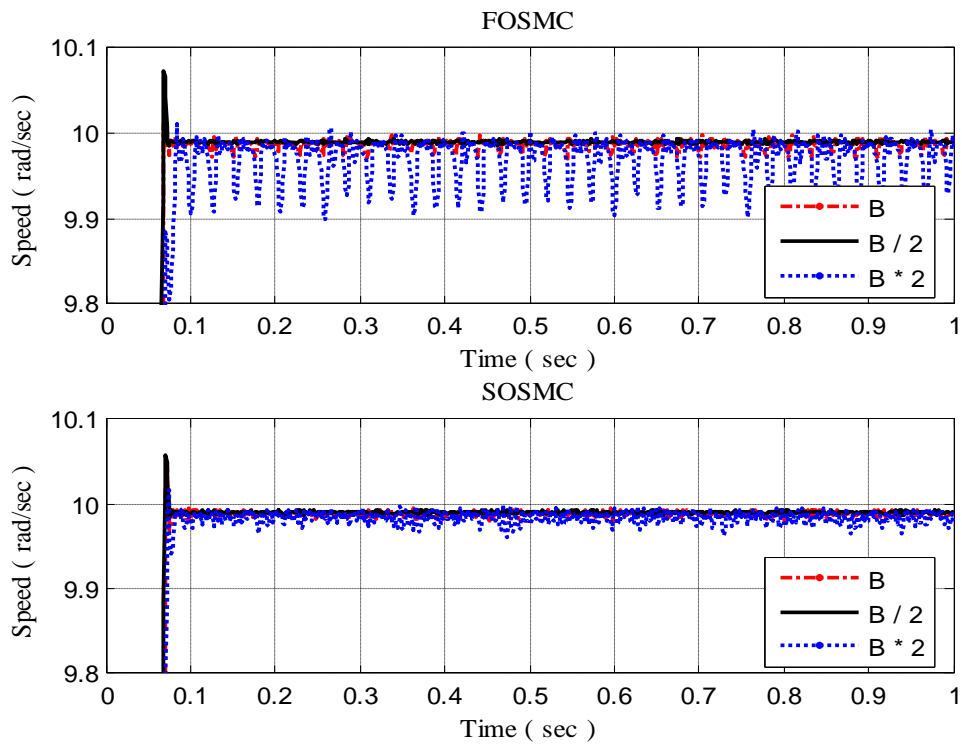


Figure 5.14: A close up view of Figure 5.12 with sudden changes in B.

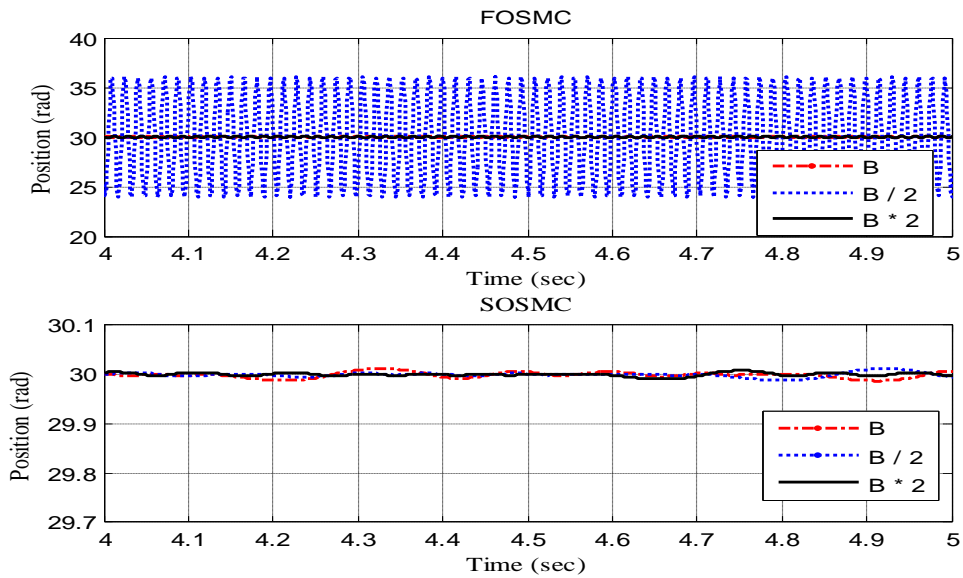


Figure 5.15: Close up view of position response of controllers during initial stage of steady state against sudden change in B

5.2.3 Comparison of Speed/Position Responses of SR Motor with Changes in R

The response of the controllers during variation of resistance is shown in Figures 5.16-5.19. In speed control problem, it can be observed that the decrement in phase resistance causes some overshoot in both the controllers and increment in phase resistance slows down the dynamic responses. The response of FOSMC is slower than SOSMC.

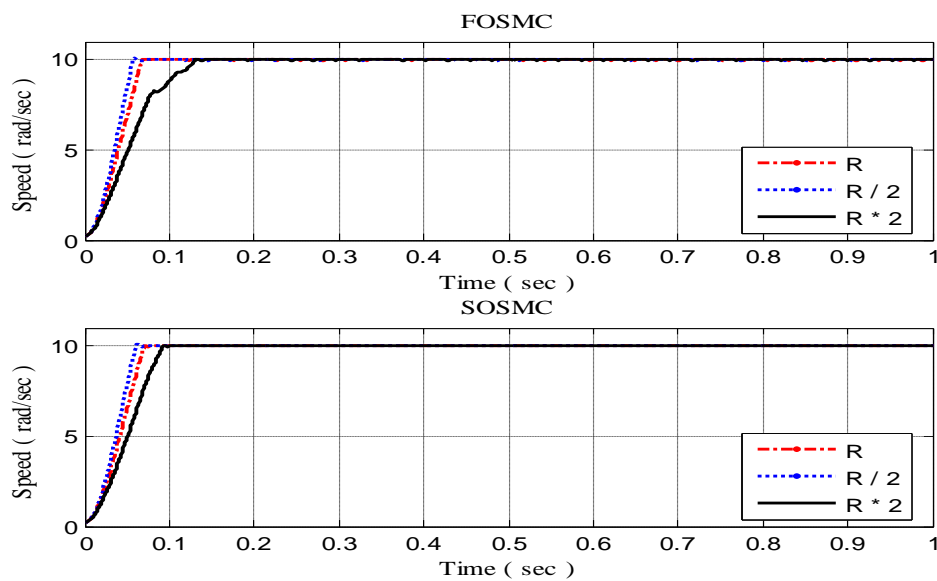


Figure 5.16: Speed response of SR motor with sudden changes in R

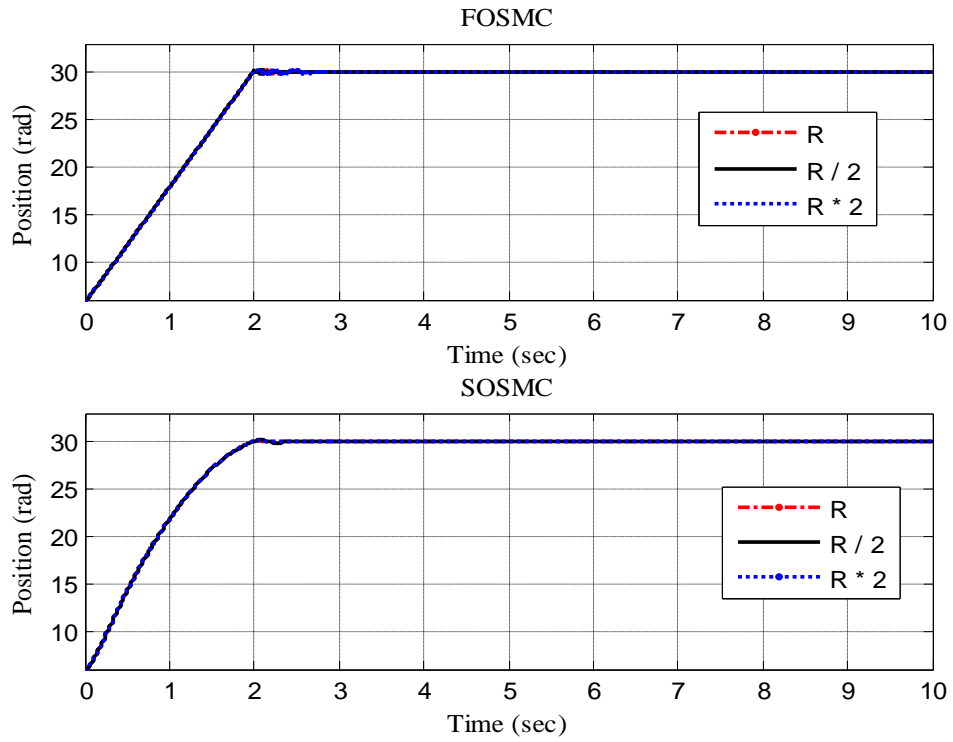


Figure 5.17: Position response of SR motor with changes in R.

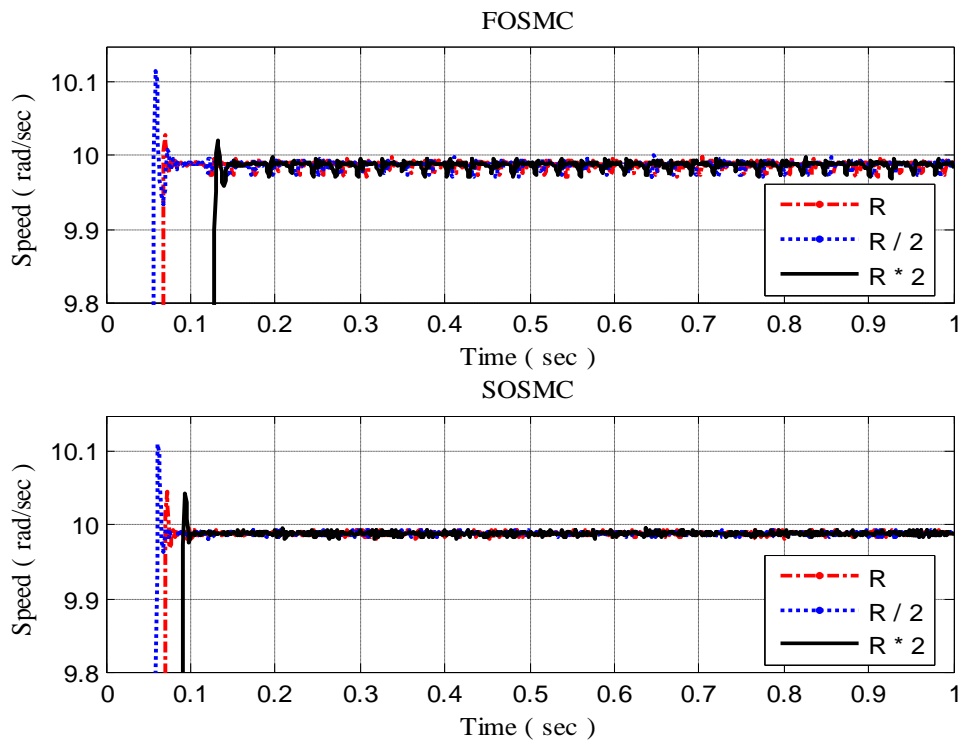


Figure 5.18: A close up view of Figure 5.16 with sudden changes in R.

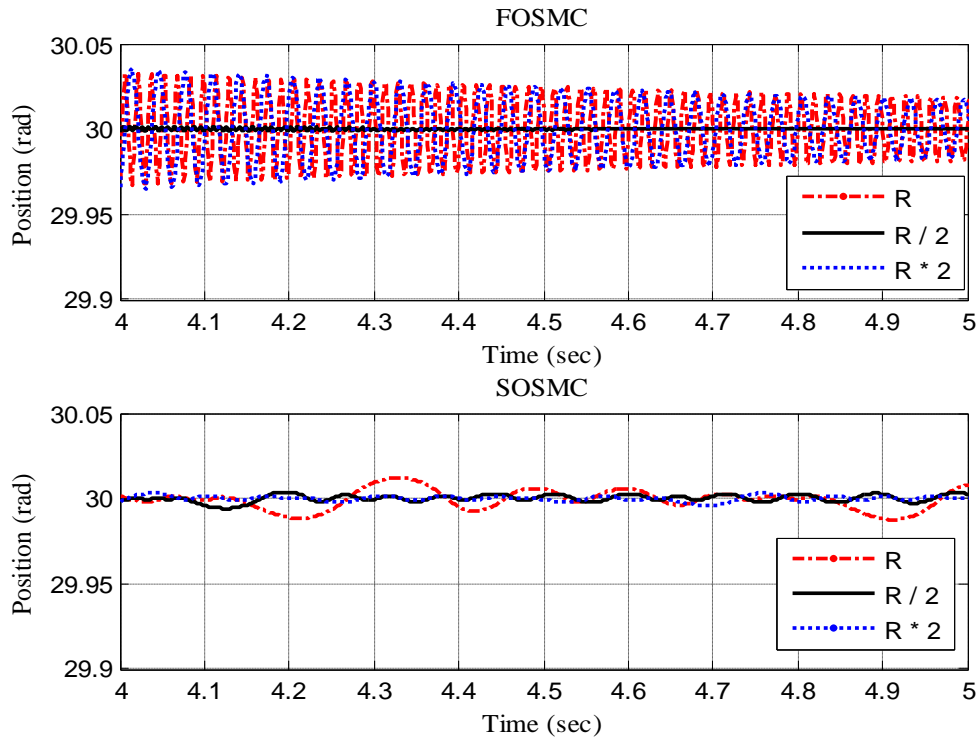


Figure 5.19: Close up view of position response of controllers during initial stage of steady state against sudden change in R

In position control problem, dynamic response of both the controllers remains the same with variations in R . However, more chattering is observed in FOSMC.

In the light of these plots, it is now clear that the proposed controller SOSMC is robust against parameter uncertainties and external disturbances.

5.3 Conclusion

FOSMC and SOSMC were simulated and their performance was analyzed against external disturbances and parameters variations. From the given results, it can be concluded that both controllers provide robustness and dynamic response of SOSMC is far better than FOSMC.

Chapter 6

CONCLUSIONS AND FUTURE WORK

This thesis presents a novel control scheme for speed regulation/tracking of Switched Reluctance (SR) motors. The control methodology is based on Higher-Order Sliding-Mode (HOSM) technique. In particular, a Second-Order Sliding-Mode Controller (SOSMC) based on Super Twisting algorithm is derived. Owing to the peculiar structural properties of SRM, torque produced by each motor phase is a function of phase current as well as rotor position. More importantly, and unlike many other motors, the polarity of the phase torque in SR motors is solely determined by the rotor position and is independent of the polarity of the applied voltage or phase current. The proposed controller takes advantage of this property and incorporates a commutation scheme which; at any time instant, selects only those motor phases for the computation of control law, which can contribute torque of the desired polarity (in the desired direction only) at that instant. This feature helps in achieving the desired speed regulation/tracking objective in a power efficient manner as control efforts are applied through selective phases and phases of opposite polarity which are counterproductive to the torque optimization are not energized. This approach also minimizes the power loss in the motor windings thereby reducing the heat generation within the motor. The losses due to heat generation; and also performance degradation are avoided.

In order to highlight the advantages of HOSM based controllers, a classical First-Order Sliding-Mode controller (FOSMC) is also developed and applied to the same system. The comparison of the two schemes shows much reduced chattering in case of SOSMC. The performance of the proposed SOSMC controller for speed regulation is also compared with a dynamic sliding mode controller (DSMC) and another sliding mode speed controller published in the literature. The proposed controller (SOSMC) outperforms the DSMC not only in tracking the desired speed but also in minimization of chattering.

Furthermore, the position control application of proposed controls has been explored and first order sliding mode controller (FOSMC) is designed for position regulation problem; making it possible candidate for servo drive applications in some cases; its stability is assured using Lyapunov stability theorem. To cater for the inherent problem of chattering in FOSMC, a second order sliding mode controller (SOSMC) has been developed based on super twisting algorithm. The proposed controller is robust against parameter variations and external disturbances also. There are a lot of open research area for optimization of torque and hence power optimization, smooth sliding mode control of SR motor, design of higher order sliding mode observers for Sensorless control of SR motor etc.

Future work may address the following issues:

- Sensorless control of SR motor by avoiding the need of position sensor and development of HOSM based observers and testing at different loads and speeds. The resulting scheme will not only increase the reliability but also will reduce the cost of the overall system.
- Performance and robustness analysis of Second Order Sliding Mode Observer with First Order Sliding Mode Observer on parameter variations and disturbances in Matlab/SIMULINK environment and finally implementation on a test bench.
- Implementation of DSMC, FOSMC and conventional sliding mode control [24] for speed regulation/tracking problem on a system bench and comparison of the simulation results with experimental results. Comparative study and analysis of behaviour against parameter variations and unknown disturbances.
- Implementation of SOSMC for speed control problem on a system bench and comparison of its results with FOSMC and DSMC. A study of response of SOSMC against parameter perturbations and its comparison with the other implemented controllers.
- Implementation of FOSMC for position regulation problems on a system bench and analyses of response at different positions against parameter variations and load disturbances.

- Implementation of SOSMC on a test bench for position regulation and its comparison with FOSMC and analyses of the performance of both controllers against parameter variations and load disturbances using simulation results as well as test bench data.
- The exact parameters are indispensable for the development of any accurate nonlinear model of the system. Because model with poor parameters produces poor dynamic response and sometimes becomes unstable. The parameters of SR motor are coefficient of friction (B), moment of inertia (J) and resistance (R) play vital role in the system dynamics. Many techniques have been reported in literature to find out accurate values of the parameters. We would intend to further explore HOSM based technique for parameter estimation of SR motor.
- Timely detection and diagnosis of faults in industrial process improves its efficiency and also increases the life of the equipments. Like other motors, different types of faults may occur in SR motor. For example one phase open circuit fault, locked rotor fault, phase to ground fault etc. HOSM based technique has been reported on DC motor, induction motor, permanent magnet synchronous motor for fault detection and isolation. We would intend to apply this technique on SR motor for fault detection and diagnosis purpose.

REFERENCES

- [1] Miller T. J. E., *Electronic control of switched reluctance machines*, 2001, Newness Power Engineering Series (Oxford Newness Publisher).
- [2] Krishnan R. *Switched Reluctance Motor Drives: Modeling, Simulation, Analysis, Design, and Applications*, 2000, CRC Press, Boca Raton London New York Washington, D.C.
- [3] Bizkevelci E., Leblebicioglu K., Ertan H. B., “A Sliding Mode Controller to Minimize SRM Torque Ripple and Noise”, Proc. in IEEE International Symposium on Industrial Electronics, Vol. 2, pp. 1333-1338, May 4-7, Turkey, 2004.
- [4] Hajatipour M., Farrokhi M., “Adaptive intelligent speed control of switched reluctance motors with torque ripple reduction”, *Energy Conversion and Management*, Vol.49, pp.1028-1038, 2008.
- [5] Nihat I., Veysel O., “Torque ripple minimization of a switched reluctance motor by using continuous sliding mode control technique”, *Electric Power Systems Research* 66 (2003) 241-251
- [6] Yang H., Panda K. S., Chii L. Y., “Performance comparison of feedback linearization control with PI control for four quadrant operation of switched reluctance motor”, *IEEE Applied Power Electronics Conference and Exposition*, Vol. 2: pp. 956 – 962, 1996.
- [7] Schmid J., Kaiserseder M., Amrhein W., Schumacher A., Knecht G., “Speed and Torque Control of Switched Reluctance Motors”, Proc. in IEEE International Conference on Power Electronics, Machines and Drives, Vol. 1, pp. 98 – 103, 31 March 2- April 2004.
- [8] Ilic-Spong M., Marino R., Peresada S.M., Taylor D.G., “Feedback linearizing control of switched reluctance motors,” *IEEE Transaction on Automatic Control*, Vol.32, No. 5, pp. 371-379, 1987.
- [9] Amor L. B., Dessaint L. A, Akhrif O., Olivier G., “Adaptive Feedback Linearization for Position Control of a Switched Reluctance Motor: Analysis and Simulation”, Proc. in IEEE International Conference on Industrial Electronics, Control, Instrumentation, and Automation, Vol.1, pp.150 – 159, November 09- 13, 1992, San Diego, CA , USA.
- [10] Bolognan S., Zigliotto M., “Fuzzy Logic Control of a Switched Reluctance Motor Drive”, *IEEE Transactions on Industry Applications*, pp. 1063-1068, Vol. 32, No. 5, 1996.
- [11] Vijayan S., Paramasivam S., Arumugam R., Dash S. S., Poornaselvan K. J., “A Practical Approach to The Design and Implementation of Speed Controller for Switched Reluctance Motor Drive using Fuzzy Logic Controller”, *Journal of Electrical Engineering*, Vol. 58, No. 1, pp. 39–46, 2007.
- [12] Liu W., Song S., “Application of Fuzzy Control in Switched Reluctance Motor Speed Regulating System”, Proc. in IEEE International Conference on

Computational Intelligence for Modelling Control and Automation, and International Conference on Intelligent Agents, Web Technologies and Internet Commerce, pp.72 – 77, November 28 -December 1, 2006, Sydney, NSW.

- [13] Buja G. S., Menis R., Valla M. I., “Variable Structure Control of An SRM Drive”, IEEE Transactions on Industrial Electronics, pp. 56-63, Vol. 40, No. 1, 1993.
- [14] Yang H., Panda S. K., Chii L. Y., “Sliding Mode Control for Switched Reluctance Motors: An Experimental Investigation”, Proc. in IEEE 22nd International Conference on Industrial Electronics, Control, and Instrumentation, Vol.1, pp. 96 – 101, August 5-10, 1996.
- [15] Husain I., Sodhi S., Ehsani M., “A Sliding Mode Observer Based Controller for Switched Reluctance Motor Drives”, Proc. In IEEE Industry Application Society Annual Meeting, vol.1, pp. 635 – 643, 1994.
- [16] Sahoo S. K., Panda S. K., Xu J. X., “Direct Torque Controller for Switched Reluctance Motor Drive using Sliding Mode Control”, Proc. in IEEE Power Electronics and Drives Systems, Vol. 2, pp.1129-1134, 2005.
- [17] Tahour A., Meroufel A., Abid H., Aissaoui A. G., “Sliding Controller of Switched Reluctance Motor”, Leonardo Electronic Journal of Practices and Technologies, Vol.12, pp. 151-162, 2008.
- [18] Yaning S., Weiping W., Dengpan Q., “Study on Switch Reluctance Motor Drive System Using Variable Structure Control with Sliding”, Proc. in IEEE International Conference on Information and Automation, pp. 2154-2157, June 20 - 23, 2010, Harbin, China.
- [19] Singh B, Sharma V. K., Murthy S. S., “Comparative Study of PID, Sliding Mode and Fuzzy Logic Controllers for Four Quadrant Operation of Switched Reluctance Motor”, Proc. in IEEE Power Electronic Drives and Energy Systems for Industrial Growth, Vol. 1, pp. 99 – 105, 1998.
- [20] Hossain S. A., Husain Iqbal, Klode H., Lequesne B., Omekanda A. M., Gopalakrishnan S., “Four-Quadrant and Zero-Speed Sensorless Control of a Switched Reluctance Motor”, IEEE Transactions on Industry applications, Vol. 39, No. 5, pp. 1343-1349, 2003.
- [21] Alrifai M., Zribi M., Rayan M., Krishnan R. “Speed control of switched reluctance motors taking into account mutual inductances and magnetic saturation effects”, Energy Conversion and Management Vol. 51, Pages 1287–1297, 2010.
- [22] Rafiq M., Rehman S. A., Butt Q. R., Bhatti A. I., “Power Efficient Sliding Mode Control of SR Motor for Speed Control Applications,”, Proc. in IEEE 13th International Multitopic Conference, pp. 1-6, December 14-15, 2009, MAJU, Islamabad.
- [23] Slotine J. J. E., “Sliding controller design for nonlinear systems”, International Journal of Control, Vol. 40, pp. 421-434, 1984.

- [24] Alrifai M. T., Zribi M., Ramirez H. S., “Static and dynamic sliding mode control of variable reluctance motors”, *International Journal of Control*, Vol. 77, No. 13, pp. 1171–1188, 2004.
- [25] Damiano A., Gianluca L. Gatto M., Ignazio and Pisano A., “Second-Order Sliding-Mode Control of DC Drive”, *IEEE Transaction on Industrial Electronics*, Vol. 51, No. 2, 2004.
- [26] Floquet T., Barbot et W J.P., Perruquetti, “Second order sliding mode control for induction motor” *Proc. 39th IEEE Conference on Decision and Control* , Sydney, Australia December, 2000.
- [27] Bartolini G., Damiano A., Gatto G, Marongiu I., Pisano A., and Usai E., “Robust Speed and Torque Estimation in Electrical Drives by Second-Order Sliding Modes”, *IEEE Transactions on Control Systems Technology*, VOL. 11, No. 1, January 2003.
- [28] Laghrouche S., Plestan F. and Glumineau A., “A higher order sliding mode controller for a class of MIMO nonlinear systems: application to PM synchronous motor control” in *Proc. 2004 American Control Conference*, Boston, Massachusetts June 30-July 2, 2004.
- [29] Milena D., Luiz C. M., “Robust Control of Permanent Magnet Synchronous Motor Based on Higher-Order Sliding Mode Approach”, in *Proc. IEEE Power Electronics Conference*, pp. 1163 – 1170, 2009.
- [30] Defoort M., Nollet F., Floquet T. and Perruquetti W., “Higher order sliding mode control of a stepper motor” in *Proc. IEEE Conference on Decision & Control San Diego, CA, USA, December 13-15, 2006*.
- [31] Saeed-ur-Rehman, “Commutation, Identification and Estimation for Switched Reluctance Motors”, PhD Thesis, Georgia Institute of Technology, Atlanta, Georgia, USA, November 27, 1996.
- [32] Pisano, *Second Order Sliding Modes: Theory and Applications*, PHD Thesis, Dipartimento di Ingegneria Elettrica ed Elettronica (DIEE) Università degli Studi di Cagliari, December 2000.
- [33] Gotovac S, “Mathematical model of switched reluctance motor”, *International Journal for Engineering Modeling*, Vol. 8, No. 1-2, 1995.
- [34] Ustun O., “A nonlinear full model of switched reluctance motor with artificial neural network”, *Energy Conversion and Management*, Vol. 50, pp. 2413–2421, 2009.
- [35] Xilian W., Yihuang Z., Huijuan L., Hui H., “Nonlinear Modeling of Switched Reluctance Motor Based on Combination of Neural Network and Genetic Algorithm”, *ICEMS 2005*, pp.572-574.
- [36] Vasquez H. and Parker J. K., “A new simplified mathematical model for a switched reluctance motor in a variable speed pumping application,” *Mechatronics*, vol. 14, No. 9, pp. 1055-1068, November 2004.

- [37] Bose B. K., Miller T. J. E., Szczesny P. M., Bicknell W. H., “Microcomputer Control of Switched Reluctance Motor”, IEEE Transactions on Industry Applications, Vol. IA-22, No. 4, pp. 708-715, 1986.
- [38] Pillay P., Liu Y., Durham O. G., “A novel switched reluctance motor drive with optical graphical programming technology”, IEEE Transactions on Industrial Electronics, Vol. 47, No. 4, pp. 915 – 919, 2000.
- [39] Wang Z., Cheok A. D., Wee L. K., “Sensorless Rotor Position Estimation Algorithm for Switched Reluctance Motors Using Fuzzy Logic”, Proc. in IEEE 32nd Annual Conference on Power Electronics Specialists, Vol. 3, pp. 1701-1706, 2001, Vancouver, BC.
- [40] Mese E., Torrey D. A., “An Approach for Sensorless Position Estimation for Switched Reluctance Motors Using Artificial Neural Networks” , IEEE Transactions on Power Electronics, Vol. 17, No. 1, pp. 66-75, 2002.
- [41] Karakas E. and Vardarbasi S., “Speed control of SR motor by self-tuning fuzzy PI controller with artificial neural network”, Sadhana, Vol. 32, No. 5, pp. 587–596, October 2007.
- [42] Yang H., Panda S.K., Chii L. Y., “Performance Comparison of Sliding Mode Control with PI Control for Four-quadrant Operation of Switched Reluctance Motors”, Proc. in IEEE International Conference on Power Electronics, Drives and Energy Systems for Industrial Growth, Vol.1, pp. 381 – 387, January 8-11, 1996.
- [43] Alrifai M. T, Chow J. H. and Torrey D.A., “Backstepping nonlinear speed controller for switched-reluctance motors”, IEE Proc. Electric Power Application, Vol. 150, No. 2, March 2003.
- [44] Alrifai M., Zribi M., Krishnan R., and Rayan M., “Nonlinear Speed Control of Switched Reluctance Motor Drives Taking into Account Mutual Inductance”, Journal of Control Science and Engineering, pp.1-11, 2008.
- [45] Chancharoensook P. and Rahman M. F., “A High Precision Speed control of a Four Phase Switched Reluctance Motor Drive Using Closed Loop Controllers of Instantaneous Torque and Current”, Proc. in IEEE 30th Annual Conference on Industrial Electronics Society, pp. November 2-6, 2004, Busan, Korea.
- [46] Chen C. G., “Sensorless Speed Control of Switched Reluctance Drives Using a Nonlinear Controller”, Proc. in IEEE International Symposium on Industrial Electronics, pp. 2256 – 2261, June 4-7, 2007, Vigo, Spain.
- [47] Muniraj C., Chandrasekar S., “Neural Network Based Speed Control for 6/4 Switched Reluctance Motor”, Proc. in IEEE, International Conference on Computational Intelligence and Multimedia Applications, pp. 227-231, 2007.
- [48] Dehkordi B. M., Parsapoor A., Moallem M., Lucas C., “Sensorless speed control of switched reluctance motor using brain emotional learning based intelligent controller”, Energy Conversion and Management, Vol. 52, pp. 85–96, 2011.
- [49] Rafael S., Costa B.P.J., Pires A. J., “Position Control of an 8/6 Switched Reluctance Machine without Current Sensor”, Proc. in IEEE, International

Conference on Power Engineering, Energy and Electrical Drives, pp. 327 - 330 , March 18-20, 2009, Lisbon Portugal.

- [50] Leviner M. D., Dawson D. M., Hu J., “Position Tracking Control of a Switched Reluctance Motor Using Partial State Feedback”, Proc in IEEE, American Control Conference, Vol. 3, pp. 3095-3098, June 29-July 1, 1994.
- [51] Baik W.S., Kim M.H., Kim D.H., Choi K. H., Hwang D.H., “A High Performance Motion Control System of Switched Reluctance Motor”, Proc. in IEEE 37th Power Electronics Specialists Conference, pp. 1-5, 2006.
- [52] Gan W. C., Cheung N.C., Qiu Li, “Position control of linear switched reluctance motors for high-precision applications”, IEEE Transactions on Industry Applications, pp. 1350-1362, 2003.
- [53] Cao G. Z., Lin L.M., Qiu H., Pan J.F., “Design and Analysis of a dSPACE-based Position Control System for a Linear Switched Reluctance Motor”, Proc. in 3rd International Conference on Power Electronics Systems and Applications, 2009.
- [54] Mademlis C. and Kioskeridis I., “Position Control of Switched Reluctance Motors by Using an Online Fine-Tuning Regulator”, Proc. in IEEE, 8th International Symposium on Advanced Electromechanical Motion Systems & Electric Drives, pp. 1-6, 1-3 July 2009, Lille, France.
- [55] Elmas C., Yigit T., “Genetic Algorithm Based On-line Tuning of a PI Controller for a Switched Reluctance Motor Drive”, Electric Power Components and Systems, Vol. 35, pp. 75–691, 2007.
- [56] Rouhani H., Sadeghzadeh A., Lucas C., and Araabi B. N., “Emotional learning based intelligent speed and position control applied to neurofuzzy model of switched reluctance motor”, Control and Cybernetics, vol. 36, No. 1, pp. 75-95, 2007.
- [57] Utkin V. I. and Chang H.C., “Sliding Mode Control on Electro-Mechanical Systems”, Mathematical Problems in Engineering, 2002, Vol. 5(4-5) pp. 451-473.
- [58] Levant A., “Sliding order and sliding accuracy in sliding mode control,” International Journal of Control, Vol. 58, Vol. 6, pp. 1247-1263, 1993.
- [59] John G., and Eastham A.R., “Speed control of switched reluctance motor using sliding mode control strategy”, Proc. in IEEE Industry Applications Conference, 13th IAS Annual Meeting, Vol. 1, pp. 263 – 270, Oct 8-12, 1995, Orlando, FL , USA.
- [60] Forrai A., Biro Z., Chiorean V., “Sliding Mode Control Of Switched Reluctance Motor Drive” Proc. in IEEE 6th International Conference on Optimization of Electrical and Electronic Equipments, Vol. 2, pp. 467 – 472, May 14-15, 1998.
- [61] Yu-zhou L., “Sliding Mode Control of Switch Reluctance Motor Based on Torque Inverse Model”, Proc. in IEEE International Conference on Measuring Technology and Mechatronics Automation, pp. 398 – 401, March 13-14, 2010, Changsha City.

- [62] Chuang T. S., Pollock C., “Robust Speed Control of a Switched Reluctance Vector Drive Using Variable Structure Approach”, IEEE Transactions on Industrial Electronics, Vol. 44, No. 6, pp. 800-808, 1997.
- [63] Edwards C. and Spurgeon S. K., Sliding Mode Control: Theory and Applications, Taylor & Francis 1998.
- [64] Iqbal S., “Robust smooth model-free control methodologies for industrial applications”, PhD Thesis, Mohammad Ali Jinnah University Islamabad, August, 2011.
- [65] Slotine J. J. E. , Weiping Li., Applied Nonlinear Control, Prentice Hall, Englewood Cliffs, New Jersey 07632, 1991.
- [66] Ben-Israel, Greville T. N. E., Generalized Inverses, Theory and Application, 2nd edition, Springer, New York, 2003.
- [67] Britz T., “The Moore-Penrose inverse of a free matrix”, Electronic Journal of Linear Algebra ISSN 1081-3810, A publication of the International Linear Algebra Society, Volume 16, pp. 208-215, August 2007.
- [68] Gupta M. K., Sharma A. K., Patidar D., “A Robust Variable Structure Position Control of DC Motor”, Journal of Theoretical and Applied Information Technology, Vol. 4, No.10, 2008.
- [69] Chen M., Hwang Y., Tomizuka M., “A state-dependent boundary layer design for sliding mode control”, IEEE Transactions on Automatic Control, Vol. 47, pp. 1677-81, 2002.
- [70] Koshkouei A.J., Burnham K.J., Zinober A.S., “Dynamic sliding mode control design”, in Proc. IEE, Control Theory and Applications, Vol. 152, No. 4, pp. 392 – 396, 2005.
- [71] Comanescu M., Batzel T., “A Novel Speed Estimator for Induction Motor based on Integral Sliding Mode Current Control”, Proc. IEEE, Power and Energy Society General Meeting - Conversion and Delivery of Electrical Energy in the 21st Century, pp. 1 – 6, 2008.
- [72] Chang J. L., “Dynamic Output Integral Sliding-Mode Control With Disturbance Attenuation”, IEEE Transactions on Automatic Control, Vol. 54, No.11, pp. 2653 – 2658, 2009.
- [73] Fallahi M., Azadi, S.; “Fuzzy PID Sliding Mode Controller Design for the position control of a DC Motor”, Proc. IEEE, International Conference on Education technology and Computer, pp. 73 – 77, 2009.
- [74] Reay D.S., Moud M. M., Williams B.W., “On the Appropriate uses of Fuzzy Systems: Fuzzy Sliding Mode Position Control of a Switched Reluctance Motor”, in Proc. IEEE International Symposium on Digital Object Identifier, pp. 371 – 376, 1995.
- [75] Chen T. C., Hsu J. U., “A Fuzzy Sliding Mode Controller for Induction Motor Position Control”, Proc. IEEE, 20th International Conference on Industrial Electronics, Control and Instrumentation, Vol. 1, pp: 44 – 49,1994.
- [76] Phakamach P., “Robust Position Control of an Induction Motor Using a Fuzzy Logic Sliding mode Model Following Controller (FLSMFC) with

- Sinusoidal Command Input”, *Journal of Research in Engineering and Technology*, Vol.6, No.4, October - December 2009.
- [77] Barrero F., Gonziilez A., Torralba A., GalvBn E., Franquelo L.G., “Speed Control of Induction Motors Using a Novel Fuzzy-Sliding Mode Structure”, *IEEE Transaction on Fuzzy Systems*, Vol. 10 , No.3 , pp. 375 – 383, 2002.
- [78] Zadeh M.H., Yazdian A., Mohamadian M., “Robust Position Control in DC Motor by Fuzzy Sliding Mode Control”, *Proc. IEEE, Power Electronics, Electrical Drives, Automation and Motion*. pp: 1413 – 1418, 2006.
- [79] Huang Y. S., Sung C. C., Yu C. S., “Reduced Order Fuzzy Sliding Mode Control for Linear Synchronous Motor Systems”, *Proc. IEEE International Conference on Industrial Technology (ICIT 2010)*, Vina del Mar, Chile, March 14-17, pp. 392-396, 2010.
- [80] Chan C.C., Zhan Y.J., Chau K.T., “Stability Analysis of Fuzzy Sliding Mode Controlled Switched Reluctance Motor Drives”, in *Proc. IEEE Power Electronics Specialists Conference*, vol.2, pp. 1283-1289,1998.
- [81] Tahour A., Abid H., Aissaoui A. G., “Speed Control of Switched Reluctance Motor Using Fuzzy Sliding Mode”, *Advances in Electrical and Computer Engineering* Vol. 8, No. 15, 2008.
- [82] Morsy M., Moteleb M., Dorrah H.T., “Design and Implementation of Fuzzy Sliding Mode Controller for Switched Reluctance Motor”, *IEEE International Conference on Industrial Technology*, Chengdu, pp. 21-24, April 2008.
- [83] Rouhani H., Lucas C., Milasi R. M., Bahrami M. N., “Fuzzy Sliding Mode Control Applied to Low Noise Switched Reluctance Motor Control”, *Proc. IEEE, International Conference on Control and Automation*, pp: 325 – 329, Vol. 1, Budapest, Hungary, June 27-29, 2005.
- [84] Miaoshan L., Yuqun W., Yunxing C., “Applied Research into Switched Reluctance Motor in Electric Vehicle”, in *Proc. IEEE International Conference on Digital Object Identifier*, pp. 1903-1907, 2011.
- [85] Qaiser S.H., Bhatti A.I., Iqbal M., Samar R., Qadir J., “Model validation and higher order sliding mode controller design for a research reactor” *Annal of Nuclear Energy*, Vol. 36, pp. 37-45, 2009.
- [86] Butt Q. R., Bhatti A. I., Iqbal M., Rizvi M. A., Mufti R., Kazmi I. H., “Estimation of Automotive Engine Parameters Part I: Discharge coefficient of throttle body”, *IBCAST 2009 January*, 2009 Islamabad, Pakistan.
- [87] Orani N., Pisano A., Usai E. “Fault diagnosis for the vertical three tank system via high-order sliding mode observation” *Journal of the Franklin Institute*, November 2009.
- [88] Rafiq M., Rehman S.U., Rehman F. R., Butt Q. R., Awan I.,” Second Order Sliding Mode Control Design of a Switched Reluctance Motor using Super Twisting Algorithm”, *Simulation Modelling Practice and Theory*, Vol. 25,2012.

- [89] Butt Q. R.; Bhatti A. I., "Estimation of Gasoline-Engine Parameters Using Higher Order Sliding Mode", *IEEE Transaction on Industrial Electronics*, 55(11): pp. 3891-3898. 2008.
- [90] Goh K. B., Spurgeon S.K., Jones N. B., "Higher-order sliding mode control of a diesel generator set", *Journal of Systems and Control Engineering*, Vol. 217, No. 3, pp. 229-241, 2003.
- [91] Huangfu Y., Liu W., Ma R., "Permanent magnet synchronous motor fault detection and isolation using second order sliding mode observer" in *Proc. 3rd IEEE Conference on Industrial Electronics and Applications*, June 2008.
- [92] Traore D., Plestan F., Glumineau A. and Leon J. d., "Sensorless Induction Motor: High-Order Sliding-Mode Controller and Adaptive Interconnected Observer", *IEEE Transactions on Industrial Electronics*, VOL. 55, NO. 11, November 2008.
- [93] Goh K.B., Dunnigan M.W., Williams B.W., "Robust chattering-free (higher order) sliding mode control for a vector-controlled induction machine", *Proc. in IEEE, 5th Asian Control Conference*. Vol. 2, PP: 1362 – 1370, 2004.
- [94] Defoort M., Nollet F., Floquet T., and Perruquetti W., "A Third Order Sliding Mode Control of a Stepper Motor" *IEEE transactions on Industrial Electronics*, VOL. 56, NO. 9, September 2009.
- [95] Rafiq M., Rehman S.U., Rehman F. U., Butt Q. R., "Power Efficient Higher Order Sliding Mode Control of Switched Reluctance Motor for Speed Control Applications", *International Journal of Computer Science Issues*. Vol. 8, No. 3, pp. 378-387, May 2011.
- [96] Rafiq M., Rehman S.U., Rehman F. R., Butt Q. R., "Performance Comparison of PI and Sliding Mode for Speed Control Applications of SR Motor", *European Journal of Scientific Research*, Vol. 50, No. 3. pp. 368-384, February 2011.
- [97] Levant A., Higher order sliding modes and their application for controlling uncertain processes. Ph.D Dissertation, Institute for System Studies of the USSR Academy Of Science, Moscow, 1987.
- [98] Fridman L. and Levant A. (2002). *Sliding mode control in engineering*, Marcel Dekker, chapter 3.
- [99] Perruquetti W., Barbot J. P., *Sliding mode control in Engineering*, Marcel Dekker, 2002.
- [100] Levant A., "Higher order sliding: Collection of design tools," *Proc. 4th European Control Conference*, Brussels, Belgium, 1997.
- [101] Capisani L. M., Ferrara A., Magnani L., "Second order sliding mode motion control of rigid robot manipulators", *Proc. 46th IEEE Conference on Decision and Control*, pp. 3691-3696, New Orleans, LA, USA, Dec. 12-14, 2007.
- [102] Kaveh P., Shtessel Y. B., "Blood Glucose Regulation in Diabetics Using Sliding Mode Control Techniques", in *Proc. IEEE 38th Southeastern Symposium on System Theory*, 2006, pp. 171 – 175.

- [103] Derafa L., Fridman L., Benallegue A. Ouldali A., “Super Twisting Control Algorithm for the Four Rotors Helicopter Attitude Tracking Problem”, in Proc. IEEE, 11th International Workshop on Variable Structure Systems, 2010, pp. 62-67.
- [104] Rashed M., Goh K.B., Dunnigan M.W., MacConnell P.F.A., Stronach A.F., Williams B.W., “Sensorless second-order sliding-mode speed control of a voltage-fed induction-motor drive using nonlinear state feedback”, in Proc. IEE, Electric Power Application, 2005, Vol. 152, No. 6. pp. 1127-1136.
- [105] Galicia M. I., Loukianov A. G., Rivera J., “Second Order Sliding Mode Sensorless Torque Regulator for Induction Motor”, in Proc. IEEE 49th international Conference on Decision and Control, 2010, pp. 78-83.
- [106] Chaal H., Jovanovic M., “ Second Order Sliding Mode Control of a DC Drive with Uncertain Parameters and Load Conditions”, in Proc. IEEE, Conference on Control and Decision, 2010, pp. 3204-3208.
- [107] Ezzat M., Leon J. D., Gonzalez N., Glumineau A, “Sensorless Speed Control of Permanent Magnet Synchronous Motor by using Sliding Mode Observer”, in Proc. IEEE, 11th International Workshop on Variable Structure Systems, 2010, pp. 227-232.
- [108] Khan M. K., Goh K. B., Spurgeon S. K., “Second Order Sliding Mode Control of a Diesel Engine”. Asian Journal of Control, Vol.5, No. 4, pp. 614-619, 2003.
- [109] Visinka R. , “Phase Resistance Estimation For Sensorless Control Of Switched Reluctance Motors”, Proc. in IEEE 28th Annual Conference of the Industrial Electronics Society November 5-8. 2002, Vol. 2, pp. 1044-1049.
- [110] Gobbi R., Sahoo N. C., Vejian R. “The measurement of mechanical parameters of a switched reluctance motor drive system”, Journal of Measurement Science and Technology, Vol. 18, pp. 2007.